

COMPARISON OF GUIDANCE NAVIGATION AND CONTROL DESIGN METHODS
FOR A 3-DOF MISSILE

A THESIS SUBMITTED TO
THE GRADUATE SCHOOL OF NATURAL AND APPLIED SCIENCES
OF
MIDDLE EAST TECHNICAL UNIVERSITY, NORTHERN CYPRUS CAMPUS

BY

TUĞRUL KOCADAL

IN PARTIAL FULFILLMENT OF THE REQUIREMENTS
FOR
THE DEGREE OF MASTER OF SCIENCE
IN MECHANICAL ENGINEERING

AUGUST 2024

Approval of the Board of Graduate Programs

Prof. Dr. Cumali Sabah

Chairperson

I certify that this thesis satisfies all the requirements as a thesis for the degree of
Master of Science

Asst. Prof. Dr. Ali Atashbar Orang

Program Coordinator

This is to certify that we have read this thesis and that in our opinion it is fully adequate, in scope and quality, as a thesis for the degree of Master of Science.

Asst. Prof. Dr. Anna Prach
Co-Supervisor

Prof. Dr. Eşref A. Eşkinat
Supervisor

Examining Committee Members

Prof. Dr. Esref Eşkinat METU NCC/MECH.

Asst. Prof. Dr. Anna Prach METU NCC/ASE

Prof. Dr. Farhad Javidrad METU NCC/ASE

Asst. Prof. Dr. Canras Batunlu METU NCC/EEE

Asst. Prof. Dr. Parvaneh Esmaili CIU/ Computer Engineering

I hereby declare that all information in this document has been obtained and presented in accordance with academic rules and ethical conduct. I also declare that, as required by these rules and conduct, I have fully cited and referenced all material and results that are not original to this work.

Name, Last name : Tuğrul, Kocadal

Signature :

ABSTRACT

COMPARISON OF GUIDANCE NAVIGATION AND CONTROL DESIGN METHODS FOR A 3-DOF MISSILE

Kocadal, Tuğrul
Master of Science, Mechanical Engineering
Supervisor: Prof. Dr. Eşref A. Eşkinat
Co-Supervisor: Asst. Prof. Dr. Anna Prach

August 2024, 127 pages

Guidance Navigation and Control (GNC) is the most crucial component of the missiles, which makes them one of the critical military implements; without this system, there is no difference from an uncontrolled object flying in the air and not knowing where to go. For this reason, designing a GNC system for a missile is researched in this work. The primary objective of this thesis is to design different Guidance Navigation Control algorithms for an air-to-air tactical missile. Three distinct GNC algorithms are utilized: Proportional Navigation (PN) with a seeker, Proportional Navigation (PN), and Proportional Navigation with Zero Effort Miss (ZEM). Inertial Navigation System (INS) and a Proportional-Integral-Derivative (PID) controller are applied to a nonlinear missile. Target and missile dynamic model are created and it is simulated in the Simulink. Situations where the missile with integrated GNC systems hit the target were determined in these simulations. The obtained results show the effectiveness of the algorithms and it is aimed to compare and find the algorithm that gives the best results. These findings will guide future research.

Keywords: Interception, GNC, PN, Seeker, PID.

Öz

COMPARISON OF GUIDANCE NAVIGATION AND CONTROL DESIGN METHODS FOR A 3-DOF MISSILE

Kocadal, Tuğrul
Yüksek Lisans., Makine Mühendisliği
Tez Yöneticisi: Prof. Dr. Eşref A. Eşkinat
Ortak Tez Yöneticisi: Asst. Prof. Dr. Anna Prach

Ağustos 2024, 127 sayfa

Güdüm Seyrüsefer ve Kontrol (GSK) sistemi füzelerin en önemli birleşenedir, bu da onları kritik askeri araçlardan biri yapar. Bu sistemin olmadığı durumda, füzenin havada uçan nereye gideceğini bilmeyen kontrolsüz bir cisimden farkı yoktur. Bundan dolayı, bu çalışmada füze için bir GSK sisteminin tasarılanması araştırılmıştır. Bu tezin ana amacı, havadan havaya atılan taktik bir füze için birbirinden farklı GSK algoritmaları tasarlamak ve simüle etmektir. Üç farklı GSK algoritması kullanılmıştır: Arayıcı ile orantısal seyrüsefer (OS), orantısal seyrüsefer (OS) ve sıfır çaba hatası (SÇH) ile oransal seyrüsefer (OS). Eylemsiz seyrüsefer sistemi (ESS) ve PID kontrolcüsü doğrusal olmayan bir füze modeline uygulanmıştır. Füze ve hedef dinamik modellerini oluşturulmuş ve SIMULINK ortamında simülasyonlar yapılmıştır. Bu simülasyonlara GSK sistemleri entegre edilerek füzenin hedefi vurduğu durumlar belirlenmiştir. Elde edilen sonuçlar algoritmaların verimliliğini göstermektedir. Bu sayede karşılaştırma yapılarak algoritmalar arasında en iyi sonuç verenin bulunması amaçlanmıştır. Bu bulgular gelecekteki araştırmalar için yol gösterici olacaktır.

Anahtar Kelimeler: Çarpışma, GKS, OS, Arayıcı, PID.

To my Parents, Family, and Friends with my Acquaintances at METU NCC, my second
home...

ACKNOWLEDGMENTS

I would like to express my sincere gratitude to Prof. Dr. Eşref A. Eşkinat and Assist. Prof. Dr. Anna Prach for their unwavering direction, support, and invaluable expertise in the field that guided me throughout my research progress. I would also like to thank the jury members during the thesis defence.

I would like to thank the Department of Mechanical Engineering (MECH) at the Middle East Technical University, Northern Cyprus Campus (NCC), for the opportunity to pursue my Master's degree successfully. Additionally, I am appreciative of the Aerospace Engineering Department for the valuable experience I gained through my role as a teaching assistant.

To all the academic and staff members at the Middle East Technical University, Northern Cyprus Campus, I express my sincere appreciation for your multitude of contributions. Additionally, my special thanks to you, Cem Yıldırım, Can Marazlı, Alpay Pilli, Selim Sergey, Sameer Noman, İlker Öner, Şebnem Akdoğan, Candan Koroğlu, Cahit Tatlı and Serkan Serkanat, who made my life at METU more bearable and fun.

Lastly, I want to express my gratitude to my parents, brother and sister-in-law, and other family members for their tremendous support and encouragement during this journey. I would also like to thank my valuable friends who were always there for me and rushed to help me whenever I was in trouble. Additionally, to all my current and prospective colleagues whose lives I have had the privilege to touch, even in the slightest way...

TABLE OF CONTENTS

ABSTRACT	vii
ÖZ.....	ix
ACKNOWLEDGMENTS.....	xi
TABLE OF CONTENTS.....	xii
LIST OF TABLES.....	xv
LIST OF FIGURES.....	xvi
LIST OF SYMBOLS.....	xix
LIST OF ABBREVIATIONS	xxi
CHAPTERS	
1. INTRODUCTION	1
1.1 Problem Statement.....	2
1.2 Objective of the Study	2
1.3 Significance of the Study	3
1.4 Scope and Limitations.....	3
1.5 Structure of Thesis.....	3
2. LITERATURE REVIEW	5
2.1 Guidance, Navigation and Control System	5
2.1.1 Navigation Systems.....	6
2.1.2 Guidance Systems.....	7
2.1.3 Control Systems	8
2.2 Mathematical Model	9
2.3 Control Strategies for a Missile.....	10
3. MATHEMATICAL MODELLING	12
3.1 Reference Coordinate System.....	12
3.1.1 Earth Fixed (Inertial) Coordinate System	13
3.1.2 Body Fixed Coordinate System	14

3.1.3	Wind Coordinate System.....	14
3.1.4	Kinematics and Transformation Matrix.....	14
3.2	Equations of Motion.....	16
3.2.1	Theory of Coriolis Usage for Vector Derivation.....	17
3.2.2	Translational Equations of Motion	18
3.2.3	Rotational Equations of Motion	20
3.2.4	The Three Degrees of Freedom (3-DOF) Assumption	22
3.2.5	Aerodynamic Forces and Moments Acting on the Missile	24
3.3	Model Characteristics and Configuration.....	29
3.4	Linearization	31
3.4.1	State Space	34
3.4.2	Aerodynamic Stability Derivatives	37
3.5	Numerical Example of Linearization in a Trim Point	39
3.6	Actuator Model	41
3.7	Atmosphere Model	43
4.	GUIDANCE NAVIGATION AND CONTROL ALGORITHMS	45
4.1	Missile Target Interception Scenario.....	45
4.2	Guidance Navigation and Controller Algorithms	46
4.2.1	Navigation System	46
4.2.2	Navigational Guidance	47
4.2.3	Open Loop Responses of Navigational Guidance Algorithms	54
4.2.4	Controller	56
5.	DYNAMIC MODELLING AND SIMULATION	59
5.1	Linear Missile Model with a Controller	59
5.1.1	Overall Transfer Function:	60
5.1.2	Pole Placement.....	62
5.2	Nonlinear Model Closed Loop System	63
6.	RESULTS	65

6.1	Case 1.....	66
6.1.1	Proportional Navigation + Seeker	67
6.1.2	Proportional Navigation.....	71
6.1.3	Proportional Navigation with ZEM	75
6.2	Case 2.....	79
6.2.1	Proportional Navigation + Seeker	80
6.2.2	Proportional Navigation.....	84
6.2.3	Proportional Navigation with ZEM	88
6.3	Case 3.....	92
6.3.1	Proportional Navigation + Seeker	93
6.3.2	Proportional Navigation.....	95
6.3.3	Proportional Navigation with ZEM	97
6.4	Case 4.....	99
6.4.1	Proportional Navigation + Seeker	99
6.4.2	Proportional Navigation.....	101
6.4.3	Proportional Navigation with ZEM	103
6.5	Limitations	106
7.	DISCUSSION	108
8.	CONCLUSION	114
	REFERENCES.....	117
	APPENDICES.....	119
A.	Linearization	119
B.	Aerodynamical Stability Derivatives	123

LIST OF TABLES

TABLES

Table 3. 1: Aerodynamical Polynomial Coefficient.....	27
Table 3. 2: Physical Characteristics of the missile. [15]	30
Table 3. 3: Aerodynamical Equations Parameters.....	37
Table 3. 4: Aerodynamical Stability Derivative Equations	38
Table 3. 5: Numerical parameters for linearization.....	40
Table 3. 6: Actuator parameters.....	42
Table 3. 7: Atmosphere model parameters.....	43
Table 4. 1: Proportional Navigation Parameters	49
Table 6. 1: Numerical parameters for case one.	66
Table 6. 2: Numerical parameters for case two.	80
Table 6. 3: Numerical parameters for case four	92
Table 6. 4: Numerical parameters for case five.	99
Table 6. 5: Case analysis for z-separation target velocity.....	106
Table 6. 6: Case analysis for x-separation target velocity.....	106
Table B. 1: Aerodynamical Stability Derivative Equations.....	127

LIST OF FIGURES

FIGURES

Figure 3. 1: Reference Coordinate Frames [3]	13
Figure 3. 2: Dynamic model of the missile	17
Figure 3. 3: Aerodynamical Coefficients Plot in x-direction.....	28
Figure 3. 4: Aerodynamical Coefficients Plot in z-direction.....	28
Figure 3. 5: Aerodynamical Pitch Moment Coefficients Plot.....	29
Figure 3. 6: AIM9-Sidewinder Missile [24].	30
Figure 3. 7: Forces acting on the missile model.	39
Figure 3. 8: Actuator model block diagram.	42
Figure 4. 1: Missile Target Interception Scenario	46
Figure 4. 2: Missile Target Interception Scenario with Parameters.....	48
Figure 4. 3: Seeker and Proportional Navigation Angles.	53
Figure 4. 4: Navigational guidance response of open loop simulation when fin deflection is minus ten degrees.....	54
Figure 4. 5: Navigational guidance response of open loop simulation when fin deflection is zero degrees.....	55
Figure 4. 6: Navigational guidance response of open loop simulation when fin deflection is ten degrees.	55
Figure 4. 7: PI Block Diagram	57
Figure 4. 8: PI block diagram with rate feedback.	58
Figure 5. 1: Controller with a linear missile model.....	60
Figure 5. 2: Nonlinear model closed loop block diagram.	64
Figure 6. 1: Missile Target interception case one scenario.....	66
Figure 6. 2: Missile Target Interception Animation.	67
Figure 6. 3: Demanded vs Measured Acceleration.....	68
Figure 6. 4: Missile Target Trajectory.	68
Figure 6. 5: Missile Target Relative Separation.....	69
Figure 6. 6: Change of Angle of Attack.....	69
Figure 6. 7: Change of Fin Deflection.....	70
Figure 6. 8: Change of Mach Number.	70
Figure 6. 9: Missile Target Interception Animation.	71
Figure 6. 10: Demanded vs Measured Acceleration.....	72
Figure 6. 11: Missile Target Trajectory.	72

Figure 6. 12: Missile Target Relative Separation	73
Figure 6. 13: Change of Angle of Attack	73
Figure 6. 14: Change of Fin Deflection	74
Figure 6. 15: Change of Mach Number	74
Figure 6. 16: Missile Target Interception Animation	75
Figure 6. 17: Demanded vs Measured Acceleration	76
Figure 6. 18: Missile Target Trajectory.....	76
Figure 6. 19: Missile Target Relative Separation	77
Figure 6. 20: Change of Angle of Attack	77
Figure 6. 21: Change of Fin Deflection	78
Figure 6. 22: Change of Mach Number.....	78
Figure 6. 23: Missile Target interception case two scenario	79
Figure 6. 24: Missile Target Interception Animation	81
Figure 6. 25: Demanded vs Measured Acceleration	81
Figure 6. 26: Missile Target Trajectory.....	82
Figure 6. 27: Missile Target Relative Separation	82
Figure 6. 28: Change of Angle of Attack	83
Figure 6. 29: Change of Fin Deflection	83
Figure 6. 30: Change of Mach Number.....	84
Figure 6. 31: Missile Target Interception Animation	85
Figure 6. 32: Demanded vs Measured Acceleration	85
Figure 6. 33: Missile Target Trajectory.....	86
Figure 6. 34: Missile Target Relative Separation	86
Figure 6. 35: Change of Angle of Attack	87
Figure 6. 36: Change of Fin Deflection	87
Figure 6. 37: Change of Mach Number.....	88
Figure 6. 38: Missile Target Interception Animation	89
Figure 6. 39: Demanded vs Measured Acceleration	89
Figure 6. 40: Missile Target Trajectory.....	90
Figure 6. 41: Missile Target Relative Separation	90
Figure 6. 42: Change of Angle of Attack	91
Figure 6. 43: Change of Fin Deflection	91
Figure 6. 44: Change of Mach Number.....	92
Figure 6. 45: Missile Target Interception Animation	93
Figure 6. 46: Demanded vs Measured Acceleration	94
Figure 6. 47: Missile Target Trajectory.....	94

Figure 6. 48: Missile Target Interception Animation.	95
Figure 6. 49: Demanded vs Measured Acceleration.....	96
Figure 6. 50: Missile Target Trajectory.	96
Figure 6. 51: Missile Target Interception Animation.	97
Figure 6. 52: Demanded vs Measured Acceleration.....	98
Figure 6. 53: Missile Target Trajectory.	98
Figure 6. 54: Demanded vs Measured Acceleration.....	100
Figure 6. 55: Missile Target Trajectory.	100
Figure 6. 56: Change of Fin Deflection.....	101
Figure 6. 57: Demanded vs Measured Acceleration.....	102
Figure 6. 58: Missile Target Trajectory.	102
Figure 6. 59: Change of Fin Deflection.....	103
Figure 6. 60: Demanded vs Measured Acceleration.....	104
Figure 6. 61: Missile Target Trajectory.	104
Figure 6. 62: Change of Fin Deflection.....	105
Figure 6. 63: Limitation of the missile according to the target velocity and x-direction relative separation.....	107
Figure 6. 64: Limitation of the missile according to the target velocity and z-direction relative separation.....	107
Figure 7. 1: Acceleration response to a pulse function. [15].....	109
Figure 7. 2: Acceleration response to a pulse function.[11].....	109
Figure 7. 3: Acceleration response to a pulse function.	110

LIST OF SYMBOLS

SYMBOLS

C_m	Aerodynamic coefficients in pitch moment
C_x	Aerodynamic coefficients in x-direction
C_z	Aerodynamic coefficients in z-direction
α	Angle of attack
ω	Angular Speed
D	Drag Force
δ_e	Fin/Elevator Deflection
X	Forces in x-direction
Z	Forces in z-direction
g	Gravitational Acceleration
L	Lift Force
M	Mach Number
I	Moment of Inertia
\dot{q}	Pitch Acceleration
θ	Pitch Angle/ Attitude
M	Pitch Moment
q	Pitch Rate
\dot{p}	Roll Acceleration
ϕ	Roll Angle
L	Roll Moment
p	Roll Rate
u	Speed in x-direction
v	Speed in y-direction
w	Speed in z-direction

a	Speed of Sound
\dot{r}	Yaw Acceleration
ψ	Yaw Angle
N	Yaw Moment
r	Yaw Rate

LIST OF ABBREVIATIONS

ABBREVIATIONS

c.g	Centre of Gravity
c.p	Centre of Pressure
CFD	Computational Fluid Dynamics
EOM	Equation of Motion
GPS	Global Positioning System
GNC	Guidance Navigation and Control
INS	Inertial Navigation System
LOS	Line of Sight
LQR	Linear Quadratic Regulator
MPC	Model Predictive Control
PD	Proportional Derivative
PI	Proportional Integral
PID	Proportional Integral Derivative
PN	Proportional Navigation
6-DOF	Six Degrees of Freedom
3-DOF	Three Degrees of Freedom
ZEM	Zero Effort Miss

CHAPTER 1

INTRODUCTION

Missile systems have various usage areas, such as military, defence, aerospace, and space exploration. Military and defence systems are among the most used areas of missiles. They have been either used for attacking or defending against opponents. For this reason, missiles are indispensable and are the leading equipment for wars. Although missiles were used before, it can be said that the actual usage of guided missiles started during World War II (WW2). During and after World War II, innovations in missiles proceeded. Thanks to the guidance navigation and control (GNC) systems, the missile and the target can easily intercept each other by ensuring accurate trajectory follow, thus increasing the target hitting rate. This shows how GNC is crucial for the missiles. During this period, not only was GNC developed, but other things related to the missiles, such as propulsion and launching systems, were also established. As a result, different types of missiles with various properties have been developed and classified differently according to type, launching, range, propulsion systems and guidance systems [1]–[3].

1.1 Problem Statement

In modern warfare, although continuous advancements have been proceeded, especially in the development of the supersonic missile systems, the dominance of operational missiles remain subsonic and may have trouble to effectively counter target with high speeds and manoeuvrability. Increasing sophistication of these targets demands further enhancement of missile speed and manoeuvrability. However, as the speed of the missile increase, the complexity of the flight proportionally grows, which ends up with the development of the more advanced guidance, navigation and control (GNC) systems. This research aims to address these challenges by developing and validating GNC algorithms tailored for supersonic missiles, thereby improving their accuracy and reliability in engaging fast, agile targets under dynamic flight conditions.

1.2 Objective of the Study

The primary objectives of this study are to design three different navigation and guidance algorithms for higher speeds that improve target missile interception accuracy. This is possible by providing suitable command, developing a powerful and effective controller that will quickly implement commands from navigation and guidance, and keep the system stable at the same time. Lastly, with the comparison of the data obtained from three different GNC systems, a decision made for which GNC algorithm is the most suitable for these kind of missile systems among them.

1.3 Significance of the Study

This research contributes to the field of missile technology by providing a comparison between three different GNCs. During this comparison, the responses of each GNC system will be investigated, and their performance characteristics will be found. According to these performance characteristics, the limitations of guidance navigation and control systems will be revealed. Aligned with these limitations, the analysis will elucidate which GNC system operates with optimal performance under specific conditions. The findings could be applied in the new faster systems, i.e. $\text{Mach} > 1$, to improve the effectiveness and reliability of missile operations, potentially leading to more successful missions and bringing strategic advantages.

1.4 Scope and Limitations

This research concentrates on three-degree-of-freedom (3-DOF) missile models and does not extend to more degrees of freedom. Furthermore, no actual testing is involved in the study; all of it is done through theoretical and visualized simulations (MATLAB Simulink). These limitations define the scope of the study and ensure that it is both manageable and relevant to the state of technology today.

1.5 Structure of Thesis

The thesis is organized as follows: Chapter 2 provides a comprehensive literature review on GNC systems for missiles. Chapter 3 details the mathematical model of the used missile. Chapter 4 presents the guidance navigation and control algorithms. Chapter 5 represents the dynamic modelling and simulations, while chapter 6 gives the results

obtained throughout the simulations and chapter 7 provides their discussions. Lastly, chapter 8 concludes the thesis. This structure ensures a logical progression from background research to presenting original findings and their implications.

CHAPTER 2

LITERATURE REVIEW

This chapter presents a literature review of guidance navigation and control systems used in missiles. It starts by explaining the GNC systems, and investigating each component individually to determine their purposes, and why a GNC system is important for missiles. Additionally, it shows different mathematical models developed before and which GNC algorithms have been used in similar research, providing the advantages and disadvantages of their strategies and conclusions.

2.1 Guidance, Navigation and Control System

GNC is the critical system of the missile to have a successful missile target interception. As explicitly implied by its name, GNC has three parts: guidance, navigation, and control systems, which are gathered together to form a system called GNC. Each part has a specific role. This system, as a whole, provides an input to the missile dynamics, which will be explained in chapter three, and ensures a smooth path for the missile to follow and makes the target and missile interception possible [4].

2.1.1 Navigation Systems

Navigation systems are one of the components of the GNC system, which provide position velocity and attitude of the missile with respect to the reference coordinate frame by using high-accuracy gyroscopes and accelerometers [4]. Since gyroscopes and accelerometers are carried within the missile, this navigational system is called an inertial navigation system (INS). This navigational system depends on gyros and accelerometers to obtain accelerations and integrate them in order to find the velocity and position of the missile. The INS system, integrated into the missile, offers dependable global navigation in all conditions without needing ground-based navigational aids. Thus, this system plays a massive role in the whole GNC system by providing all the dynamical parameters of the vehicle for the guidance part of the system [3], [5].

Additionally, there is a system called the Global Positioning System (GPS), which also provides the vehicle's position around the Earth by using external sources, i.e. satellites in all weather conditions around or near the Earth within the atmosphere [6]. By combining GPS and INS, the performance of the navigation system can be enhanced by taking into account the strengths of both systems. In the GPS/INS system, INS provides the position, velocity and acceleration of the vehicle, while GPS also provides the position of the vehicle as well; by comparing two positional data, drift errors can be corrected and create a more robust and reliable navigation system [3], [4].

Alternative navigation aids, such as terrain counter matching, are used on top of an inertial navigation system for position correction, similar to the GPS. Instead of using satellites, this system uses an already created terrain map of the area and compares

the actual instant terrain by using sensors on board and matching them to find the exact location of the vehicle [7]. Although it is an effectively working system, the fact that it requires previously prepared data can be shown as a minor disadvantage.

2.1.2 Guidance Systems

The guidance system is another component of the GNC system, which is a matter of finding the appropriate compensation network to place in series with the plant in order to accomplish an intercept. In other words, guidance calculates the motion variables, i.e. demanded accelerations and puts them in series to flow the desired trajectory to have the missile target interception by providing these data to the controller [1], [3], [4],[8]. One of the guidance used in ancient times is called Parallel Navigation (PN). This navigational algorithm assumes a constant bearing angle, which is measured clockwise from north, and a constant speed for both the tracker and target. By using geometry and knowing the position and speed of the target, the tracker's velocity can be estimated easily and ensures that the target and pursuer meet. Moreover, this algorithm is the basic start-up algorithm, which makes it possible to create more advanced guidance systems [1].

One of the most commonly used guidance algorithms is proportional navigation guidance because of its success rate and effectiveness. This algorithm creates acceleration commands perpendicular to the instantaneous missile target line of sight (LOS), which is proportional to the closing velocity and line of sight rate [1], [2], [4]. In order to make this navigation guidance system, which has a high success rate, even more powerful, some additions can be made to make the system more efficient. One of these additions is using a seeker, which is a sensor that tracks the target and gives

the information, like position and speed, to the proportional navigation guidance to rearrange the commands in order to create the most accurate trajectory for the interception [2], [4].

Zero Effort Miss (ZEM) is the distance that the missile misses the target if no further command is performed. This technique can be integrated together with the PN to continuously adjust the missile's trajectory to minimize the zero effort miss (ZEM), which effectively improves the interception accuracy and makes the guidance algorithm more robust through real-time adjustments [2].

2.1.3 Control Systems

The control system is the last component of the GNC system, which is used in order to stabilize and guide the missile by controlling the pitch, roll and yaw motions via either control surfaces or thrust vectoring. The working principle of the control system is that it takes the demanded acceleration command coming from the guidance stem and creates a controlling input for the missile in order to follow the desired trajectory to make the target and missile interception happen [3], [4], [8]. One of the most commonly used controllers is Proportional Integral and Derivative (PID) controller, because of its simplicity and robustness. In some cases, different variants of PID controllers like Proportional Integral (PI), Proportional Derivative (PD), and simple proportional controllers might have been used depending on the requirements of the missile systems [9]. In particular scenarios, the PID controller might not meet the requirements in order to follow the desired acceleration. In these cases, rate feedback can be used to increase the effectiveness of the controller [10].

In some situations, the PID controller's gains might work adequately for all the flight conditions because of their variations. Therefore, these gains should be adjusted according to the variable flight conditions and parameters such as Mach number, angle of attack, sideslip angle, etc. In such a case, a gain scheduling controller comes in handy. This controller adjusts the PID gains by using flight parameters in order to make the missile work in all weather conditions and ensure a smooth trajectory for missile target interception [11].

There are also controllers, which are known as optimal controllers i.e. Linear Quadratic Regulator (LQR), Model Predictive Control (MPC). The Linear Quadratic Regulator (LQR) is an ideal control technique that balances state and control input efforts by minimising a cost function for linear systems. It can also handle more complex dynamical behaviours than a PID controller [12]. On the other hand, MPC solves the optimization problem at each step to calculate the control inputs that will optimize the objective function for the future horizon, and this controller works for both linear and non-linear stems, which makes it more powerful and versatile than the other controllers [13].

2.2 Mathematical Model

The mathematical model of missiles involves a comprehensive set of equations and reference frames to describe the missile's dynamics, control and guidance system. In order to identify the missile's motion with respect to itself or the Earth, inertial reference frames and body axis reference frames are used. The core of the mathematical model depends on the Equation of Motions (EOM), which is derived from Newton's second law. In addition to the EOM, kinematic equations are used to identify the velocities and angular rates of the missile. Aerodynamical forces and moments are

the other crucial parameters for the missile dynamics. GNC algorithm are the other factor that plays a role in the missile dynamics and has an enrolment in the mathematical model [2], [14]. In addition, while doing the simulation and modelling in this thesis, three different journal articles were used besides the above two sources. As mentioned in the upper part of the paragraph, these three references also provide step-by-step instructions on how to make a mathematical model of the missile in order to be used in the modelling and simulation in MATLAB Simulink [11], [15], [16].

2.3 Control Strategies for a Missile

Various control and guidance algorithms can be used to control the missile. As explained in the previous paragraph, different navigation algorithms with multiple guidance algorithms and various controllers can be used. To illustrate, an initial navigation system (INS), proportional navigation (PN), and a Proportional Integral Derivative (PID) controller can be gathered together to create a Guidance Navigation and Control (GNC) system. Similarly, a completely different GNC algorithm can be obtained by adding a seeker to the guidance system and a Global Positioning System (GPS) to the navigation system and keeping the PID the same. Thus, many combinations can be done to have a working GNC system, but the primary objective has to meet the requirements of the missile system. At the same time, the system should respond to the target's dynamics in order to have proper trajectory and interception.

In order to understand different control strategies that are applied in the missiles, a master's thesis was reviewed [18]. This thesis uses a six-degree-of-freedom (6-DOF) tactical missile; while designing the missile, 6-DOF motional and kinematic equations with aerodynamic forces and moments were used. In order to calculate aerodynamical

forces and moments, aerodynamical coefficients were required, and these coefficients were obtained by Missile DATCOM in this thesis. As a GNC algorithm, an inertial navigation system with proportional navigation (PN) and linear quadratic regulator (LQR) was used.

In another thesis [17], a control strategy for a powered reusable rocket booster landing case was created, similar to the previous thesis equation of motions, kinematic equations, and aerodynamic forces and moments were used to develop the missile model, but in this case, a 3-DOF model was created. In this thesis, there is no GNC system since navigation and guidance systems were not used because it assumed that the location of the landing area is known and given as input directly to the controller. However, as a controller, three different controllers, PID, LQR, and MPC, were used, and their comparisons were made. As a result, the findings clearly demonstrated which controller operates most efficiently under the given conditions.

CHAPTER 3

MATHEMATICAL MODELLING

This section describes the fundamental aspects of mathematical modelling, focusing on its application to missile dynamics. In the beginning, coordinate frames and the transformation between them are expressed, which are crucial for accurately describing the missile's motion in different coordinate systems than the missile's behaviour during its flight. The mathematical model created for the missile brought about three degrees of freedom (3DOF) rigid body dynamics providing position and attitude of the missile by considering the forces: thrust, aerodynamical forces and gravity. Lastly, a comprehensive linearization of the nonlinear equations of motion, illustrated with a detailed numerical example, is shown, which is helpful in the stability and controllability analysis. To begin with, reference coordinate frames are handled.

3.1 Reference Coordinate System

A reference coordinate system is a rigid body or a set of rigidly connected points used to describe objects' position, orientation, and movement in the atmosphere. It provides a point of origin and a set of axes for making measurements, and it is widely used in areas such as physics, astronomy, engineering and navigation for consistent and accurate descriptions [3]. There are various reference coordinate systems, but two of them are the most used ones, which are the Body Fixed Coordinate system and Earth Fixed Coordinate system, which is shown in Fig 3.1.

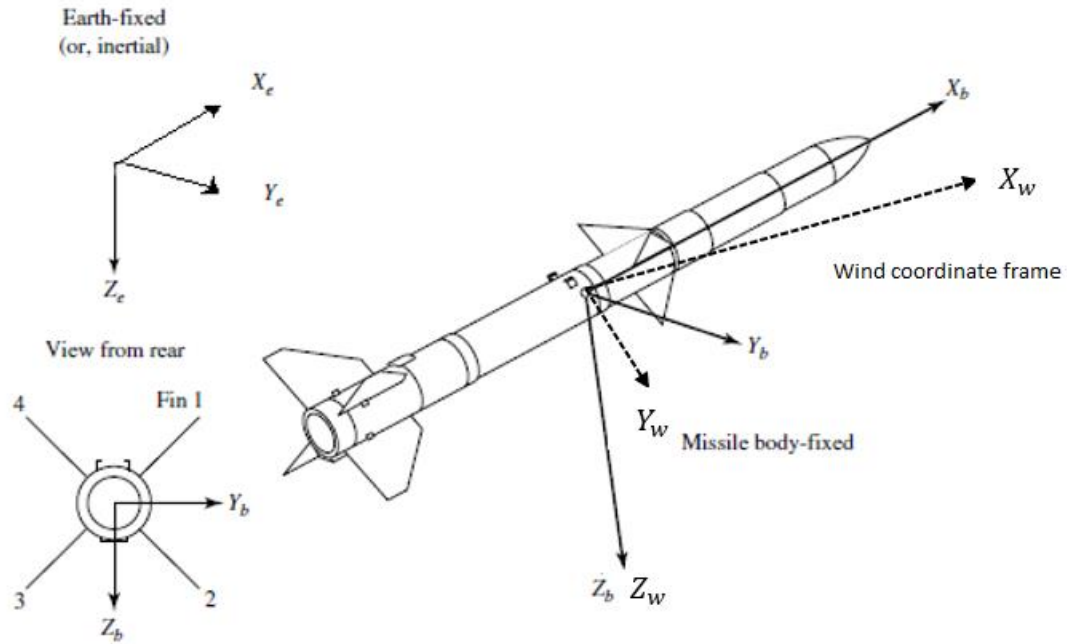


Figure 3. 1: Reference Coordinate Frames [3]

3.1.1 Earth Fixed (Inertial) Coordinate System

The Earth Fixed Coordinate is a cartesian coordinate system $[X_E, Y_E, Z_E]$ which is at a location where the horizontal (X-axis) displacement relative to the missile's position is zero, but there is a vertical (Z-axis) displacement, indicating an altitude difference between the missile and the Earth-fixed frame. In this study, the missile is assumed to be moving longitudinally, meaning moving in the X and Z axis of the inertial coordinate system and rotating around the Y_E [3].

3.1.2 Body Fixed Coordinate System

The Body Fixed Coordinate is a cartesian coordinate system $[X_B, Y_B, Z_B]$ which is attached to the missile's centre of mass, where its centre denoted by (O_B) , and as the missile moves and rotates, it moves and rotates with itself. Coordinate system's X_B axis is along with the nose of the missile, Z_B axis point towards downwards, in the plane of symmetry and Y_B axis completes the right hand coordinate system [3].

3.1.3 Wind Coordinate System

The Wind Coordinate is a cartesian coordinate system $[X_w, Y_w, Z_w]$ attached to the missile's centre of pressure, where its centre denoted by (O_w) , and as the missile moves and rotates, it does not rotate with the missile. Coordinate system's X_w axis is along with the wind direction, along with the freestream (\vec{V}_∞) vector, Z_w axis point towards downwards perpendicular to the velocity direction and Y_w axis completes the right-hand coordinate system [3].

3.1.4 Kinematics and Transformation Matrix

A missile position and velocity are defined by using an inertial reference frame coordinate system. However, the attitude of a missile is defined as the angle between the horizontal axis of the earth fixed reference frame and the X-axis of the boy coordinate system (X_B). As a result, a coordinate transformation is required in order to relate all the missile's motions and parameters with respect to the inertial reference coordinate system [3]. The velocity vectors of the missile with respect to the inertial coordinate system and body axis coordinate system are:

$$\vec{V}^{(E)} = \begin{bmatrix} \dot{x} \\ \dot{y} \\ \dot{z} \end{bmatrix}, \vec{V}^{(B)} = \begin{bmatrix} u \\ v \\ w \end{bmatrix}, \quad (3.1)$$

Similarly, the position of the missile is written in the inertial axis as:

$$O^I = \begin{bmatrix} x \\ y \\ z \end{bmatrix}, \quad (3.2)$$

The variables defined in one coordinate system are transformed into another coordinate system using the transformation matrices. In this model, the transformation between the body axis and inertial reference coordinate frame is needed. In order to do that, either a transformation matrix from the body axis to an inertial reference frame coordinate system or vice versa is used [3], [14].

$$L_{EB} = \begin{bmatrix} \cos \theta & 0 & \sin \theta \\ 0 & 1 & 0 \\ -\sin \theta & 0 & \cos \theta \end{bmatrix}, \quad (3.3)$$

$$L_{BE} = L_{EB}^{-1} = \begin{bmatrix} \cos \theta & 0 & \sin \theta \\ 0 & 1 & 0 \\ -\sin \theta & 0 & \cos \theta \end{bmatrix}^{-1}, \quad (3.4)$$

$$L_{BW} = \begin{bmatrix} \cos \alpha & 0 & -\sin \alpha \\ 0 & 1 & 0 \\ \sin \alpha & 0 & \cos \alpha \end{bmatrix}, \quad (3.5)$$

$$L_{WB} = L_{BW}^{-1} = \begin{bmatrix} \cos \alpha & 0 & -\sin \alpha \\ 0 & 1 & 0 \\ \sin \alpha & 0 & \cos \alpha \end{bmatrix}^{-1}. \quad (3.6)$$

Using this transformation matrices, velocity components on coordinates can be obtained easily.

$$\vec{V}^{(E)} = \vec{V}^{(B)} \times L_{EB} \Rightarrow \begin{bmatrix} \dot{x} \\ \dot{y} \\ \dot{z} \end{bmatrix} = \begin{bmatrix} \cos \theta & 0 & \sin \theta \\ 0 & 1 & 0 \\ -\sin \theta & 0 & \cos \theta \end{bmatrix} \times \begin{bmatrix} u \\ v \\ w \end{bmatrix} \quad (3.7)$$

Since there is no velocity in the Y_B direction, $v = 0$. Thus, velocity components become:

$$\dot{x} = u \cos \theta + w \sin \theta \quad (3.8)$$

$$\dot{z} = -u \sin \theta + w \cos \theta \quad (3.9)$$

3.2 Equations of Motion

The mathematical model defines the position and attitude of the missile using rigid body dynamics with using Newton's second law for forces and moments separately. In real life, missiles' has six degree of freedom (6-DOF) of motion, but in this study for simplicity a 3-DOF missile model has been used as illustrated in Fig. 3.2. Weight, aerodynamical forces and thrust are the forces that act on the missile [3].

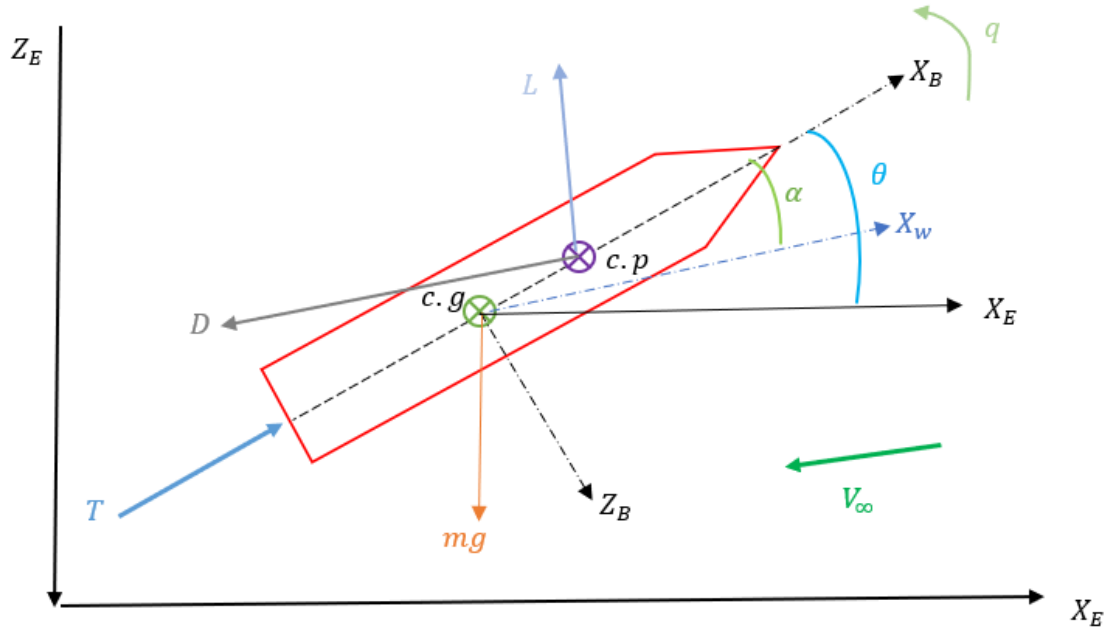


Figure 3.2: Dynamic model of the missile

3.2.1 Theory of Coriolis Usage for Vector Derivation

The Coriolis theorem should be used when the derivative of a vector is expressed as components of a rotating frame (body-fixed) with respect to a non-rotating frame (earth-fixed or inertial). For finding the derivative of vector \vec{V} in an earth fixed coordinate system with respect to the time, theorem is expressed as [3], [19]:

$$\frac{d\vec{V}}{dt} \Big|_E = \frac{d\vec{V}}{dt} \Big|_B + \vec{\omega}_B \times \vec{V}_B \quad (3.10)$$

where $\vec{\omega}_B$ is the angular velocity of the rotating coordinate system, i.e. body coordinate system with respect to the non-rotating frame, earth fixed coordinate frame.

$$\vec{\omega}_B = \begin{bmatrix} p \\ q \\ r \end{bmatrix}, \quad (3.11)$$

3.2.2 Translational Equations of Motion

Applying Newton's second law of motion for the forces, at the centre of gravity (c.g) , these equations are obtained [3], [19].

$$\sum \vec{F} = m\vec{a} = m \frac{d\vec{V}}{dt} \Big|_I = m \left(\frac{d\vec{V}}{dt} \Big|_B + \vec{\omega}_B \times \vec{V}_B \right). \quad (3.12)$$

There are three forces acting on the missile body which are $[X, Y, Z]$ and they indicate the sum of the forces acting on the missile in x ,y and z directions respectively.

$$\vec{F}_B = \begin{bmatrix} X \\ Y \\ Z \end{bmatrix}, \quad (3.13)$$

There is also gravitational acceleration force acting on the missile, and it needs to be considered in the calculations by applying the earth coordinate frame to the body axis frame transformation matrix. As a result, sum of the forces become:

$$\sum \vec{F} = \vec{F}_B + L_{BE} \begin{bmatrix} 0 \\ 0 \\ mg \end{bmatrix}, \quad (3.14)$$

Using equation 3.1, derivative of the velocity component can be written as:

$$\frac{d\vec{v}}{dt} \Big|_B = \begin{bmatrix} \dot{u} \\ \dot{v} \\ \dot{w} \end{bmatrix}, \quad (3.15)$$

The 2nd law of Newton can be written as :

$$\Sigma \vec{F} = \begin{bmatrix} X \\ Y \\ Z \end{bmatrix} + L_{BE} \begin{bmatrix} 0 \\ 0 \\ mg \end{bmatrix} = m \left\{ \begin{bmatrix} \dot{u} \\ \dot{v} \\ \dot{w} \end{bmatrix} + \begin{bmatrix} p \\ q \\ r \end{bmatrix} \times \begin{bmatrix} u \\ v \\ w \end{bmatrix} \right\}. \quad (3.16)$$

Expanding the matrices and rearranging, simplified equations can be obtained as:

$$\dot{u} = rv - qw + \frac{X}{m} - g \sin \theta, \quad (3.17)$$

$$\dot{v} = pw - ru + \frac{Y}{m} + g \cos \theta \sin \phi, \quad (3.18)$$

$$\dot{w} = qu - pv + \frac{Z}{m} + g \cos \theta \cos \phi. \quad (3.19)$$

3.2.3 Rotational Equations of Motion

Applying Newton's second law of motion for the moments, denoted by \vec{G} , at the centre of the gravity (c.g) , these equations are obtained [3], [19] .

$$\Sigma \vec{G}_B = \begin{bmatrix} L \\ M \\ N \end{bmatrix}, \quad (3.20)$$

where L, M, N denotes the moments action on x, y and z directions respectively. \vec{H}_B is the angular momentum acting in body axis and has an equation of :

$$\vec{H}_B = I_B \vec{\omega}_B, \quad (3.21)$$

where I_B represents the inertia matrix and $\vec{\omega}_B$ represents the angular velocity defined at eq. 3.11. Inertia matrix I_B is donated as:

$$I_B = \begin{bmatrix} I_{xx} & -I_{xy} & -I_{xz} \\ -I_{xy} & I_{yy} & -I_{yz} \\ -I_{xz} & -I_{yz} & I_{zz} \end{bmatrix}, \quad (3.22)$$

where

$$I_{xx} = \int (y^2 + z^2) dm, \quad (3.23)$$

$$I_{yy} = \int (x^2 + z^2) dm, \quad (3.24)$$

$$I_{zz} = \int (x^2 + y^2) dm , \quad (3.25)$$

$$I_{xy} = \int (xy) dm , \quad (3.26)$$

$$I_{yz} = \int (yz) dm , \quad (3.27)$$

$$I_{xz} = \int (xz) dm , \quad (3.28)$$

Relation between \vec{H}_B and \vec{G}_B :

$$\Sigma \vec{G}_B = \frac{d\vec{H}_B}{dt} \Big|_I , \quad (3.29)$$

$$\frac{d\vec{H}_B}{dt} \Big|_I = \dot{H}_B + \vec{\omega}_B \times \vec{H}_B , \quad (3.30)$$

$$\dot{H}_B = \frac{d}{dt} (I_B \vec{\omega}_B) = I_B \vec{\omega}_B + I_B \dot{\vec{\omega}}_B , \quad (3.31)$$

From eq. 3.11. it can be found as:

$$\dot{\vec{\omega}}_B = \begin{bmatrix} \dot{p} \\ \dot{q} \\ \dot{r} \end{bmatrix} , \quad (3.32)$$

The moment equation can be represented as:

$$\Sigma \vec{G}_B = \bar{I}_B \dot{\vec{\omega}}_B + \vec{\omega}_B \times \vec{H}_B , \quad (3.33)$$

$$\begin{bmatrix} L \\ M \\ N \end{bmatrix} = I_B \cdot \begin{bmatrix} \dot{p} \\ \dot{q} \\ \dot{r} \end{bmatrix} + \begin{bmatrix} P \\ q \\ r \end{bmatrix} \times \left(I_B \cdot \begin{bmatrix} P \\ q \\ r \end{bmatrix} \right) , \quad (3.34)$$

$$\begin{bmatrix} L \\ M \\ N \end{bmatrix} = \begin{bmatrix} I_{xx} & -I_{xy} & -I_{xz} \\ -I_{xy} & I_{yy} & -I_{yz} \\ -I_{xz} & -I_{yz} & I_{zz} \end{bmatrix} \cdot \begin{bmatrix} \dot{p} \\ \dot{q} \\ \dot{r} \end{bmatrix} + \begin{bmatrix} P \\ q \\ r \end{bmatrix} \times \left(\begin{bmatrix} I_{xx} & -I_{xy} & -I_{xz} \\ -I_{xy} & I_{yy} & -I_{yz} \\ -I_{xz} & -I_{yz} & I_{zz} \end{bmatrix} \cdot \begin{bmatrix} P \\ q \\ r \end{bmatrix} \right) . \quad (3.35)$$

Expanding the matrices and rearranging them, simplified equations can be obtained as:

$$L = I_{xx}\dot{p} - I_{xz}(\dot{r} + pq) - (I_{yy} - I_{zz})qr - I_{yz}(q^2 - r^2) - I_{xy}(\dot{q} - rp) , \quad (3.36)$$

$$M = I_{yy}\dot{q} - I_{xz}(r^2 - p^2) - (I_{zz} - I_{xx})rp - I_{xy}(\dot{p} + qr) - I_{yz}(\dot{r} - pq) , \quad (3.37)$$

$$N = I_{zz}\dot{r} - I_{xz}(\dot{p} - qr) - (I_{xx} - I_{yy})pq - I_{xy}(p^2 - q^2) - I_{yz}(\dot{q} + rp) , \quad (3.38)$$

3.2.4 The Three Degrees of Freedom (3-DOF) Assumption

Whenever a missile is launched, it experiences a six degrees of freedom motion in the flight condition similar to an aircraft's flight condition. During this flight, it might fly at a flight level, climb, descent, or manoeuvre. This means the missile could have any

configuration where all the translational and rotational components of accelerations and velocities may be included.

During most of the flight, the missile flies at a constant velocity, altitude and attitude with the same heading. This flight condition is known as a trim condition, in other words, when the sum of the forces and moments acting on the missile is zero. In such a flight condition, if a laterally symmetrical missile is launched, there should be no lateral motion as long as there is no lateral disturbance. As a result, the missile should act in the longitudinal direction, eliminating only two rotational and one translational degree of freedom and having three degrees of freedom motion. There is always some lateral movement due to the perturbations and coupling, but this is only an assumption longitudinally, which is actually a startup point.

In the three degrees of freedom (3-DOF) assumption, motion is restricted into two dimensions with two forces and a pitching moment. In this research, the missile is restricted to travel in the longitudinal directions meaning that no force or moment is acting on the lateral direction. The missile motion is limited to travel only in the x-direction and z-direction and rotates around the pitch axis in the body axis coordinate frame.

By applying these conditions to the translational and rotational equations of motions with the assumption of plane of symmetry $I_{xy} = I_{yz} = 0$ and $I_{xz} \approx 0$, which can be neglected, equations become as [3], [19]:

$$\dot{u} = \frac{x}{m} - qw - g\sin\theta , \quad (3.39)$$

$$\dot{w} = \frac{z}{m} + uq + g\cos\theta , \quad (3.40)$$

$$\dot{q} = \frac{M}{I_{yy}} , \quad (3.41)$$

$$q = \dot{\theta} . \quad (3.42)$$

Where forces defined as:

$$X = X_{aero} + T , \quad (3.43)$$

where T is Thrust.

$$Z = Z_{aero} , \quad (3.44)$$

$$M = M_{aero} . \quad (3.45)$$

3.2.5 Aerodynamic Forces and Moments Acting on the Missile

The missile has a propulsive force acting on the x-axis along the body axis, and there are controller fins located at the end of the missile in order to control the missile movement. Consequently, forces acting on the missile are aero-propulsive forces, and the moment is only aerodynamical. These forces and moments are drag, lift and pitch moments, and they are defined in the wind reference frame as [3], [19]–[21]:

$$D = X_{aero} = \frac{1}{2} \rho V^2 S(C_x), \quad (3.46)$$

$$L = Z_{aero} = \frac{1}{2} \rho V^2 S(C_z), \quad (3.47)$$

$$M_{aero} = \frac{1}{2} \rho V^2 S d_{ref} (C_m). \quad (3.48)$$

In these aerodynamical forces and moments, aerodynamical coefficients play a massive role in the design process and optimising the missile performance, stability, and control, ensuring efficient and successful interception. These coefficients C_x , C_z , and C_m quantify the aerodynamical forces and moments acting on the missile proportional to the size, speed and atmospheric conditions.

3.2.5.1 Aerodynamical Coefficients

In order to calculate aerodynamical coefficients, there are several ways that can be followed. The first one is to use a wind tunnel experiment using a small, scaled model of the missile and measure the forces and moments directly for different conditions. This method provides highly accurate results on aerodynamical behaviour. Secondly, a computational flight dynamics (CFD) program can be used to obtain data without needing a physical model. These programs solve the fluid flow equations around the missile for different regimes by using numerical methods. Lastly, Missile DATCOM, which is a software, can be used for calculations. This program uses empirical and semi-empirical methods to estimate aerodynamic behaviour based on the missile's geometry and flight conditions, providing a quick and cost-effective aerodynamical analysis. Overall, a real-life experiment, a wind tunnel test, provides the most accurate results

compared to the CFD analysis, which provides more reasonable results than the Missile DATCOM [20], [21].

In this thesis, a polynomial model was utilized to estimate the aerodynamical coefficient of the missile, which is based on the AIM-9 Sidewinder geometry [15], [22], [23]. Instead of conducting a wind tunnel experiment, computational fluid dynamics (CFD) simulation or utilizing tools such as Missile DATCOM, aerodynamical behaviours was approximated by this polynomial model sourced from existing literature. This polynomial model for aerodynamical coefficients (C_x, C_z, C_m) is represented as the functions of key flight parameters, including Mach number, angle of attack, pitch rate, and fin deflection (M, α, q, δ_e). By applying established model, it was possible to avoid direct aerodynamical analysis while still achieving a realistic representation of the missile's aerodynamical characteristics, which is suitable for guidance, navigation and control (GNC) analysis conducted in this study. With this polynomial representation, the aerodynamical forces and moments acting on the missile throughout its flight envelope can be calculated easily and accurately [11], [15], [16]. The polynomial representation of the coefficients is:

$$C_x = a_a , \quad (3.49)$$

$$C_z = a_n \alpha^3 + b_n \alpha |\alpha| + c_n \left(2 - \frac{M}{3}\right) \alpha + d_n \delta_e , \quad (3.50)$$

$$C_m = a_m \alpha^3 + b_m \alpha |\alpha| + c_m \left(-7 + \frac{8M}{3}\right) \alpha + d_m \delta_e + e_m q . \quad (3.51)$$

Where The polynomial coefficients are summarized in Table 3.1:

Table 3. 1: Aerodynamical Polynomial Coefficient

Normal Force	Pitch Moment
$a_n = 19.373$	$a_m = 40.44$
$b_n = -31.023$	$b_m = -64.015$
$c_n = -9.717$	$c_m = 2.922$
$d_n = -1.948$	$d_m = -11.803$
$a_a = -0.3$	$e_m = -1.719$

Using this polynomial aerodynamical model, lookup tables have been created for each aero dynamical coefficient by defining the working range for Mach number (M) from 2 to 4 in the increments of 0.5 and the angle of attack (α) from -20 to 20 in the increment of 1. This tables include the calculated data for aerodynamical coefficients for each combination of M and α within the specified ranges. The figures 3.3 - 3.5 shows the variation of aerodynamical coefficients for this Mach number (M) and angle of attack (α) ranges.

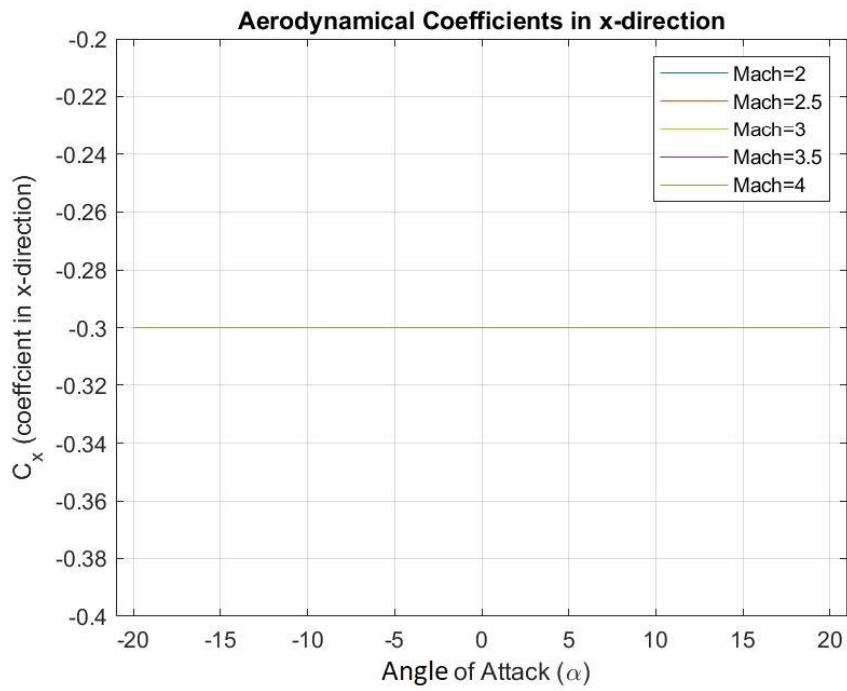


Figure 3. 3: Aerodynamical Coefficients Plot in x-direction

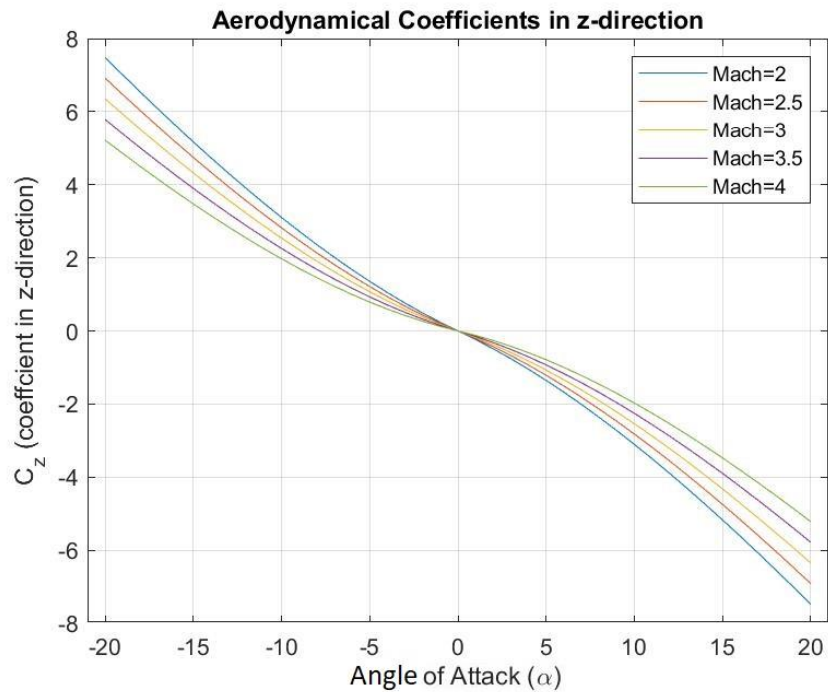


Figure 3. 4: Aerodynamical Coefficients Plot in z-direction

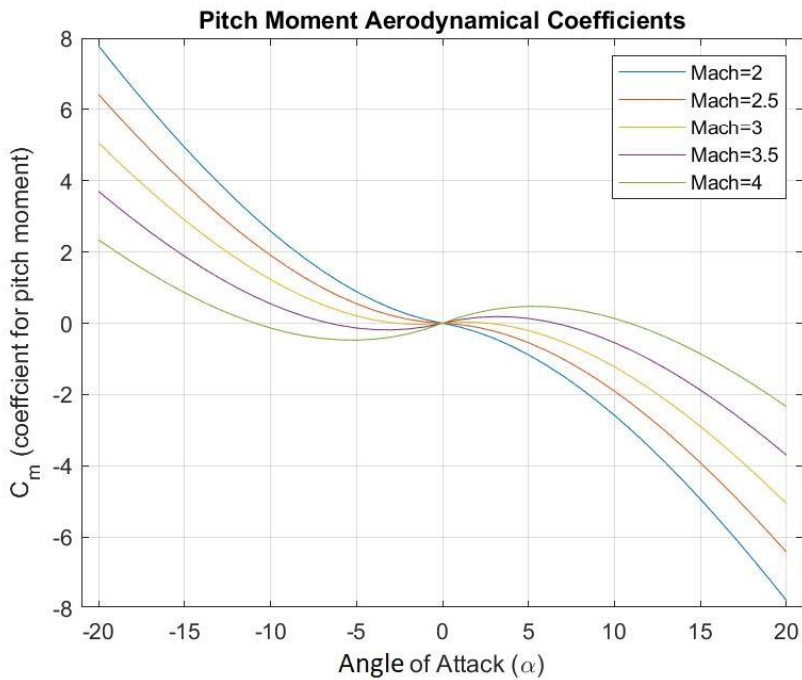


Figure 3. 5: Aerodynamical Pitch Moment Coefficients Plot

3.3 Model Characteristics and Configuration

The model characteristics of the missile are composed of various different physical parameters, which are critical to the aerodynamical performance and structural design of the missile. One of the key physical parameters is surface area (S), which is determined by the length (l) and the diameter (d_{ref}) of the missile, and has a great effect on the missile's drag, lift and stability. The other one is that moment of inertia (I_{yy}), which indicates the resistance of the missile in the rotational motion and has an influence on manoeuvrability and control. Additionally, the missile's working range is defined by the Mach Number (2 to 4) and angle of attack (-20 to 20), and aerodynamical coefficients have been calculated and validated for this flight envelope.

Table 3. 2: Physical Characteristics of the missile. [15]

Symbol	Name	Value
S	Reference Area	0.0409 m^2
d_{ref}	Reference Diameter	0.2286 m
l	Length	3.02 m
I_{yy}	Moment of Inertia	247.44 kgm^2
m	Mass	204.023 kg
g	Gravity	$9.81 \frac{\text{kg m}}{\text{s}^2}$

As missile configuration, it has four fins and canards as it seen in figure down below (fig 3.6). Canards are located at the front of the missile and they have a triangular shape, while fins are located at the end of the missile and they have a trapezoidal shape. All canards and fins are located at the same direction.



Figure 3. 6: AIM9-Sidewinder Missile [24].

3.4 Linearization

The missile model, which is used in this study, is a non-linear model with a single input and single output. Thus, a linear model is derived besides the non-linear model in order to decrease the complexity of the controller design and make the stability analysis possible. Therefore, using Taylor series expansion, the nonlinear equations are linearized by using steady level flight assumption [19], [25]. The linear model is only valid in the vicinity of an equilibrium point, but this point is a very small margin for the missile because of fast dynamical changes [25]. Using plenty of equilibrium points, the linear model's response and stability can be checked. In order to make the linearization possible, the nonlinear equation of motions (3.39), (3.40), (3.41), (3.42) are used.

The variables of the trim conditions are $u = u_0, w = w_0, \theta = \theta_0, \dot{u} = \dot{w} = \dot{q} = 0, q_0 = 0, \Delta q = q, \Delta \dot{q} = \dot{q}, \alpha \neq 0, \theta \neq 0$.

Linearization of equation of motions, using Taylor series expansion [19], [25] (see Appendix A) :

$$\Delta \dot{u} = \frac{\Delta X}{m} - w_0 q - g \cos \theta_0 \Delta \theta, \quad (3.52)$$

$$\Delta \dot{w} = \frac{\Delta Z}{m} + u_0 \Delta q - g \sin \theta_0 \Delta \theta, \quad (3.53)$$

$$\Delta \dot{q} = \frac{\Delta M}{I_{yy}}, \quad (3.54)$$

$$\Delta \dot{\theta} = \Delta q. \quad (3.55)$$

In the steady state assumption, the angle of attack (α) and pitch angle (θ) is small, so small angle assumption is used to further simplify the linearized equations (3.52), (3.53).

$$\Delta \dot{u} = \frac{\Delta X}{m} - g \Delta \theta, \quad (3.56)$$

$$\dot{\alpha} = \frac{\Delta Z}{m} + \Delta q. \quad (3.57)$$

These aero propulsive forces are functions of u, w, q, α, θ , and δ_c , so they need to be expanded and written in terms of these variables. Additionally, in the condition of pitching missile only control variable δ_c is the elevator, so it can be represented as δ_e . As a result, these forces are expressed as [10]:

$$\Delta X = X_u \Delta u + X_\alpha \Delta \alpha + X_{\delta_e} \Delta \delta_e \quad (3.58)$$

$$\Delta Z = \frac{Z_u}{V} \Delta u + \frac{Z_\alpha}{V} \Delta \alpha + Z_{\delta_e} \Delta \delta_e \quad (3.59)$$

$$\Delta M = M_u \Delta u + M_\alpha \Delta \alpha + M_q \Delta q + M_{\delta_e} \Delta \delta_e \quad (3.60)$$

By putting these equations into the previous equations ,which are eq. 3.54, 3.55, 3.56, 3.57, updated linearized version can be obtained as [10] :

$$\Delta \dot{u} = \frac{X_u}{m} \Delta u + \frac{X_\alpha}{m} \Delta \alpha + \frac{X_{\delta_e}}{m} \Delta \delta_e - g \Delta \theta, \quad (3.61)$$

$$\Delta\dot{\alpha} = \frac{z_u}{mV} \Delta u + \frac{z_\alpha}{mV} \Delta\alpha + \frac{z_{\delta_e}}{mV} \Delta\delta_e + \Delta q, \quad (3.62)$$

$$\Delta\dot{q} = \dot{q} = \frac{M_u}{I_{yy}} \Delta u + \frac{M_\alpha}{I_{yy}} \Delta\alpha + \frac{M_q}{I_{yy}} \Delta q + \frac{M_{\delta_e}}{I_{yy}} \Delta\delta_e, \quad (3.63)$$

$$\Delta\dot{\theta} = \Delta q. \quad (3.64)$$

$$\begin{aligned} X_u &= \frac{\partial X}{\partial u}, X_\alpha = \frac{\partial X}{\partial \alpha}, Z_u = \frac{\partial Z}{\partial u}, Z_\alpha = \frac{\partial Z}{\partial \alpha}, M_u = \frac{\partial M}{\partial u} \\ M_\alpha &= \frac{\partial M}{\partial \alpha}, M_q = \frac{\partial M}{\partial q}, X_{\delta_e} = \frac{\partial X}{\partial \delta_e}, Z_{\delta_e} = \frac{\partial Z}{\partial \delta_e}, M_{\delta_e} = \frac{\partial M}{\partial \delta_e} \end{aligned} \quad (3.65)$$

In this linearized equations of motion, step size or delta (Δ) values are determined by considering small perturbations, often ranging between 0.1% and 1% of the state variables, around the trim point. Expanding the nonlinear equations around the trim point, and keeping the first order terms, which are proportional to these small deviations. Therefore, the choice of the step size is crucial, as it must be sufficiently small to ensure the higher order terms can be neglected to accurately approximate the nonlinear model with linearized one. The appropriate step size is often determined empirically or based on the sensitivity of the system to perturbations, ensuring the linear model remains valid [10], [19], [25]. These linearized equations can be represented in the matrix form to obtain the state space representation. In this case, the state vector become as $[\Delta u \ \Delta\alpha \ q \ \Delta\theta]^T$.

3.4.1 State Space

The obtained linearized equations are represented in the matrix form to obtain the state space, which is a state of dynamical set of physical quantities. State space has a representation of:

$$\dot{x} = Ax + Bu , \quad (3.66)$$

$$y = Cx + Du . \quad (3.67)$$

In this representation, x represents the state vector, u is the input, and y is the output. A is the state matrix, B is the input matrix, C is the output matrix, and D is the feedthrough matrix [14], [19], [25].

In many cases the coupling of the change in the velocity Δu normal to the longitudinal axis into the equations for angle of attack (α) and pitch rate (q) is negligible, so X_u, Z_u, M_u are insignificant. Additionally, the pitch angle usually not of interest, hence the differential equation $\dot{\theta} = q$ can be omitted [10]. In this case the equation 3.62 and 3.63 are further simplified as:

$$\Delta\dot{\alpha} = \frac{Z_\alpha}{mV} \Delta\alpha + \frac{Z_{\delta_e}}{mV} \Delta\delta_e + \Delta q , \quad (3.68)$$

$$\dot{q} = \frac{M_\alpha}{I_{yy}} \Delta\alpha + \frac{M_q}{I_{yy}} \Delta q + \frac{M_{\delta_e}}{I_{yy}} \Delta\delta_e . \quad (3.69)$$

In these equations δ_e is the control input, which is elevator deflection. On the other hand, the output is dependent on the missile guidance laws which are generally

expressed in terms of the component of acceleration normal to the velocity vector of the missile, in proportional navigation, for example, it is desired that this acceleration is to be proportional to the initial line-of-sight rate. As a result, the output of interest in a typical missile is the normal component of the acceleration a_N [10]. In the planar case:

$$a_N \cong -V\dot{\gamma}, \quad (3.68)$$

Where γ is the flight path angle and V is the missile velocity. However, $\gamma = \theta - \alpha$, so $\dot{\gamma} = q - \dot{\alpha}$. Therefore, the normal acceleration can be expressed as:

$$a_N \cong Z_\alpha \alpha + Z_{\delta_e} \delta_e, \quad (3.69)$$

Using this algorithm to the final linearization equation, this form is obtained:

$$x = [\Delta\alpha \ q]^T, \quad (3.70)$$

$$A = \begin{bmatrix} \frac{Z_\alpha}{mV} & 1 \\ \frac{M_\alpha}{I_y} & \frac{M_q}{I_y} \end{bmatrix}, \quad (3.71)$$

$$B = \begin{bmatrix} \frac{Z_{\delta_e}}{mV} \\ \frac{M_{\delta_e}}{I_y} \end{bmatrix}, \quad (3.72)$$

$$u = \delta_e, y = a_N \text{ and } q , \quad (3.73)$$

$$C = \begin{bmatrix} Z_\alpha & 0 \\ 0 & 1 \end{bmatrix}, \quad (3.74)$$

$$D = \begin{bmatrix} Z_{\delta_e} \\ 0 \end{bmatrix}. \quad (3.75)$$

The transfer function (H_1) from input $u = \delta_e$ to the output $y = a_N$ is given by:

$$H_1(s) = C(sI - A)^{-1}B + D \quad (3.76)$$

$$H_1(s) = [Z_\alpha 0] \begin{bmatrix} s - \frac{Z_\alpha}{mV} & -1 \\ -\frac{M_\alpha}{I_y} & s - \frac{M_q}{I_y} \end{bmatrix}^{-1} \begin{bmatrix} \frac{Z_{\delta_e}}{mV} \\ \frac{M_{\delta_e}}{I_y} \end{bmatrix} + Z_{\delta_e} \quad (3.77)$$

$$H_1(s) = \frac{Z_\alpha \left(\left(s - \frac{M_q}{I_y} \right) \frac{Z_{\delta_e}}{mV} + \frac{M_\alpha}{I_y} \frac{M_{\delta_e}}{I_y} \right)}{\left(s - \frac{Z_\alpha}{mV} \right) \left(s - \frac{M_q}{I_y} \right) - \frac{M_\alpha}{I_y}} + Z_{\delta_e} \quad (3.78)$$

The transfer function (H_2) from input $u = \delta_e$ to the output $y = q$ is given by:

$$H_2(s) = [1 \ 0] \begin{bmatrix} s - \frac{Z_\alpha}{mV} & -1 \\ -\frac{M_\alpha}{I_y} & s - \frac{M_q}{I_y} \end{bmatrix}^{-1} \begin{bmatrix} \frac{Z_{\delta_e}}{mV} \\ \frac{M_{\delta_e}}{I_y} \end{bmatrix} \quad (3.79)$$

$$H_2(s) = \frac{\left(s - \frac{M_q}{I_y} \right) \frac{Z_{\delta_e}}{mV} + \frac{M_\alpha}{I_y} \frac{M_{\delta_e}}{I_y}}{\left(s - \frac{Z_\alpha}{mV} \right) \left(s - \frac{M_q}{I_y} \right) - \frac{M_\alpha}{I_y}} \quad (3.80)$$

3.4.2 Aerodynamic Stability Derivatives

The aerodynamical derivatives, represented at eq. 3.65, are known as aerodynamic stability derivatives, and they are most often obtained through experiments or CFD analysis. However, there is a way to calculate these derivatives, and this method is called an empirical method. In this method, forces and moments partial derivatives are taken, and aerodynamical stability derivatives can be obtained by applying a trim condition [19], [26] (see Appendix B).

Aerodynamical forces and moments:

$$X = \frac{1}{2} \rho V^2 S(C_x) \quad (3.46)$$

$$Z = \frac{1}{2} \rho V^2 S(C_z) \quad (3.47)$$

$$M = \frac{1}{2} \rho V^2 S d_{ref}(C_m) \quad (3.48)$$

Where

Table 3. 3: Aerodynamical Equations Parameters

Parameter	Explanation
ρ (kg/m^3)	Air density
V (m/s^2)	Velocity of the missile
δ_e (rad)	Fin deflection of the missile
a (m/s)	Speed of sound
M	Mach number
C_x	Aerodynamical coefficient of missile in x direction
$C_z(\alpha, M, \delta_e)$	Aerodynamical coefficient of missile in z direction where it is function of angle of attack ,Mach number and fin deflection(δ_e).
$C_m(\alpha, M, \delta_e, q)$	Pitch moment coefficient of missile where it is function of angle of attack, Mach number, fin deflection (δ_e) and pitch rate (q) .

Table 3. 4: Aerodynamical Stability Derivative Equations

	X	Z	M
u	$\rho V_0 \cos\theta_0 S C_{x_0}$	$\frac{1}{2} \rho V_0^2 S \left(\frac{\partial C_z}{\partial \alpha} \Big _{M_0} \cdot \frac{w_0}{V_0^2} + \frac{\partial C_z}{\partial M} \Big _{\alpha_0} \cdot \frac{u_0}{aV_0} \right)$ $+ \rho V_0 \cos\theta_0 S (C_{z_0})$	$\frac{1}{2} \rho V_0^2 S d_{ref} \left(\frac{\partial C_m}{\partial \alpha} \Big _{M_0} \cdot \frac{w_0}{V_0^2} + \frac{\partial C_m}{\partial M} \Big _{\alpha_0} \cdot \frac{u_0}{aV_0} \right)$ $+ \rho V_0 \cos\theta_0 S d_{ref} (C_{m_0})$
α	0	$\frac{1}{2} \rho V_0^2 S \left(\frac{\partial C_z}{\partial \alpha} \Big _{M_0} \right)$	$M_\alpha = \frac{1}{2} \rho V_0^2 S d_{ref} \left(\frac{\partial C_m}{\partial \alpha} \Big _{M_0} \right)$
q	0	0	$\frac{1}{2} \rho V_0^2 S d_{ref} (C_{m_q})$
δ_e	0	$\frac{1}{2} \rho V_0^2 S C_{z_{\delta_e}}$	$\frac{1}{2} \rho V_0^2 S d_{ref} C_{m_{\delta_e}}$

3.5 Numerical Example of Linearization in a Trim Point

In this part, a numerical example of the linearization is done and represented in state space form. In order to do the linearization, a trim condition is needed to be found under the assumption of a steady level flight where there is no acceleration or altitude gain. In order to find the trim angle of attack (α_{trim}) equation of motion need to be solved for the specified Mach number which is $M = 3$.

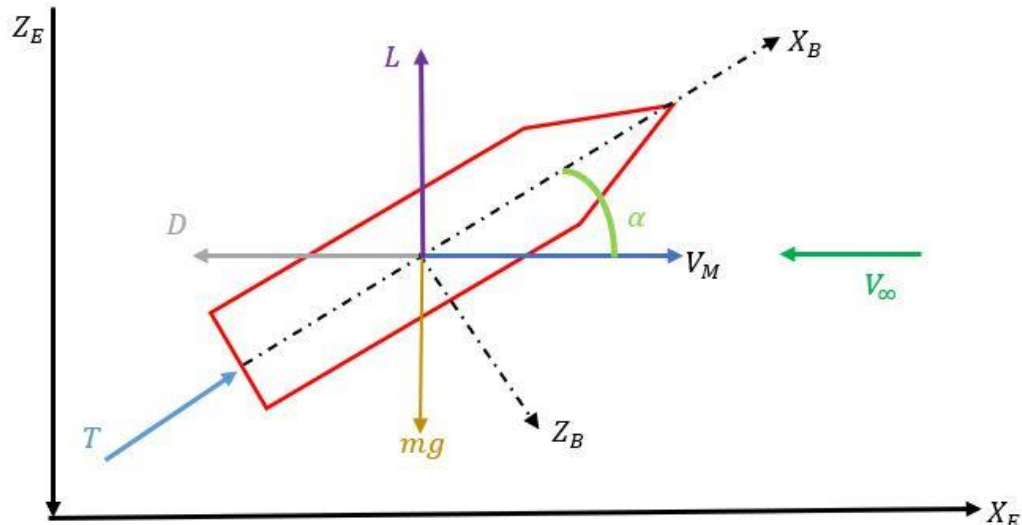


Figure 3. 7: Forces acting on the missile model.

Sum of the forces in z-direction must be equal to the zero at the trim condition. Additionally, there is no fin deflection ($\delta_e = 0^\circ$) and thrust force (T) is constant throughout the flight. Before getting to the calculation, atmospheric and missile parameters are needed which are represented in the table (Table 3.5) down below.

Table 3. 5: Numerical parameters for linearization.

Parameters	Numerical Values
M_0	3
a	328 m/s
m	204.0277 kg
S	0.0409 m ²
ρ	0.9 kg/m ³
g	9.81 kgm/s ²
T	10000 N

Using these parameters and equilibrium equation in z-direction, angle of attack for trim (α_{trim}) can be calculated as:

$$mg = L + T \sin(\alpha_{trim}), \quad (3.81)$$

$$L = \frac{1}{2} \rho V^2 S(C_z), \quad (3.82)$$

Where aerodynamical coefficient in z direction (C_z) is:

$$C_z = 19.373\alpha^3 + 31.0230\alpha^2 - 9.717\left(2 - \frac{M}{3}\right)\alpha, \quad (3.83)$$

$$204.0277 \times 9.81 = 10000 \times \sin(\alpha_{trim}) + 0.5 \times 0.9 \times (3 \times 328)^2 \times 0.0409 \times \\ (19.373\alpha_{trim}^3 + 31.0230\alpha_{trim}^2 - 9.717\left(2 - \frac{M}{3}\right)\alpha_{trim}), \quad (3.84)$$

$$\alpha_{trim} = -0.01180 \text{ rad} = -0.68^\circ. \quad (3.85)$$

Using these parameters, state space representation of the linearized model can be obtained at the trim point ($\alpha_0 = -0.68^\circ, M = 3$) as :

$$\begin{bmatrix} \dot{\alpha} \\ \dot{q} \end{bmatrix} = \begin{bmatrix} -0.9268 & 1 \\ 23.5127 & -28.3014 \end{bmatrix} \begin{bmatrix} \Delta\alpha \\ q \end{bmatrix} + \begin{bmatrix} -0.1729 \\ -194.3232 \end{bmatrix} [\Delta\delta_e], \quad (3.86)$$

$$\begin{bmatrix} a_N \\ q \end{bmatrix} = \begin{bmatrix} Z_\alpha & 0 \\ 0 & 1 \end{bmatrix} \begin{bmatrix} \alpha \\ q \end{bmatrix} + \begin{bmatrix} Z_{\delta_e} \\ 0 \end{bmatrix}. \quad (3.87)$$

3.6 Actuator Model

The actuator is a mechanical component, i.e. a small engine, that takes an input signal and converts it to the physical action. Actuators in missiles are the responsible components for moving or controlling the control surfaces, such as fins, by using the input signal [1], [2]. In this missile model, a second-order nonlinear actuator model is used in order to reflect the real-world behaviour of the actuators, including effects such as saturation and rate limits. In the figure down (Figure 3.8) the actuator model block diagram is given:

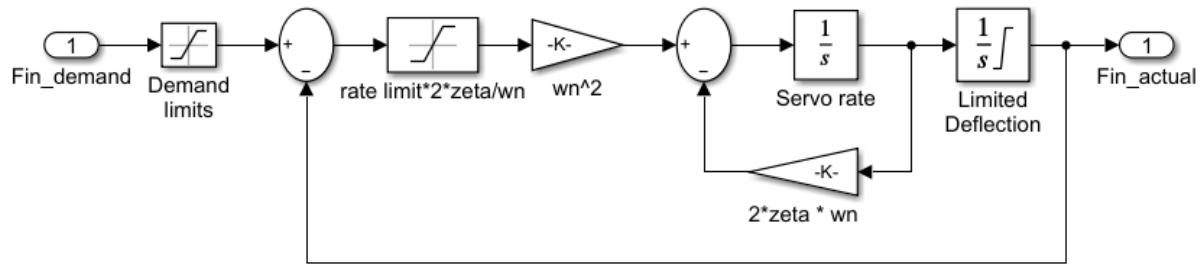


Figure 3. 8: Actuator model block diagram.

Mathematical representation of the actuator model:

$$\ddot{\delta}_e + 2\zeta\omega_n\dot{\delta}_e + \omega_n^2\delta_e = \omega_n^2\delta_{e_{dem}}, \quad (3.88)$$

Where

Table 3. 6: Actuator parameters.

Parameters	Explanation
δ_e	Actual elevator deflection
$\delta_{e_{dem}}$	Demanded elevator deflection
ω_n	Natural frequency of the actuator
ζ	Damping ratio
$\delta_{e_{max}}$	Maximum elevator deflection
$\dot{\delta}_{e_{max}}$	Maximum elevator rate

In this actuator model used numerical values are:

$$\begin{aligned}\omega_n &= 150 \text{ Hz} \\ \zeta &= 0.7 \\ \delta_{e_{max}} &= \pm 30^\circ \\ \dot{\delta}_{e_{max}} &= 500^\circ/\text{s}\end{aligned}\tag{3.89}$$

3.7 Atmosphere Model

The atmosphere model provides the speed of sound (a) and air density (ρ) using the altitude, which is actually the height difference from the sea level and calculates continuously as the altitude changes [14], [21]. These parameters are expressed mathematically as:

Table 3. 7: Atmosphere model parameters.

Parameters with Numerical Values	Explanation
$\rho_0 = 1.225 \text{ kg/m}^3$	Sea-level standard density
$L = 0.0065 \text{ K/m}$	Temperature lapse rate
$h \text{ (m)}$	Altitude
$T_0 = 288.15 \text{ K}$	Sea-level standard temperature
$T \text{ (K)}$	Temperature at altitude h
$g = 9.81 \text{ m/s}^2$	Gravitational acceleration
$R = 287.05 \text{ J/kgK}$	Specific gas constant
$\gamma = 1.4$	Heat capacity ratio

$$\text{Air density: } \rho = \rho_0 \left(1 - \frac{Lh}{T_0}\right)^{\frac{g}{RL}-1} \quad (3.90)$$

$$\text{Temperature: } T = T_0 - Lh \quad (3.91)$$

$$\text{Speed of sound: } a = \sqrt{\gamma RT} = \sqrt{\gamma R(T_0 - Lh)} \quad (3.)$$

CHAPTER 4

GUIDANCE NAVIGATION AND CONTROL ALGORITHMS

This section describes the fundamental aspects of designing the guidance, navigation and control algorithms of an air-to-air missile, which is launched either from a fighter jet or a carrier. It also explains the mathematics behind these algorithms. At the beginning, a missile target interception scenario was described in order to be able to design the GNC algorithm. After that, the navigation system algorithm, which is used in the missile system, is explained. Three navigational guidance algorithms and their maths are processed with their open loop responses according to the fin deflections. Lastly, controller design is handled, and their mathematical algorithms are given with their block diagrams.

4.1 Missile Target Interception Scenario

In order to create a working guidance navigation and control algorithm (GNC), first of all a scenario has to be created. The scenario discussed in this article is formatted as follows: there is a target which flies at a constant altitude with constant speed towards the missile with initial separation in x and z directions. The main objective in this scenario is to create a GNC system for the missile to eliminate the altitude difference between the missile and target in the shortest time and distance and ensure missile target interception, as shown in Fig 4.1.

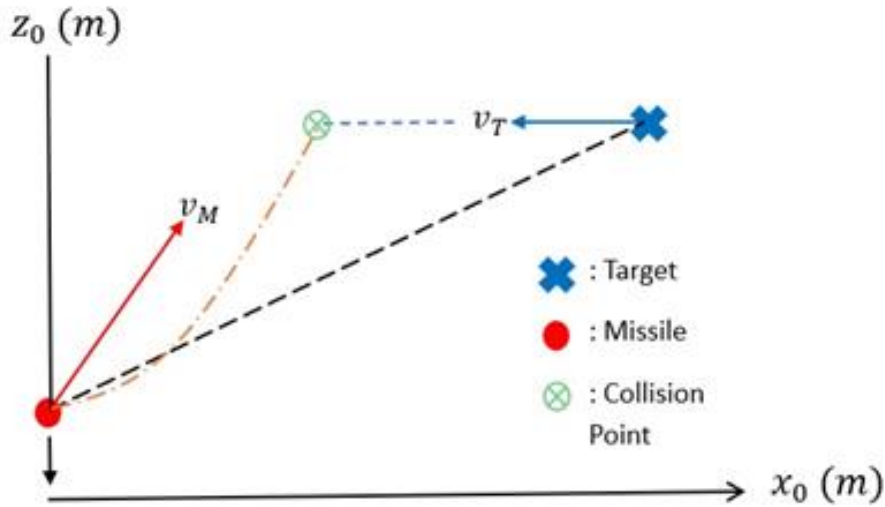


Figure 4. 1: Missile Target Interception Scenario

4.2 Guidance Navigation and Controller Algorithms

GNC algorithm is the most crucial system of the missile in order to have a successful missile and target interception [1], [2]. Different from the literature review, in this section, GNC, which is used for the designing of the missile, and the maths behind each component is expressed.

4.2.1 Navigation System

In designing the guidance, navigation, and control algorithms for the missile, the navigation system plays a vital role. In the missile designed for the simulations, the INS is used to accurately measure accelerations and pitch rates by using accelerometers and gyroscopes. Processing this initial data, the system determines the missile's position and velocity in real-time. These crucial parameters are then fed into the

navigational guidance subsystem, which uses them as inputs to continuously update and refine the missile's trajectory to enable missile target interception with high accuracy [1], [2], [4]. Thus, the INS system is the foundation of the GNC algorithm with robustness and reliability.

4.2.2 Navigational Guidance

There are various navigational guidance algorithms that are used in the GNC systems, and one of the most known ones is Proportional Navigation (PN) [2]. For this missile's GNC system, three Proportional Navigation with different algorithms are used, and in the upcoming part of the paper, the algorithms for each navigation are investigated, and open loop results are presented. In addition, according to the results, a comparison will be made among their performance, reliability, effectiveness and robustness in the comparison section. The figure below, which contains important parameters, shows the scenario of the missile target interception, which is used in the design of navigation algorithms.

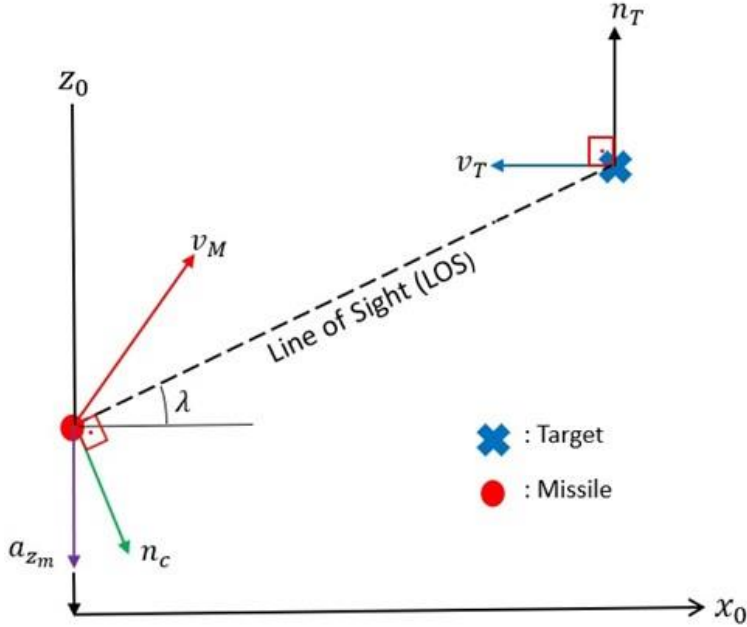


Figure 4. 2: Missile Target Interception Scenario with Parameters

4.2.2.1 Proportional Navigation

Proportional navigation guidance law provides acceleration directives that are orthogonal to the instantaneous line-of-sight between the missile and target, which is proportional to the line-of-sight rate and closing velocity [2]. Additionally, for this navigation to work correctly, the initial location of the target must be known. Mathematically the proportional navigation guidance can be shown as:

$$n_c = N' V_c \dot{\lambda}, \quad (4.1)$$

where n_c is the acceleration command which is instantly perpendicular to the line of sight and has a unit of m/s^2 . N' is a constant chosen by the designer, which is known

as an effective navigation ratio and has a value between 3-5 usually. V_c is the closing velocity between missile and target in m/s . λ is the line of sight angle in degree and $\dot{\lambda}$ is the rate of change in the line of sight angle. V_c and $\dot{\lambda}$ need to be calculated in order to calculate n_c . Table 4.1 presents the proportional navigation parameters that is used in the calculation of the demanded acceleration [2]:

Table 4. 1: Proportional Navigation Parameters

Parameters	Explanation
V_T	Target velocity (m/s)
V_{T_x}, V_{T_z}	Target velocity in x and z directions (m/s)
V_{M_x}, V_{M_z}	Missile velocity in x and z-directions (m/s)
V_{TM_x}, V_{TM_z}	Relative velocity components in x and z directions (m)
R_{T_x}, R_{T_z}	Target position with respect to the inertial reference frame (m)
R_{M_x}, R_{M_z}	Missile position with respect to the inertial reference frame (m)
R_{TM_x}, R_{TM_z}	Relative distance components in x and z directions (m)
R	Relative separation magnitude (m)
λ	Line of sight angle ($^\circ$)
$\dot{\lambda}$	Line of sight rate ($^\circ/s$)
V_c	Closing velocity (m/s)
n_c	Missile guidance command (m/s^2)
a_{z_d}	Demanded acceleration (m/s^2)

$$\text{Relative velocity in x- direction: } V_{TM_x} = V_{T_x} - V_{M_x}, \quad (4.2)$$

$$\text{Relative velocity in z- direction: } V_{TM_z} = V_{T_z} - V_{M_z}, \quad (4.3)$$

$$\text{Relative distance in x-direction: } R_{TM_x} = R_{T_x} - R_{M_x}, \quad (4.4)$$

$$\text{Relative distance in z-direction: } R_{TM_z} = R_{T_z} - R_{M_z}, \quad (4.5)$$

$$\text{Relative distance: } R = \sqrt{R_{TM_x}^2 + R_{TM_z}^2}, \quad (4.6)$$

$$\text{Line-of-sight angle: } \lambda = \tan^{-1}(|R_{TM_z}|/R_{TM_x}), \quad (4.7)$$

$$\text{Line-of-sight rate: } \dot{\lambda} = \frac{R_{TM_x} \times V_{TM_z} - R_{TM_z} \times V_{TM_x}}{R^2}, \quad (4.8)$$

$$\text{Closing velocity: } V_c = -(R_{TM_x} \times V_{TM_x} + R_{TM_z} \times V_{TM_z})/R, \quad (4.9)$$

$$\text{Missile guidance command: } n_c = N' V_c \dot{\lambda}, \quad (4.10)$$

$$\text{Demanded acceleration: } a_{z_d} = n_c \cos(\lambda). \quad (4.11)$$

Proportional navigation guidance law provides the demanded acceleration according to the missile and target parameters which is used as an input in the controller to create the desired trajectory to follow and make the missile target interception happen.

4.2.2.2 Proportional Navigation with Zero Effort Miss (ZEM)

Zero effort miss (ZEM) is the miss distance between the missile and the target if there is no further adjustment is made. ZEM is integrated into the proportional navigation, proportional navigation with zero effort miss is obtained. This algorithm aims to minimize the ZEM to zero by adjusting the proportional navigation command continuously to adjust the trajectory of the missile in order to keep the missile on a collision triangle. With this integration, proportional navigation's effectiveness and robustness improve, and interception accuracy increases [2]. Mathematically the proportional navigation with zero effort miss is :

$$\text{Zero effort miss in x- direction : } ZEM_x = R_{TM_x} + V_{TM_x} t_{go}, \quad (4.12)$$

$$\text{Zero effort miss in z- direction : } ZEM_z = R_{TM_z} + V_{TM_z} t_{go}, \quad (4.13)$$

Where t_{go} is the time to go until interception.

$$\text{Zero effort miss perpendicular to LOS: } ZEM_{PLOS} = \frac{t_{go}(R_{TM_x}V_{TM_z} - R_{TM_z}V_{TM_x})}{R}, \quad (4.14)$$

$$\text{Line of sight rate: } \lambda = \frac{ZEM_{PLOS}}{Rt_{go}}, \quad (4.15)$$

$$\text{Relative distance: } R = V_c t_{go}, \quad (4.16)$$

$$\text{Missile guidance command: } n_c = \frac{N' ZEM_{PLOS}}{t_{go}^2}, \quad (4.17)$$

$$\text{Demanded acceleration. } a_{z_d} = n_c \cos(\lambda) . \quad (4.18)$$

Similar to proportional navigation, this algorithm provides the acceleration and creates input commands for the controller.

4.2.2.3 Proportional Navigation + Seeker

Although, it is the same algorithm with the proportional navigation, which was covered previously, there is an additional component added to the navigation guidance algorithm, which is a seeker, that makes the algorithm the most complex among these algorithms. The initial position of the target does not have to be a known cause of the seeker. Seeker is a device integrated into the missile body that works for detecting the target and giving the target's location information to the navigation guidance part of the missile in order to find the desired acceleration to flow the intended path [1]–[3], [15]. Here is both mathematical explanation of the navigation guidance method:

$$\text{Sightline angle : } \theta_s = \tan^{-1}(|R_{TM_z}|/R_{TM_x}) , \quad (4.19)$$

$$\text{Look angle: } \sigma_l = \theta_s - \theta_b , \quad (4.20)$$

$$\text{Dish angle: } \sigma_d = \theta_b + \sigma_g , \quad (4.21)$$

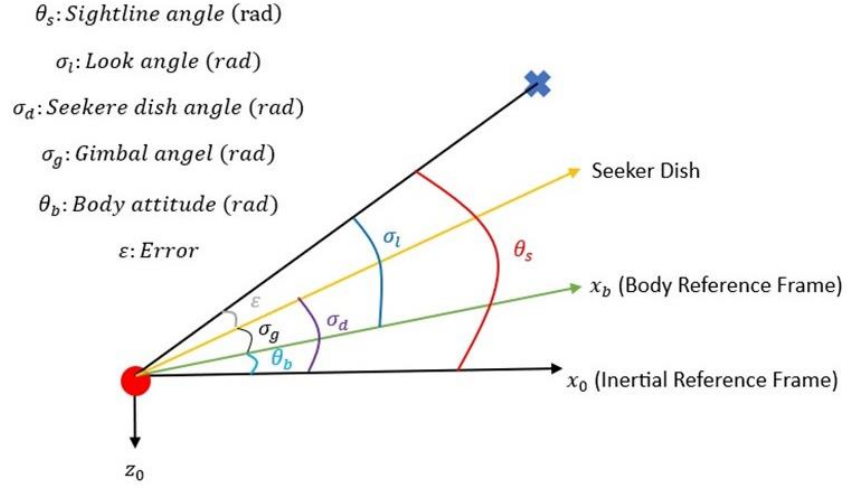


Figure 4. 3: Seeker and Proportional Navigation Angles.

This navigation guidance algorithm has two parts, which are seeker and guidance. The first part is the seeker part, which calculates the line rate of sightline angle with using the equations (4.4), (4.5), (4.6).

$$\text{Closing velocity : } V_c = V_{TM} \times \hat{R}, \quad (4.22)$$

$$\text{Unit vector along LOS : } \hat{R} = \frac{R}{|R|}, \quad (4.23)$$

$$\text{Sightline angle rate : } \dot{\theta}_s = \frac{V_c}{R}, \quad (4.24)$$

The second part, which is the proportional navigation part, is where the desired acceleration is calculated to follow the intended course. This part takes the seeker outputs, which is sightline angle rate, as input and calculates the demanded acceleration.

$$\text{Demand acceleration : } a_{z_d} = N' V_c \dot{\theta}_s = \frac{N' V_c^2}{R}. \quad (4.25)$$

4.2.3 Open Loop Responses of Navigational Guidance Algorithms

After creating the navigation guidance algorithms, several open loop tests have been done in order to find the responses of the algorithms and make comparison between them. Since in the missile model there is only single input, which is fin deflection (δ_e), a step function as an input, which initiates at one second, is used with the final values of -10, 0, and 10 indicating elevator angles as $-10^\circ, 0^\circ, 10^\circ$. Furthermore, while obtaining these results, the designer coefficient (N') for proportional navigation and proportional navigation with zero effort miss is chosen as three (3) while proportional navigation with seeker as three point five (3.5).

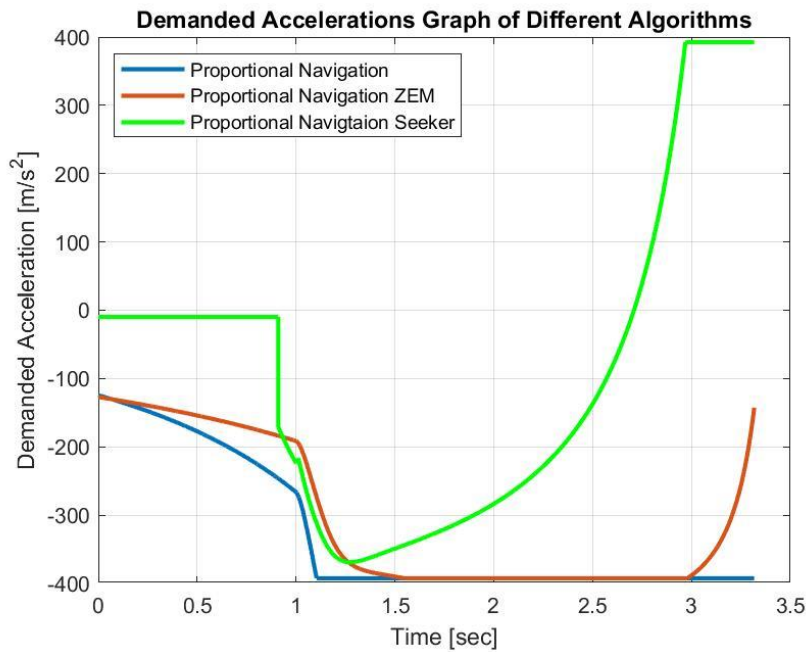


Figure 4. 4: Navigational guidance response of open loop simulation when fin deflection is minus ten degrees.

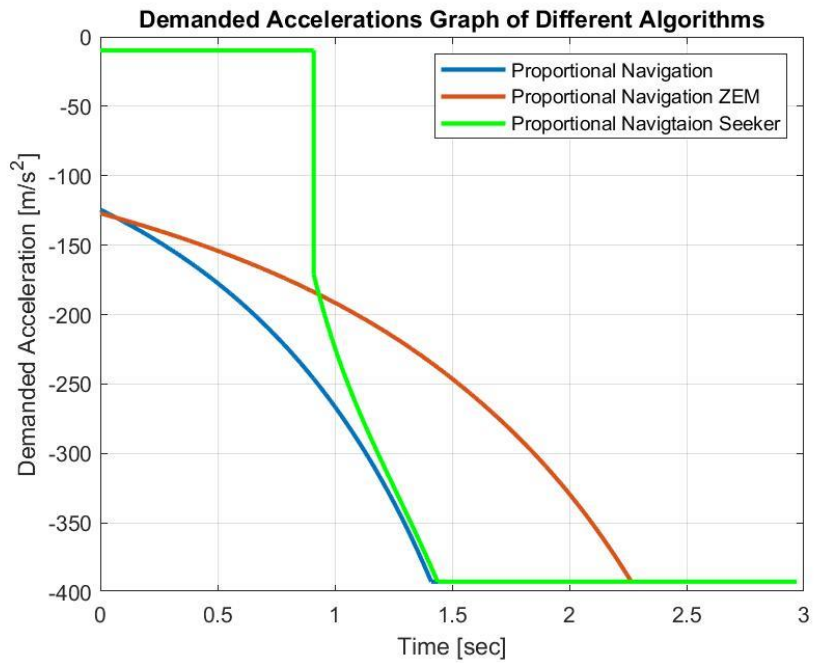


Figure 4. 5: Navigational guidance response of open loop simulation when fin deflection is zero degrees.

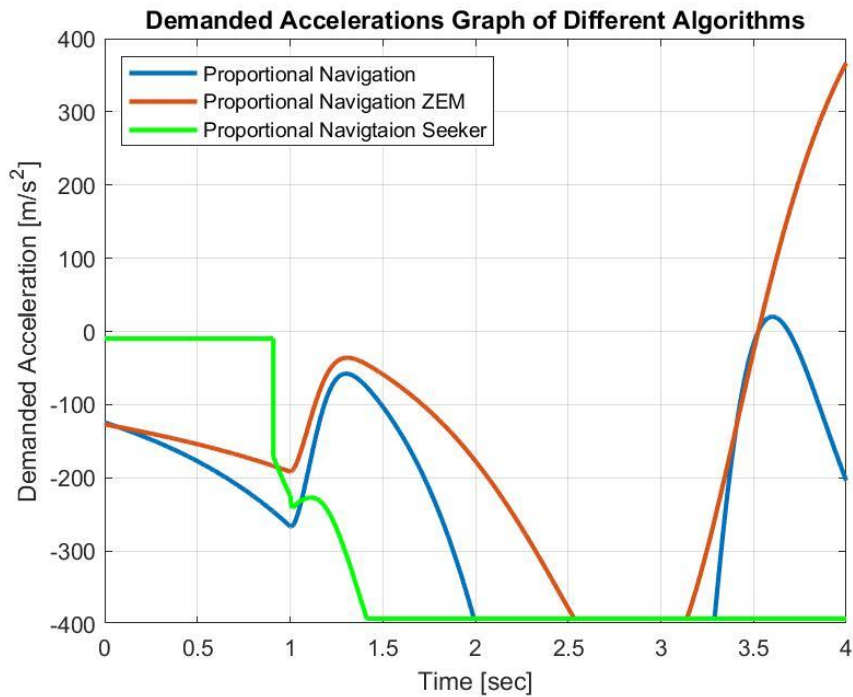


Figure 4. 6: Navigational guidance response of open loop simulation when fin deflection is ten degrees.

The responses show that these algorithms provide different demanded accelerations than each other, but in terms of the trends, it is seen that they have similar behaviour. Moreover, while proportional navigation and proportional navigation with zero effort miss start immediately to provide demanded acceleration, proportional navigation with the seeker is constant until the seeker finds the target, and then it gives the acceleration command.

4.2.4 Controller

The main objective of these controllers is to adjust the fin deflection to guide the interceptor missile along the desired trajectory [3], [4], [10]. In this missile model, a Proportional-Integral-Derivative (PID) controller is used.

4.2.4.1 Proportional Integral Derivative (PID) Controller

PID controller works based on the feedback principle, which aims to increase the actual acceleration when the desired acceleration is higher than the actual one or vice versa. The PID controller has three components which are proportional (P), Integral (I), and Derivative (D) and each has a specific objective for the controller. The Proportional term represents the present and it determines how fast the system responds and represented by the gain K_p . Integral term represents the past and it determines how fast the steady state error eliminated and represented by K_i . Derivative term represents the future by predicting the change to create a faster response and represented by K_d . However, the derivative term (K_d) is not generally used due to the noise creation in the signal, which is cause of oscillation, so instead proportional and

integral terms are used to create PI controller [9], [27], [28]. The figure below represents the block diagram version of the PI controller.

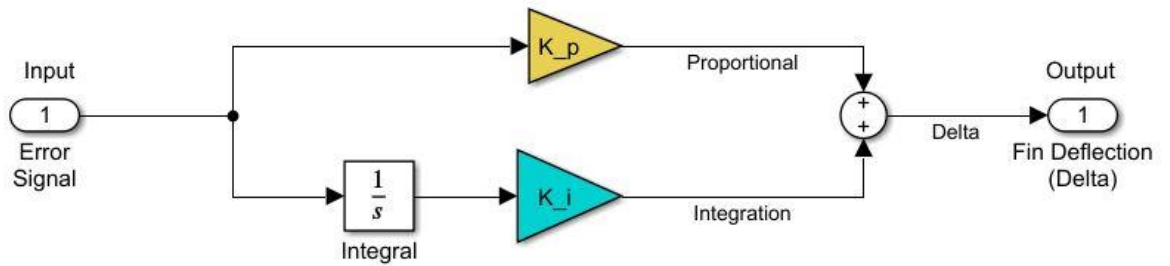


Figure 4. 7: PI Block Diagram

Mathematical representation of a PI controller [10]:

$$\delta_e = K_p e(t) + K_i \int_0^t e(t) dt , \quad (4.26)$$

where δ_e and $e(t)$ represent the fin deflection and error as a function of time, respectively.

The performance of the controller can be improved by using rate feedback [10]. The figure below represents the block diagram version of the PID controller with rate feedback.

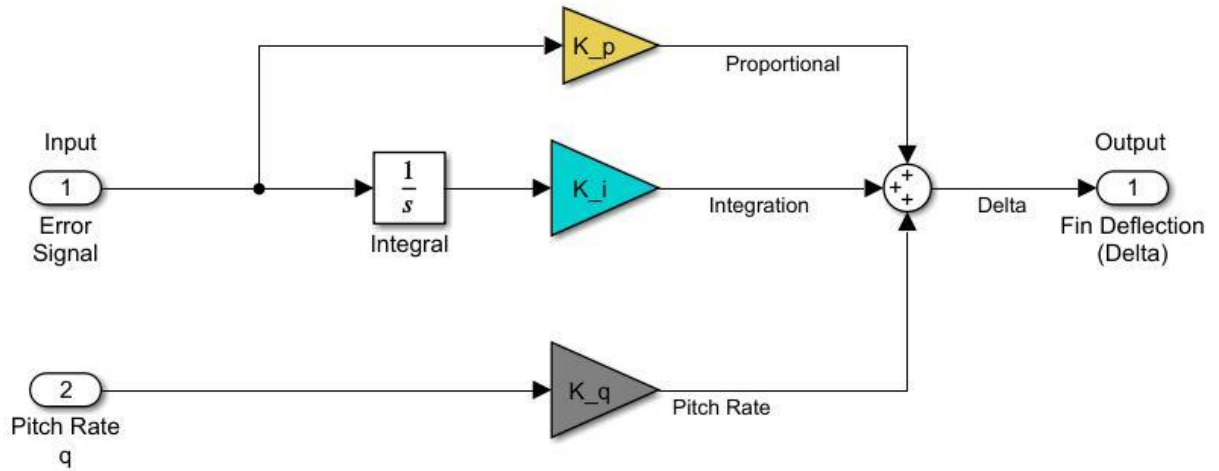


Figure 4. 8: PI block diagram with rate feedback.

The control input is [10]:

$$\delta_e = K_p e(t) + K_i \int_0^t e(t) dt + K_q q . \quad (4.27)$$

where δ_e , $e(t)$, q represents the fin deflection, error as a function of time, and pitch rate respectively.

CHAPTER 5

DYNAMIC MODELLING AND SIMULATION

This section explains the dynamic modelling and simulation analysis for the used air to air missile. The linear model closed loop with the controller is elaborated to find the gains of the controller. The nonlinear missile model closed loop ,which used to obtain the results, is explained detailly.

5.1 Linear Missile Model with a Controller

In this section, the linearized closed loop system with a controller is derived from the previously linearized model in section 3.4. In this closed loop system, the PI controller is implemented as a controller to continuously adjust the control input for the system. The main aim of the closed loop linearized model is to calculate the overall transfer function of the system and use it for the gain calculation of the controller via pole placement. The fig 5.1 represents controller with a linear missile model.

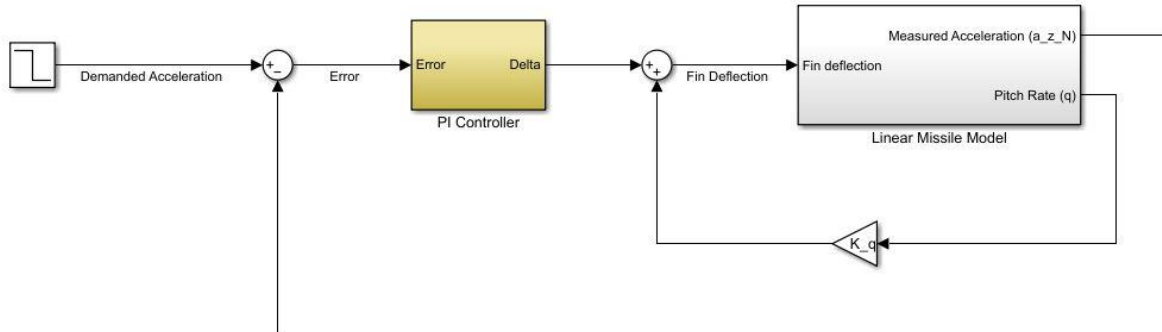


Figure 5. 1: Controller with a linear missle model.

In this block diagram, demanded acceleration is represented as a step function, but in the real case, this input is provided by navigational guidance. State space matrixes are obtained through the linearization at the trim point and used in the linear missile model dynamics to provide measured acceleration and pitch rate.

5.1.1 Overall Transfer Function:

The overall transfer function of the linear missile model closed loop is calculated by the block diagram simplification using the signals. It is needed to be found in order to find the controller gains through a pole placement. In this linearized model there are two transfer function for the linearized model, which one provides the demanded acceleration and the other one provides the pitch rate with the controller transfer function.

Controller Transfer Function :

Controller transfer function is obtained by taking the Laplace of the eq. 4.26.

$$\delta_e = K_p e(t) + K_i \int_0^t e(t) dt, \quad (4.26)$$

$$\frac{\delta_e}{e(s)} = G_c = K_p + \frac{K_i}{s}. \quad (5.1)$$

Measured Acceleration Transfer Function:

This transfer function relates the measured acceleration to the input fin deflection. It is calculated through using the state space matrixes eq. (3.71)(3.72)(3.74)(3.75)

$$G_{a_N}(s) = C(sI - A)^{-1}B + D \quad (5.2)$$

$$G_{a_N}(s) = [Z_\alpha 0] \begin{bmatrix} s - \frac{Z_\alpha}{mV} & -1 \\ -\frac{M_\alpha}{I_y} & s - \frac{M_q}{I_y} \end{bmatrix}^{-1} \begin{bmatrix} Z_{\delta_e} \\ \frac{mV}{M_{\delta_e}} \end{bmatrix} + Z_{\delta_e} \quad (5.3)$$

$$G_{a_N}(s) = \frac{(-I_y V Z_{\delta_e} m)s^2 + (M_q V Z_{\delta_e} m)s + (M_\alpha Z_{\delta_e} - M_{\delta_e} Z_\alpha)}{(-I_y V M)s^2 + (I_y Z_\alpha + M_q V m)s - M_q Z_\alpha + M_\alpha V m} \quad (5.4)$$

Pitch Rate Transfer Function:

This transfer function relates the pitch rate to the input fin deflection. It is calculated through using the state space matrixes eq. (3.71)(3.72))(3.74)(3.75).

$$G_q(s) = C(sI - A)^{-1}B + D \quad (5.5)$$

$$G_q(s) = [1 \ 0] \begin{bmatrix} s - \frac{Z_\alpha}{mV} & -1 \\ -\frac{M_\alpha}{I_y} & s - \frac{M_q}{I_y} \end{bmatrix}^{-1} \begin{bmatrix} \frac{Z_{\delta_e}}{mV} \\ \frac{M_{\delta_e}}{I_y} \end{bmatrix} \quad (5.6)$$

$$G_q(s) = \frac{-(M_{\delta_e}Vm)s + (M_{\delta_e}Z_\alpha - M_\alpha Z_{\delta_e})}{(-I_yVm)s^2 + (I_yZ_\alpha + M_qVm)s + (-M_qZ_\alpha + M_\alpha Vm)} \quad (5.7)$$

Overall Transfer Function:

Using signals, block diagram is simplified to have an overall transfer function which relates the measured acceleration to the demanded acceleration.

$$G_{overall}(s) = \frac{G_c G_{aN}}{1 - K_q G_q + G_c G_{aN}} \quad (5.8)$$

5.1.2 Pole Placement

Pole placement is a method used to assign the closed-loop poles of a system to desired location in the complex s plane. Choosing the poles appropriately, system behaviour can be controlled in terms of stability, damping and response speed [10]. In order to the pole placement, overall transfer function needs to be found at a trim condition, which is $M = 3$ and $\alpha = -0.0118 \text{ rad}$. After applying trim condition to the state matrices transfer functions for measured acceleration and pitch rate is calculated as:

$$G_{aN}(s) = \frac{-34710s^2 - 982500s + 36970000}{s^2 + 29.23s + 2.718} \quad (5.9)$$

$$G_q(s) = \frac{-194.3s - 184.2}{s^2 + 29.23s + 2.718} \quad (5.10)$$

Using the controller transfer function and applying the eq. (5.9)(5.10), overall transfer function is obtained as:

$$G_{overall}(s) = \frac{-34710K_p s^3 - (34710K_i + 982500K_p)s^2 + (-982500K_i + 36970000K_p)s + 36970000K_i}{(1 - 34710K_p)s^3 + (-34710K_i - 982500K_p - 194.3K_q + 29.23)s^2 + (-982500K_i + 36970000K_p - 184.2K_q + 2.718)s + 3.6970000K_i} \quad (5.11)$$

After finding the overall transfer function, poles need to be chosen and they are chosen as $p_1 = -52$, $p_2 = -18$, and $p_3 = -0.7$. Using this poles denominator can be found as:

$$-85.775s^3 - 2986.44s^2 + 77653.38s + 55455 \quad (5.12)$$

Equating this equation to the denominator of the overall transfer function, controller gains can be calculated as:

$$K_p = 0.0025, K_i = 0.015, \text{ and } K_q = 0.2 \quad (5.13)$$

5.2 Nonlinear Model Closed Loop System

The closed-loop system for the three degrees of freedom (3-DOF) nonlinear model, which is handled in chapter 3, is derived. This nonlinear model has been used to build up the closed loop system within the simulation and dynamical modelling environment.

Fig 5.2 represents the nonlinear model:

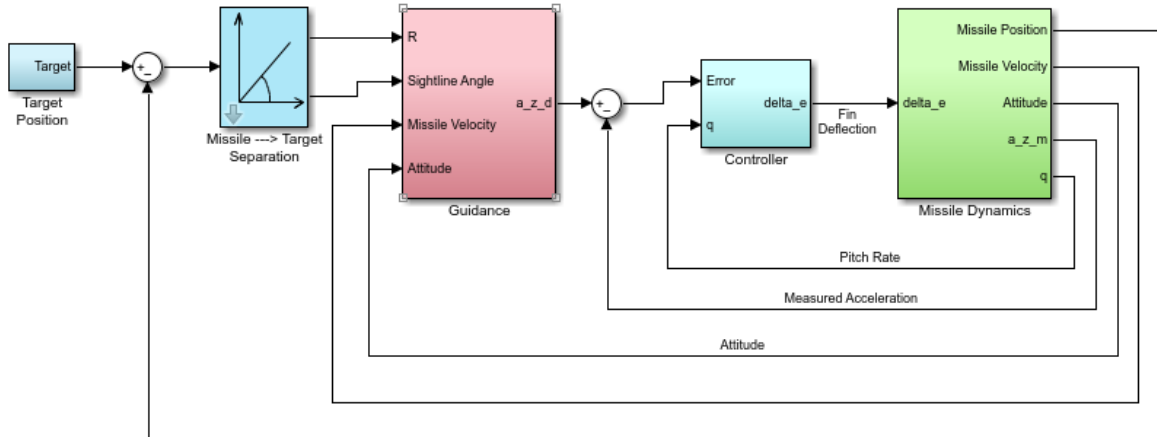


Figure 5. 2: Nonlinear model closed loop block diagram.

In this model subblock diagrams are introduced in the missile dynamics block to enhance the missile model's fidelity. The missile dynamics block, main block, includes nonlinear model equations of the missile, which is discussed in section 3.2 . Target model provides the target position and the speed to calculate the relative distance and line-of-sight angle according to the missile position to be used in the guidance part . In the guidance block, navigational guidance algorithms, elaborated in section 4.2.2, are implemented to obtain the demanded acceleration with the feedback from the missile dynamics block. As a controller, handled in the section 4.2.4, a PI controller with pitch rate feedback is used to calculate the fin deflection (δ_e) that goes to the missile dynamics block as an input.

CHAPTER 6

RESULTS

In this section, the nonlinear model with the guidance navigation and control system integration, which were all handled in the previous chapters, is investigated for multiple different cases to see the nonlinear model system response for different GNC algorithms. Among these cases, three major results are presented, and the rest are used in order to find the limitations of the missile, which will be detailed in the upcoming parts.

During this case simulation, three different guidance navigation and control algorithms are used. In all the algorithms, the navigation and controller parts are the same, but the only part that changes is the navigational guidance part. In all the simulations same controller gains, which are $K_p = 0.0025$, $K_i = 0.015$ and $K_q = 0.2$, are used. After all the simulation results are displayed, the GNC algorithms are compared and discussed. These comparisons and discussions will help to determine the most effective and robust algorithm.

For major cases, different initial conditions are given to both the target and missile for their velocities and positions. Hereby, this will prove that the algorithms work under different conditions. It is shown with different graphs for each algorithm that they work under these conditions.

6.1 Case 1

In this case, the missile and target fly toward each other, and the target is flying at a constant altitude, where it is at a higher altitude than the missile, and speed. The missile's velocity and altitude change according to the GNC algorithm input. The initial separation of target and missile in the x-direction is 4500 meters, while in the z-direction, it is -500 meters. The figure below represents the missile target interception for case one.

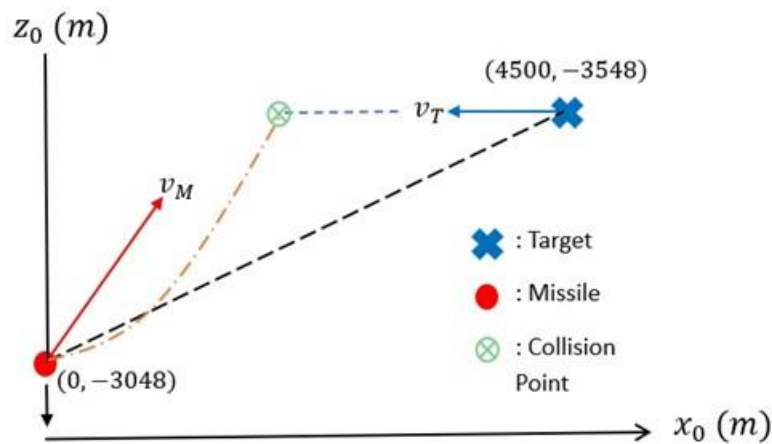


Figure 6. 1: Missile Target interception case one scenario.

Table 6. 1: Numerical parameters for case one.

Parameters	Numerical Values
V_T	328 m/s
X_{sep}	4500 m
Z_{sep}	-500 m

Using these numerical initial conditions and the case one algorithm GNC algorithms are obtained and presented as:

6.1.1 Proportional Navigation + Seeker

Graphical results of the proportional navigation with a seeker for case one is represented in this section .

Figure 6.2 illustrates the missile-target interception instant using the proportional navigation algorithm with a seeker for Case 1.

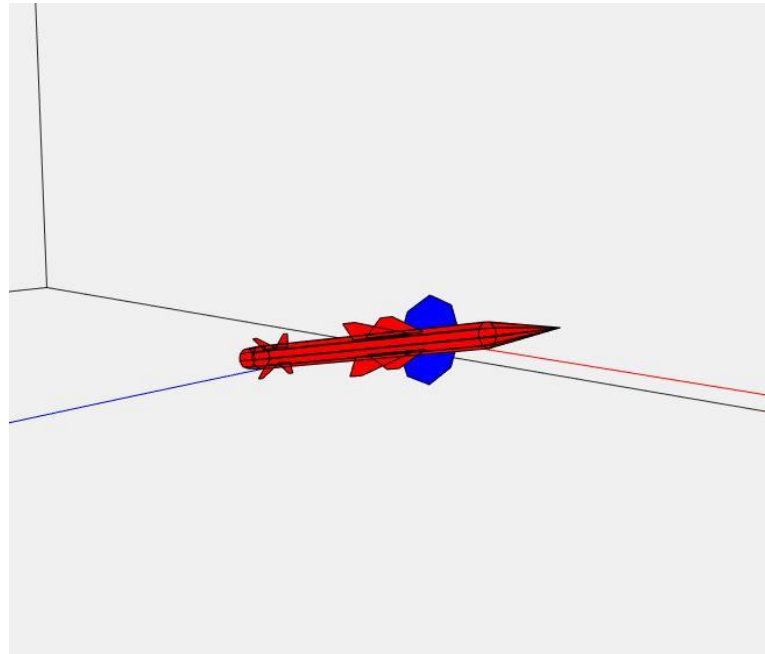


Figure 6. 2: Missile Target Interception Animation.

Fig 6.3 depicts demanded acceleration generated by proportional navigation with a seeker, alongside the measured acceleration from the missile dynamics for Case 1.

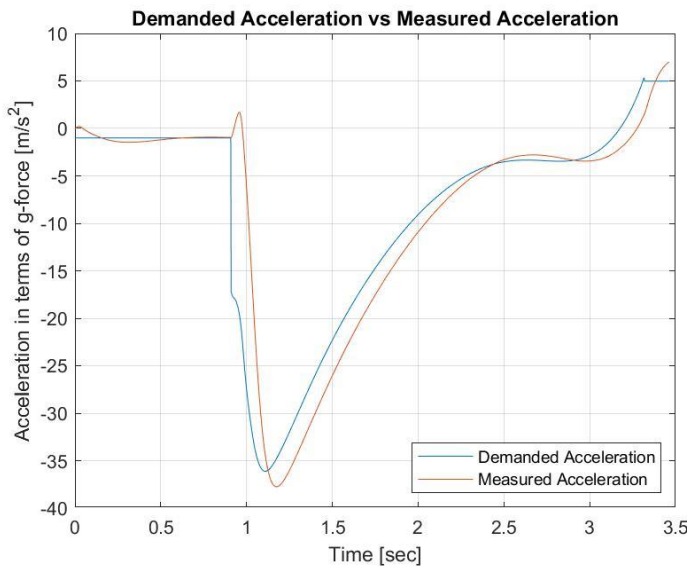


Figure 6. 3: Demanded vs Measured Acceleration.

Fig 6.4 represents missile's and target's followed trajectory until interception using proportional navigation with a seeker for Case 1.

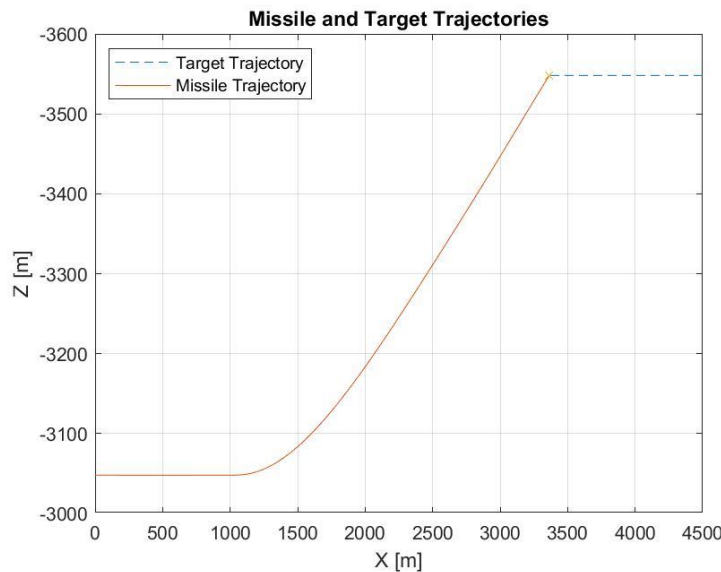


Figure 6. 4: Missile Target Trajectory.

Fig 6.5 shows missile and target separation in both x and z directions until interception using proportional navigation with a seeker for Case 1.

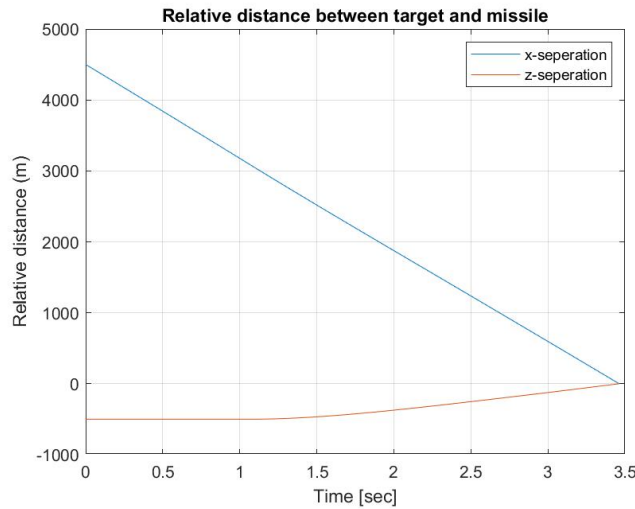


Figure 6. 5: Missile Target Relative Separation.

Fig 6.6 demonstrates the change of angle of attack (α) of the missile until the interception utilizing proportional navigation with a seeker for Case 1.

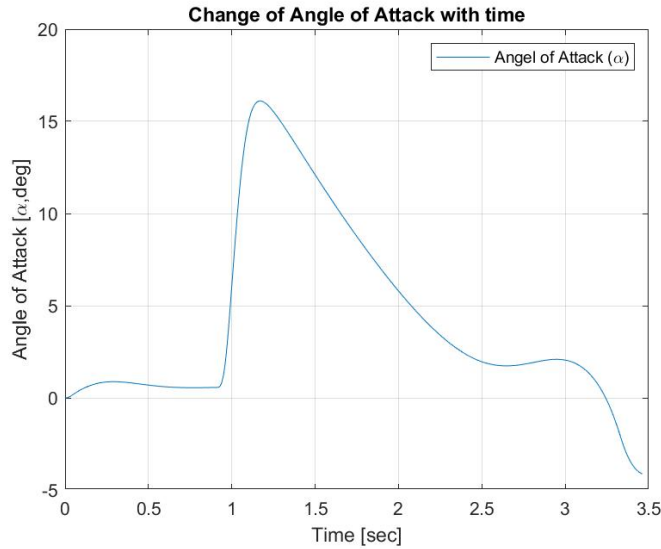


Figure 6. 6: Change of Angle of Attack.

Fig 6.7 presets the change of fin deflection(δ_e) of the missile until the interception utilizing proportional navigation with a seeker for Case 1.

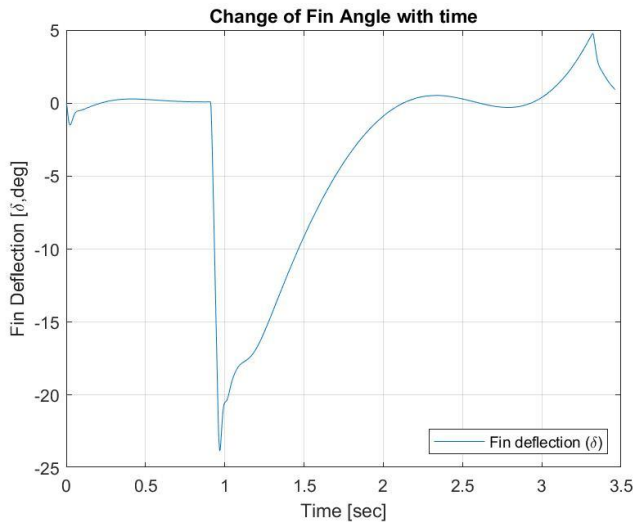


Figure 6. 7: Change of Fin Deflection.

Fig 6.8 reveals the change of Mach number of the missile till the interception utilizing proportional navigation with a seeker for Case 1.

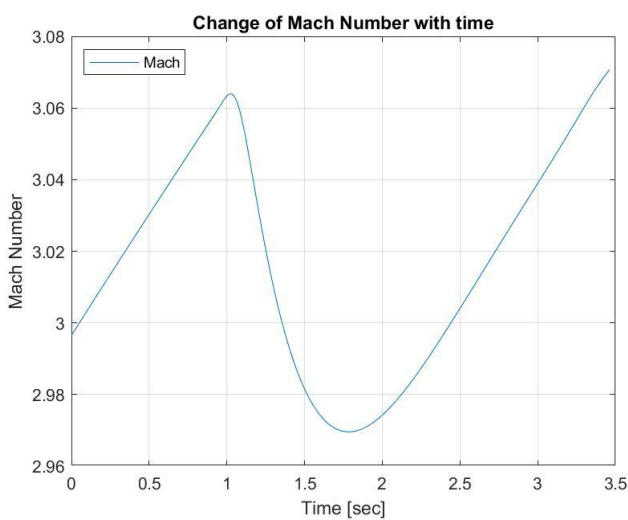


Figure 6. 8: Change of Mach Number.

6.1.2 Proportional Navigation

Graphical results of the proportional navigation for case one is demonstrated in this section.

Figure 6.9 illustrates the missile-target interception instant using the simple proportional navigation algorithm for Case 1.

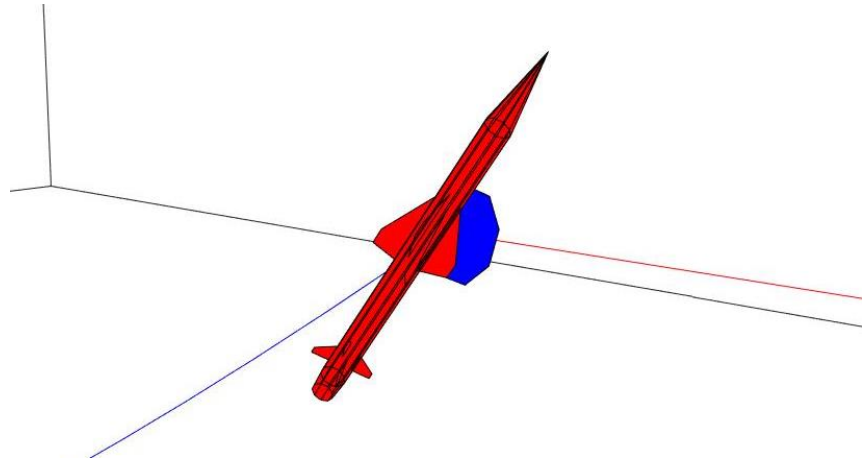


Figure 6. 9: Missile Target Interception Animation.

Fig 6.10 depicts demanded acceleration generated by proportional navigation, alongside the measured acceleration from the missile dynamics for Case 1.

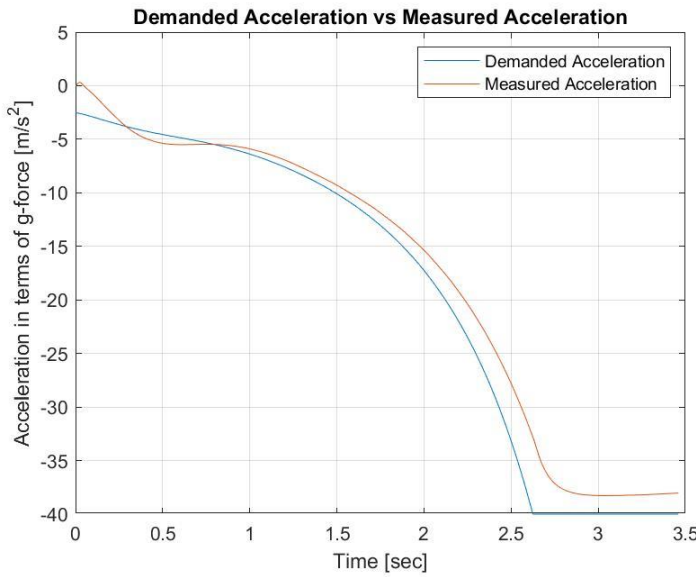


Figure 6. 10: Demanded vs Measured Acceleration.

Fig 6.11 represents missile's and target's followed trajectory until interception using proportional navigation for Case 1.

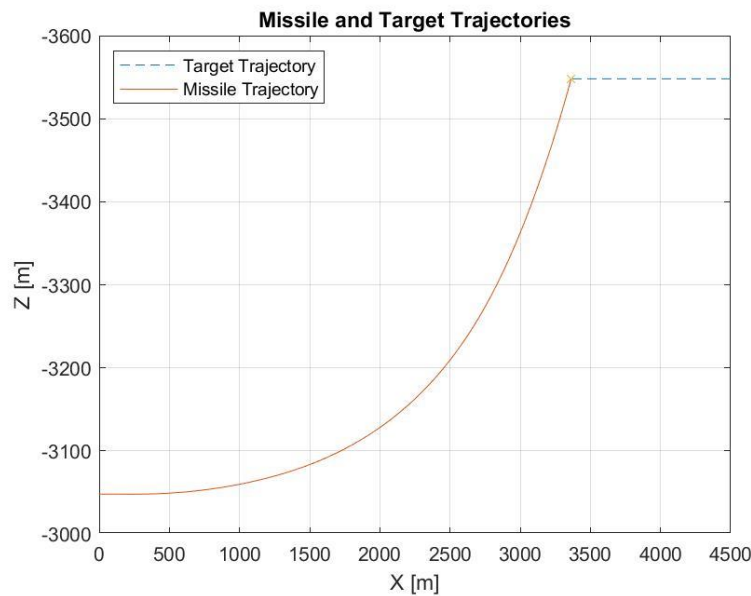


Figure 6. 11: Missile Target Trajectory.

Fig 6.12 shows missile and target separation in both x and z directions until interception using proportional navigation for Case 1.

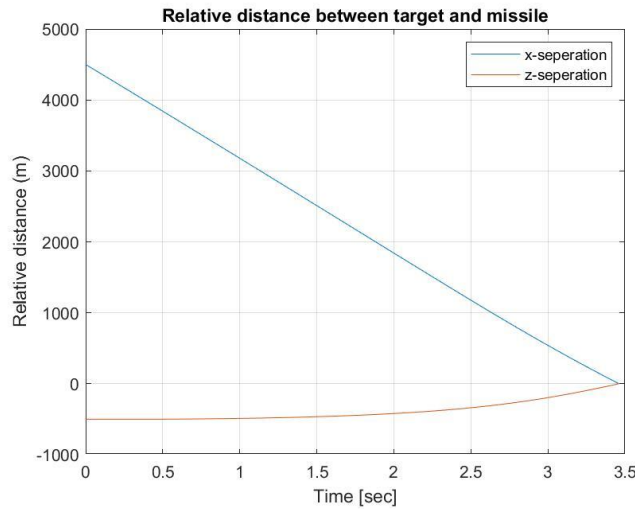


Figure 6. 12: Missile Target Relative Separation.

Fig 6.13 demonstrates the change of angle of attack (α) of the missile until the interception utilizing simple proportional navigation for Case 1.

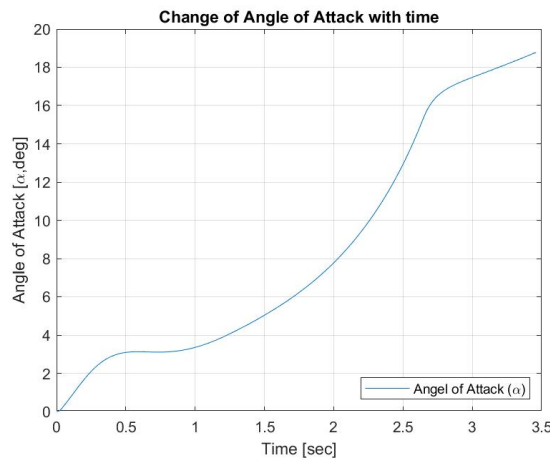


Figure 6. 13: Change of Angle of Attack.

Fig 6.14 presets the change of fin deflection(δ_e) of the missile until the interception utilizing simple proportional navigation for Case 1.

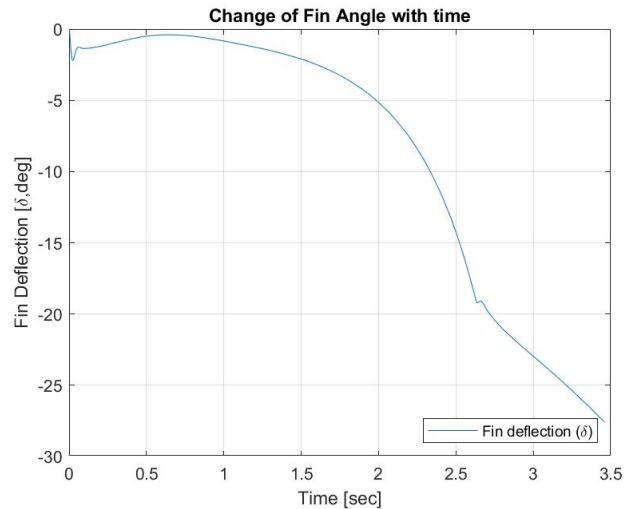


Figure 6. 14: Change of Fin Deflection.

Fig 6.15 reveals the change of Mach number of the missile till the interception utilizing proportional navigation for Case 1.

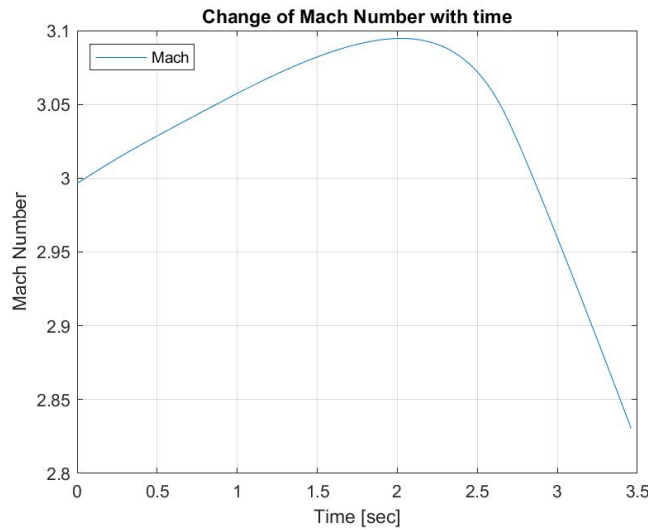


Figure 6. 15: Change of Mach Number

6.1.3 Proportional Navigation with ZEM

Graphical results of the proportional navigation with zero effort miss (ZEM) for case one is demonstrated in this section.

Figure 6.16 illustrates the missile-target interception instant using the simple proportional navigation with ZEM algorithm for Case 1.

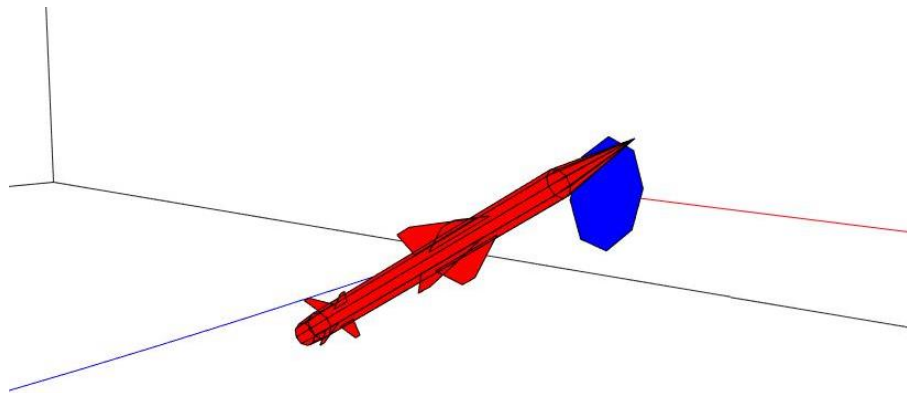


Figure 6. 16: Missile Target Interception Animation.

Fig 6.17 depicts demanded acceleration generated by proportional navigation with ZEM, alongside the measured acceleration from the missile dynamics for Case 1.

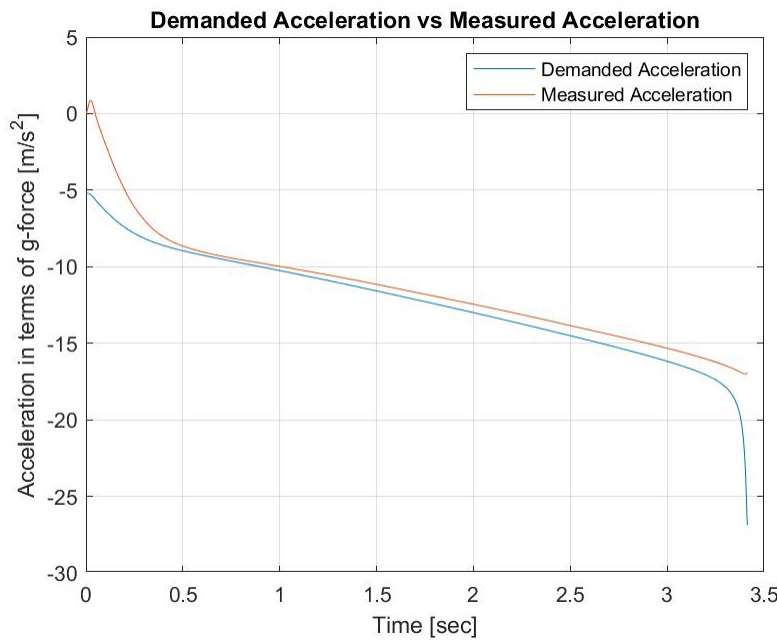


Figure 6. 17: Demanded vs Measured Acceleration.

Fig 6.18 represents missile's and target's followed trajectory until interception using proportional navigation with ZEM for Case 1.

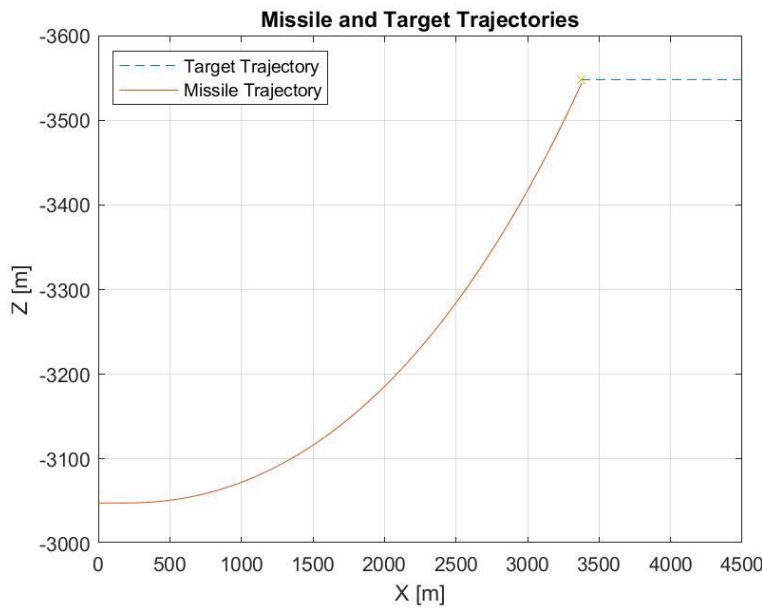


Figure 6. 18: Missile Target Trajectory.

Fig 6.19 shows missile and target separation in both x and z directions until interception using proportional navigation with ZEM for Case 1.

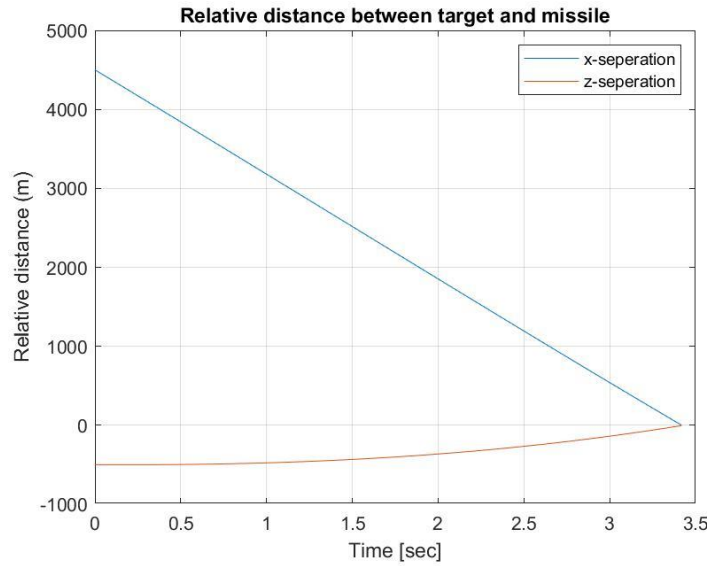


Figure 6. 19: Missile Target Relative Separation.

Fig 6.20 demonstrates the change of angle of attack (α) of the missile until the interception utilizing simple proportional navigation with ZEM for Case 1.

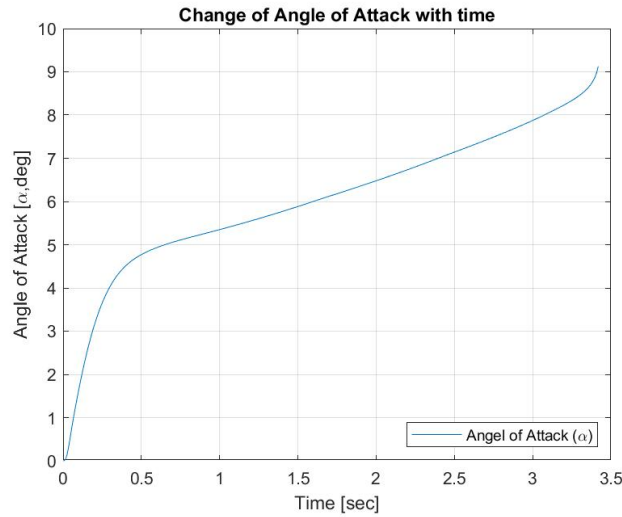


Figure 6. 20: Change of Angle of Attack.

Fig 6.21 presets the change of fin deflection(δ_e) of the missile until the interception utilizing simple proportional navigation with ZEM for Case 1.

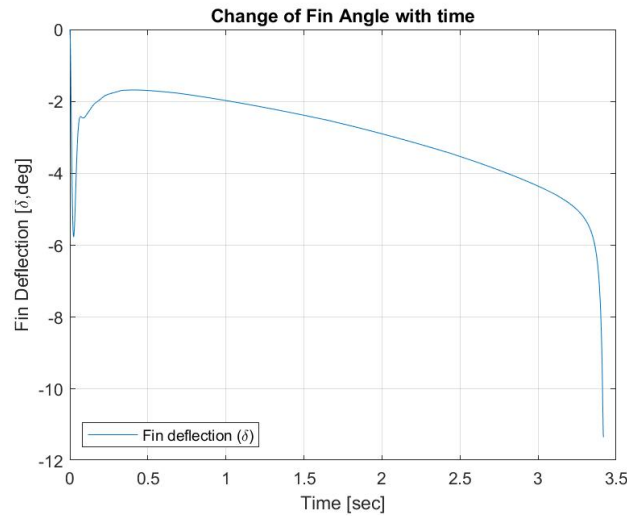


Figure 6. 21: Change of Fin Deflection.

Fig 6.22 reveals the change of Mach number of the missile till the interception utilizing proportional navigation with ZEM for Case 1.

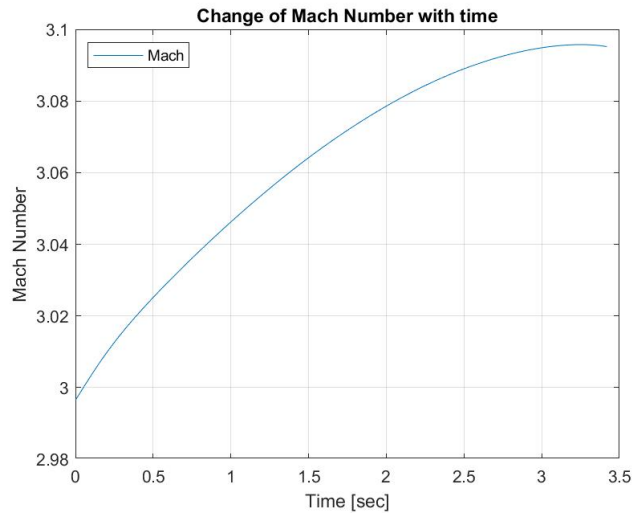


Figure 6. 22: Change of Mach Number.

6.2 Case 2

Similar to the case one, in this case, the missile and target fly toward each other, and the target is flying at a constant altitude and speed. The only difference is the target is at the lower altitude than the missile. The initial separation of target and missile in the x-direction is same with case one, 4500 meters, while in the z-direction it is different, 500 meters. The figure below represents the missile target interception for case two.

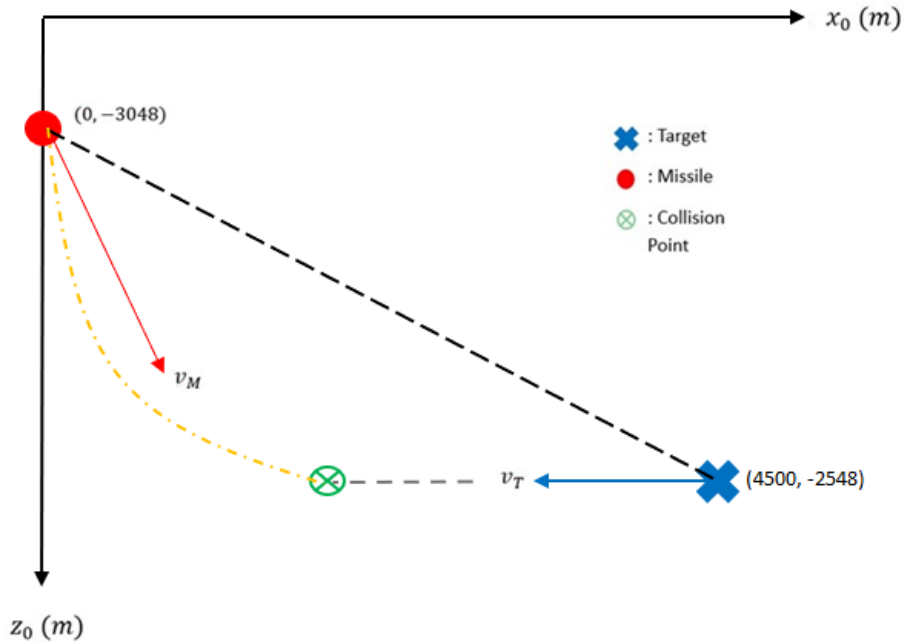


Figure 6. 23: Missile Target interception case two scenario.

Table 6. 2: Numerical parameters for case two.

Parameters	Numerical Values
V_T	328 m/s
X_{sep}	4500 m
Z_{sep}	500 m

By using these numerical initial conditions and the case one algorithm GNC algorithms are obtained and presented as:

6.2.1 Proportional Navigation + Seeker

Graphical results of the proportional navigation with a seeker for case two is represented in this section .

Figure 6.24 illustrates the missile-target interception instant using the proportional navigation algorithm with a seeker for Case 2.

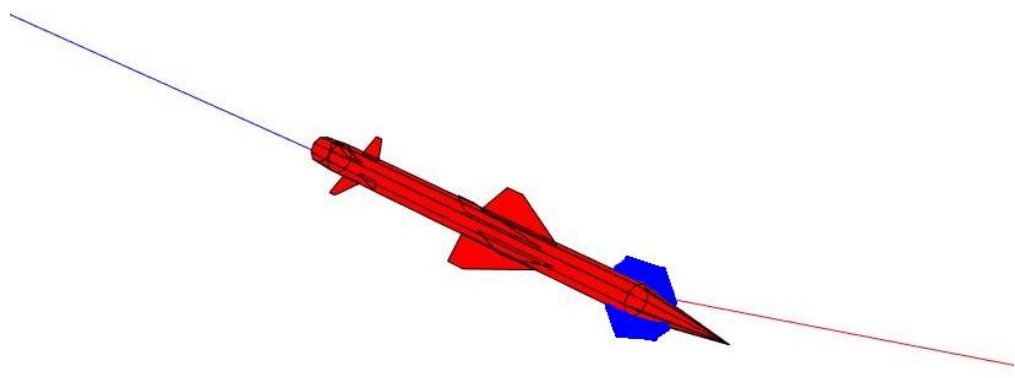


Figure 6. 24: Missile Target Interception Animation.

Fig 6.25 depicts demanded acceleration generated by proportional navigation with a seeker, alongside the measured acceleration from the missile dynamics for Case 2.

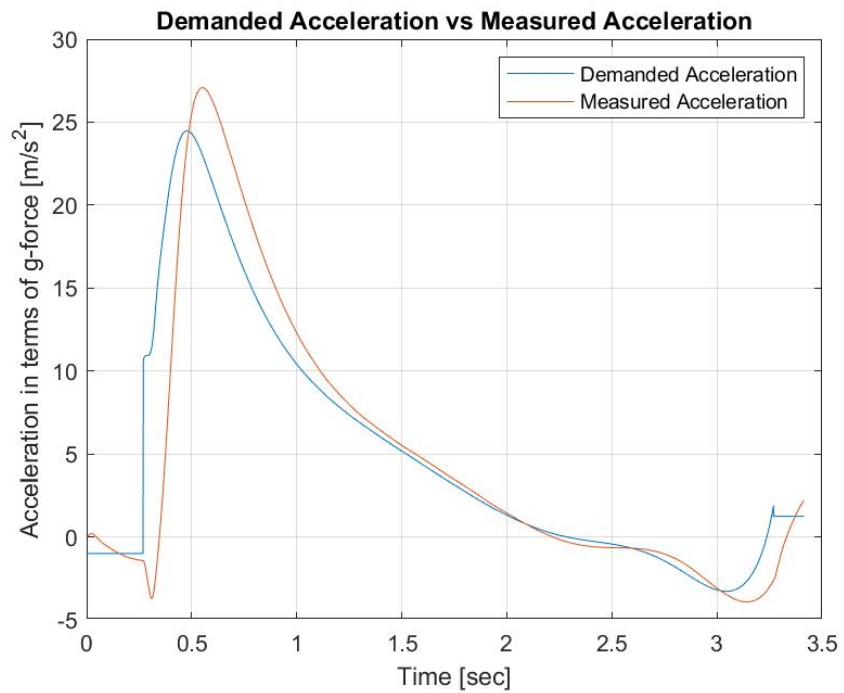


Figure 6. 25: Demanded vs Measured Acceleration.

Fig 6.26 represents missile's and target's followed trajectory until interception using proportional navigation with a seeker for Case 2.

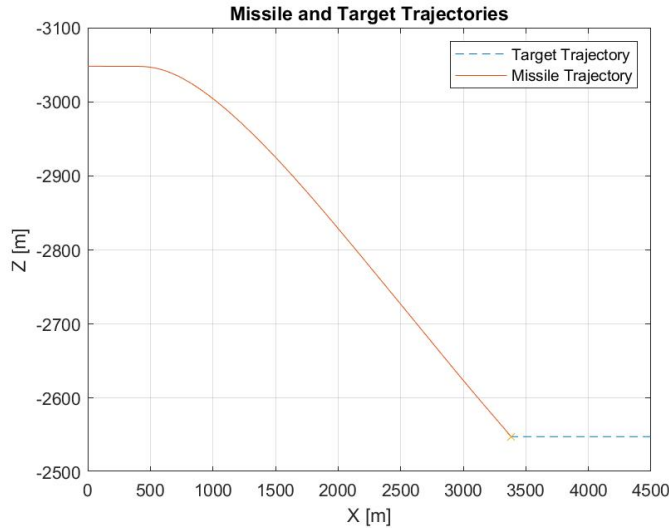


Figure 6. 26: Missile Target Trajectory.

Fig 6.27 shows missile and target separation in both x and z directions until interception using proportional navigation with a seeker for Case 2.

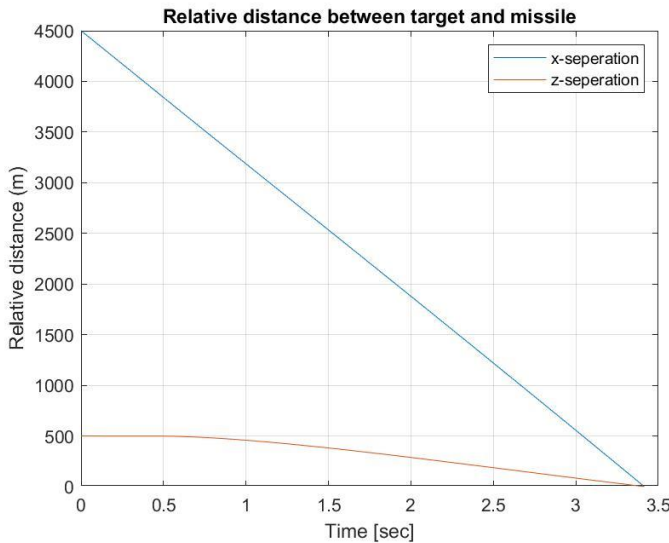


Figure 6. 27: Missile Target Relative Separation.

Fig 6.28 demonstrates the change of angle of attack (α) of the missile until the interception utilizing proportional navigation with a seeker for Case 2.

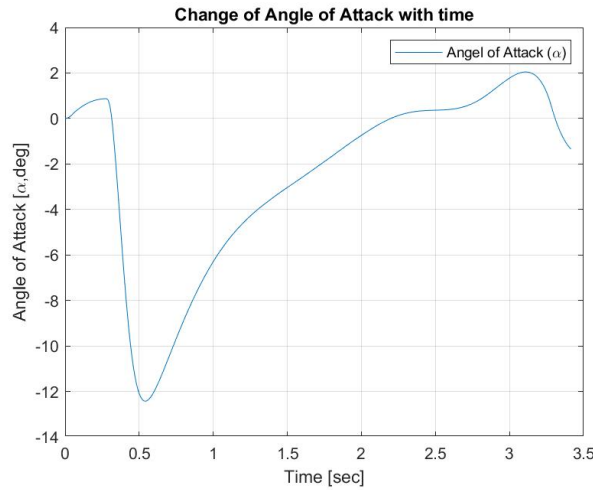


Figure 6. 28: Change of Angle of Attack.

Fig 6.29 presets the change of fin deflection(δ_e) of the missile until the interception utilizing proportional navigation with a seeker for Case 2.

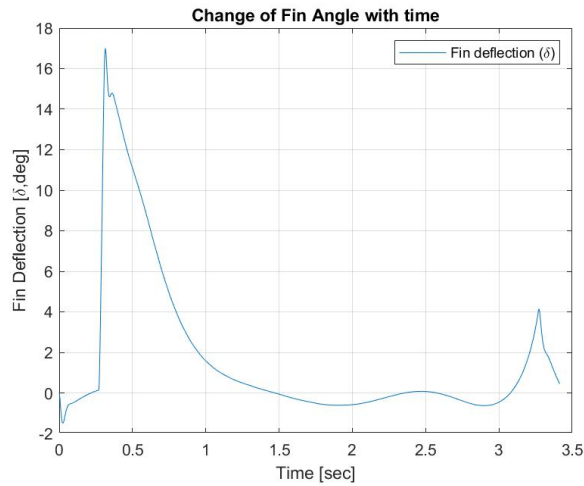


Figure 6. 29: Change of Fin Deflection.

Fig 6.30 reveals the change of Mach number of the missile till the interception utilizing proportional navigation with a seeker for Case 2.

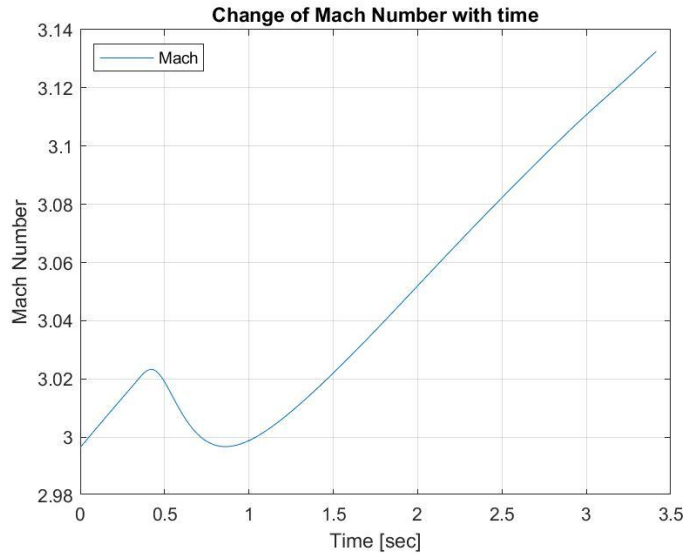


Figure 6. 30: Change of Mach Number.

6.2.2 Proportional Navigation

Graphical results of the proportional navigation for case two is demonstrated in this section.

Figure 6.31 illustrates the missile-target interception instant using the simple proportional navigation algorithm for Case 2.

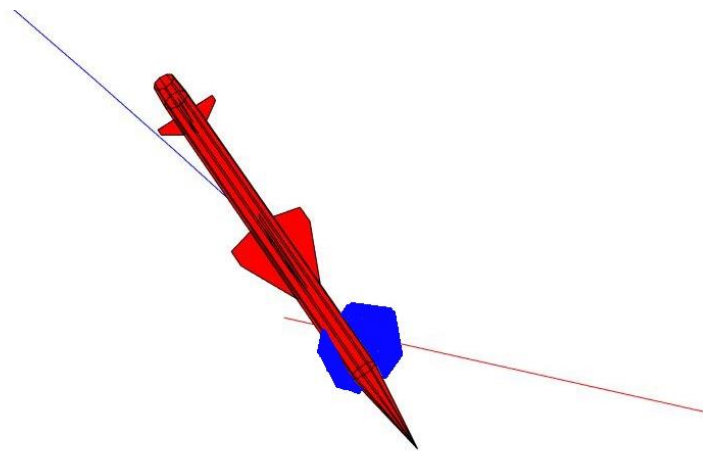


Figure 6. 31: Missile Target Interception Animation.

Fig 6.32 depicts demanded acceleration generated by proportional navigation, alongside the measured acceleration from the missile dynamics for Case 2.

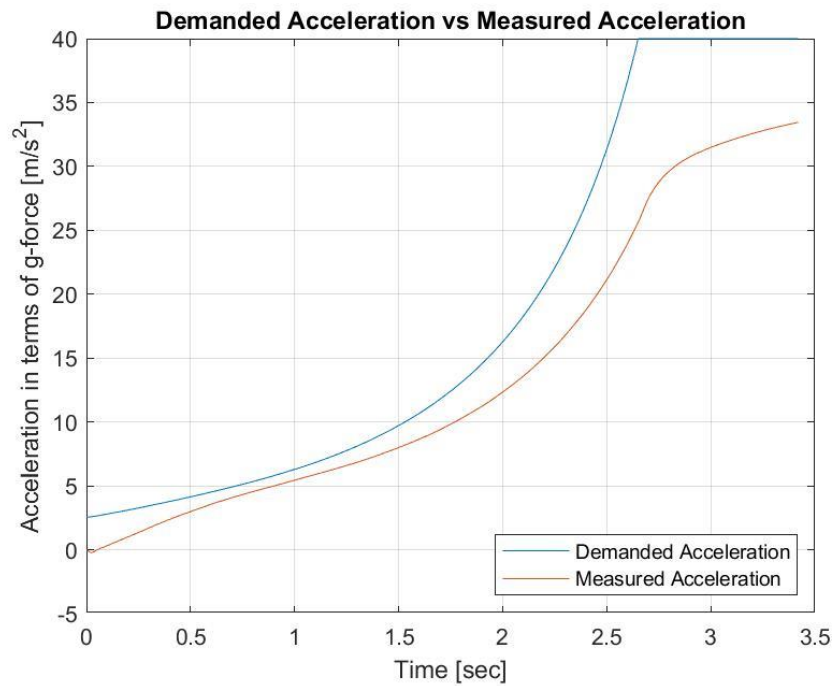


Figure 6. 32: Demanded vs Measured Acceleration.

Fig 6.33 represents missile's and target's followed trajectory until interception using proportional navigation for Case 2.

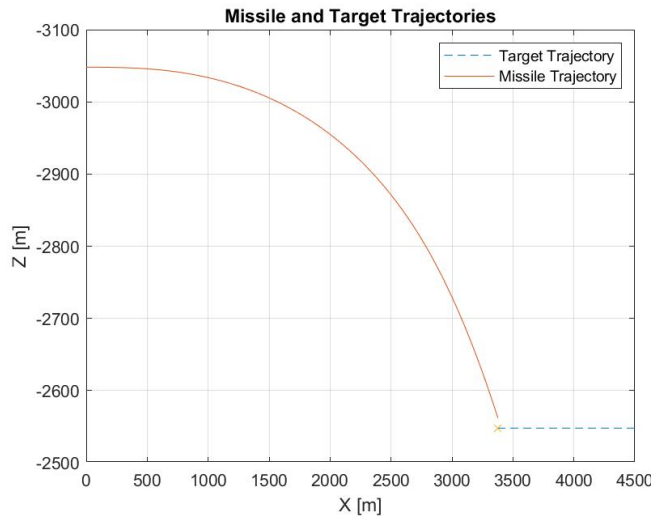


Figure 6. 33: Missile Target Trajectory.

Fig 6.34 shows missile and target separation in both x and z directions until interception using proportional navigation for Case 2.

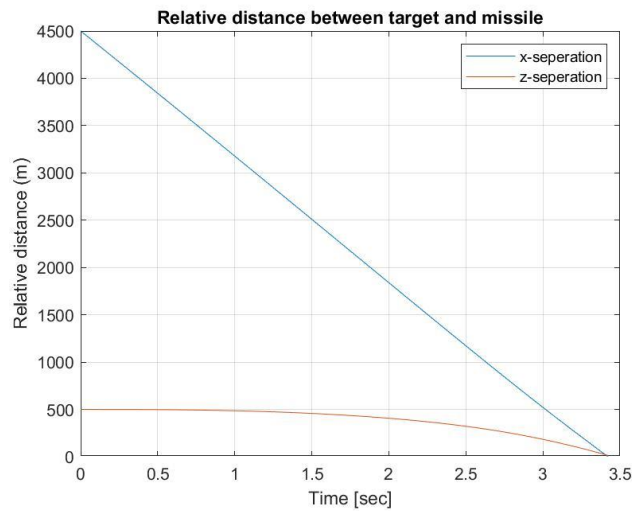


Figure 6. 34: Missile Target Relative Separation.

Fig 6.35 demonstrates the change of angle of attack (α) of the missile until the interception utilizing simple proportional navigation for Case 2.

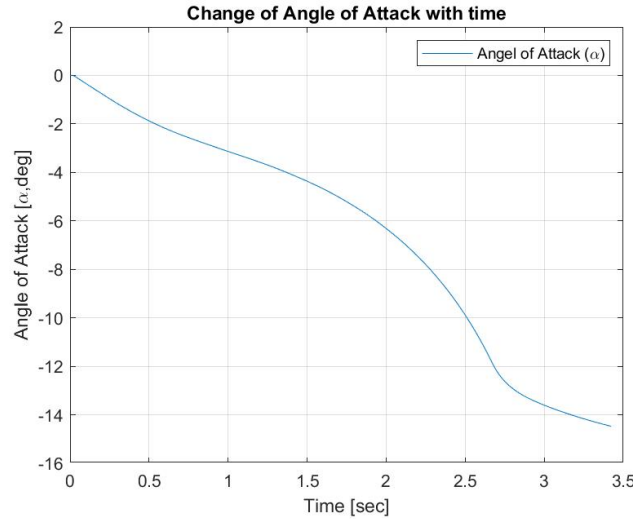


Figure 6. 35: Change of Angle of Attack.

Fig 6.36 presets the change of fin deflection(δ_e) of the missile until the interception utilizing simple proportional navigation for Case 2.

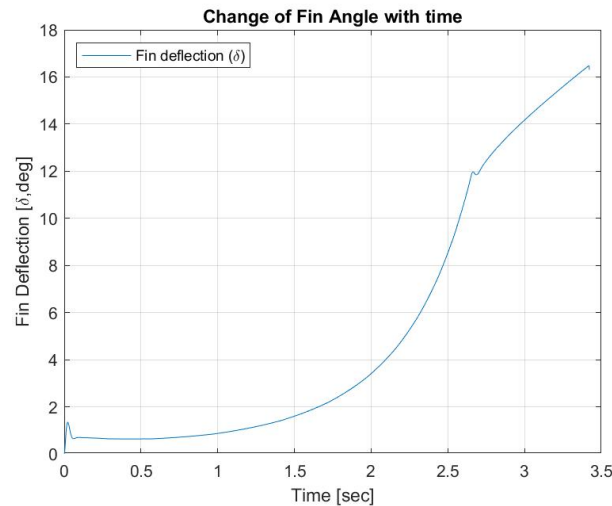


Figure 6. 36: Change of Fin Deflection.

Fig 6.37 reveals the change of Mach number of the missile till the interception utilizing proportional navigation for Case 2.

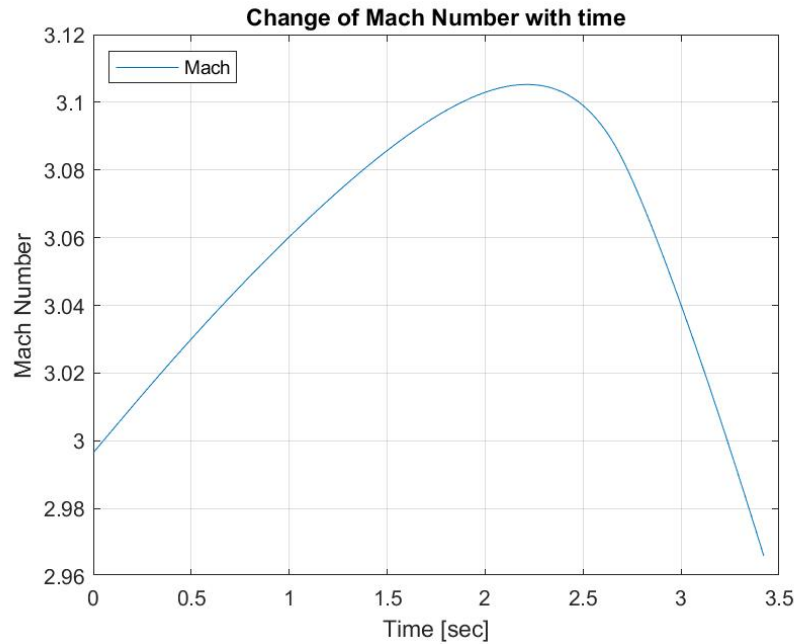


Figure 6. 37: Change of Mach Number.

6.2.3 Proportional Navigation with ZEM

Graphical results of the proportional navigation with zero effort miss (ZEM) for case two is demonstrated in this section.

Figure 6.38 illustrates the missile-target interception instant using the simple proportional navigation with ZEM algorithm for Case 2.

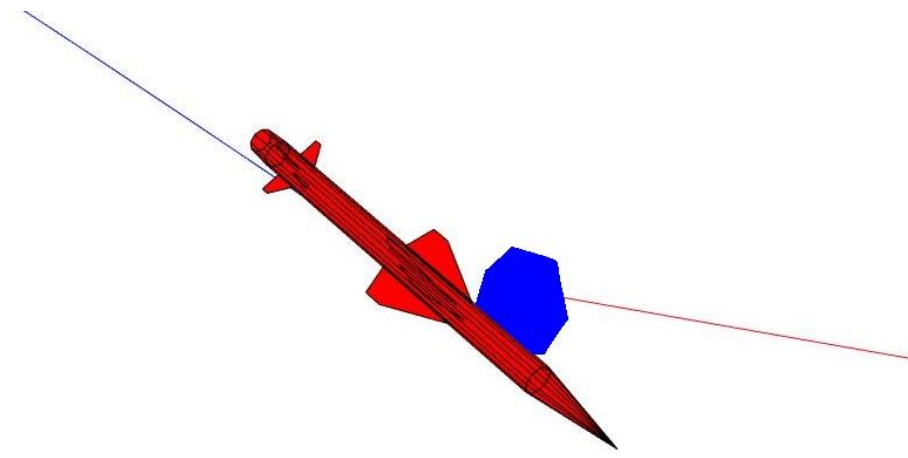


Figure 6. 38: Missile Target Interception Animation.

Fig 6.39 depicts demanded acceleration generated by proportional navigation with ZEM, alongside the measured acceleration from the missile dynamics for Case 2.

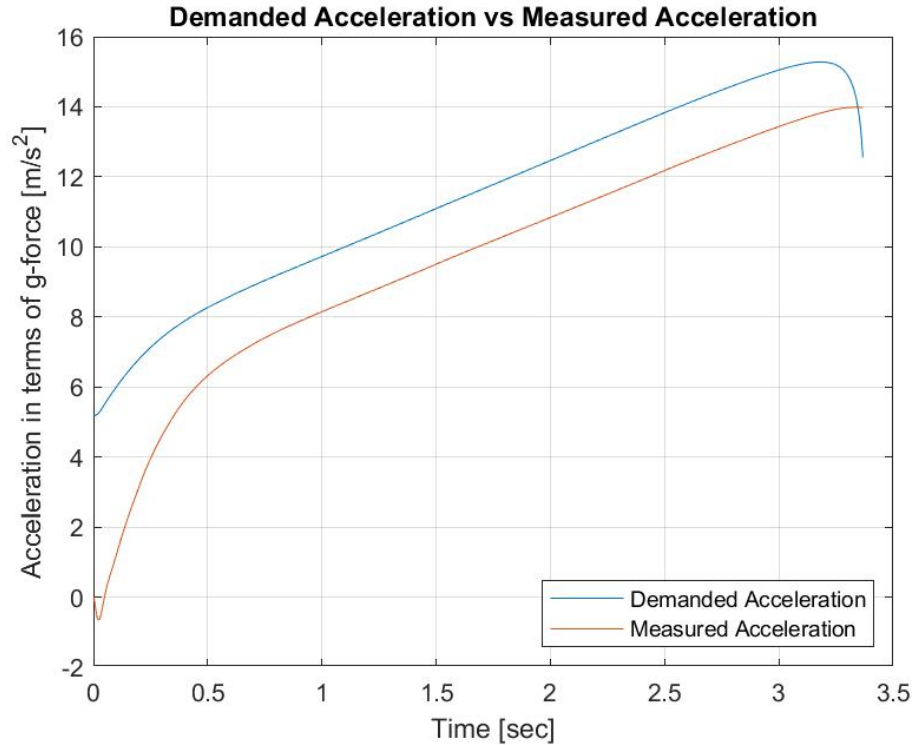


Figure 6. 39: Demanded vs Measured Acceleration.

Fig 6.40 represents missile's and target's followed trajectory until interception using proportional navigation with ZEM for Case 2.

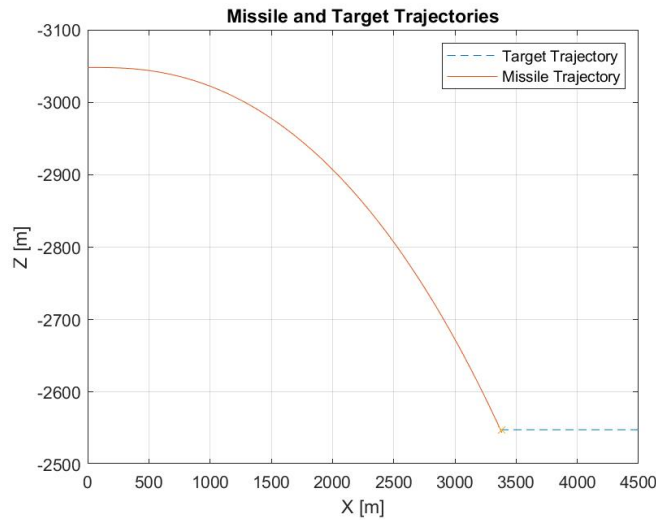


Figure 6. 40: Missile Target Trajectory.

Fig 6.41 shows missile and target separation in both x and z directions until interception using proportional navigation for Case 2.

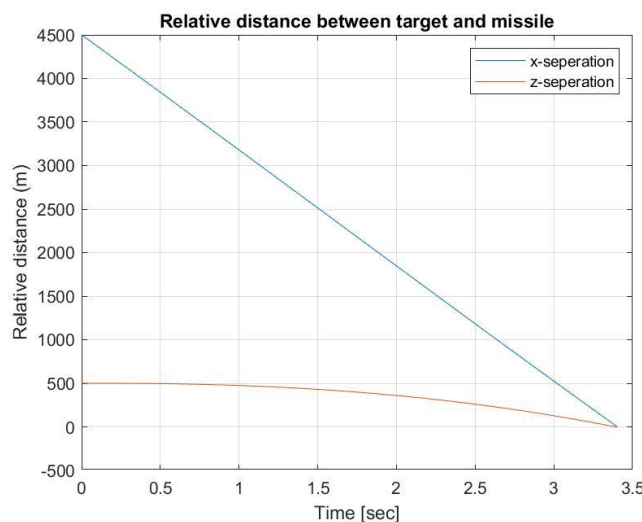


Figure 6. 41: Missile Target Relative Separation.

Fig 6.42 demonstrates the change of angle of attack (α) of the missile until the interception utilizing simple proportional navigation with ZEM for Case 2.

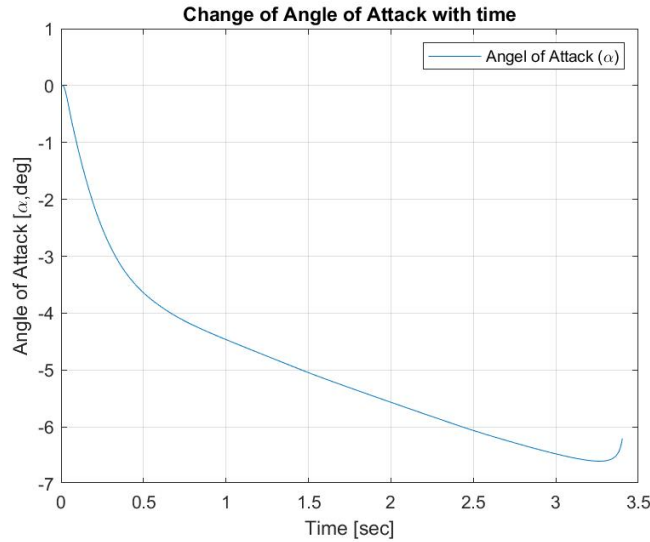


Figure 6. 42: Change of Angle of Attack.

Fig 6.43 presets the change of fin deflection(δ_e) of the missile until the interception utilizing simple proportional navigation with ZEM for Case 2.

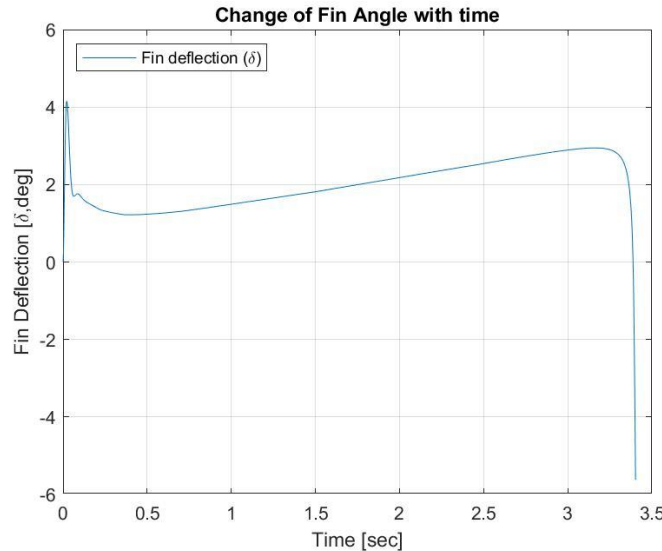


Figure 6. 43: Change of Fin Deflection.

Fig 6.44 reveals the change of Mach number of the missile till the interception utilizing proportional navigation with ZEM for Case 2.

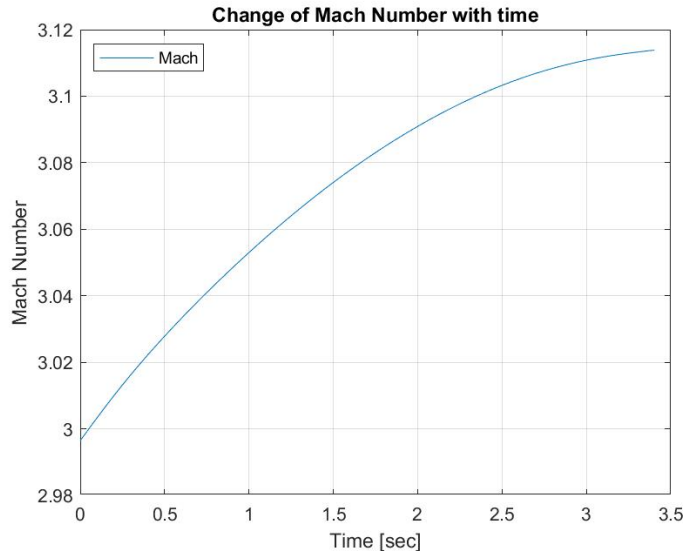


Figure 6. 44: Change of Mach Number.

6.3 Case 3

This case is exactly same with the first case with an only difference which is the speed of the target. Initial separation of target and missile in the x-direction is 4500 meters while in the z-direction is – 500 meters. The table down below represents the initial conditions and target's speed. Only three graphs are presented in this section, because others are similar to the case one results.

Table 6. 3: Numerical parameters for case four

Parameters	Numerical Values
V_T	400 m/s
X_{sep}	4500 m
Z_{sep}	-500 m

6.3.1 Proportional Navigation + Seeker

Graphical results of the proportional navigation with a seeker for case three is represented in this section .

Figure 6.45 illustrates the missile-target interception instant using the proportional navigation algorithm with a seeker for Case 3.

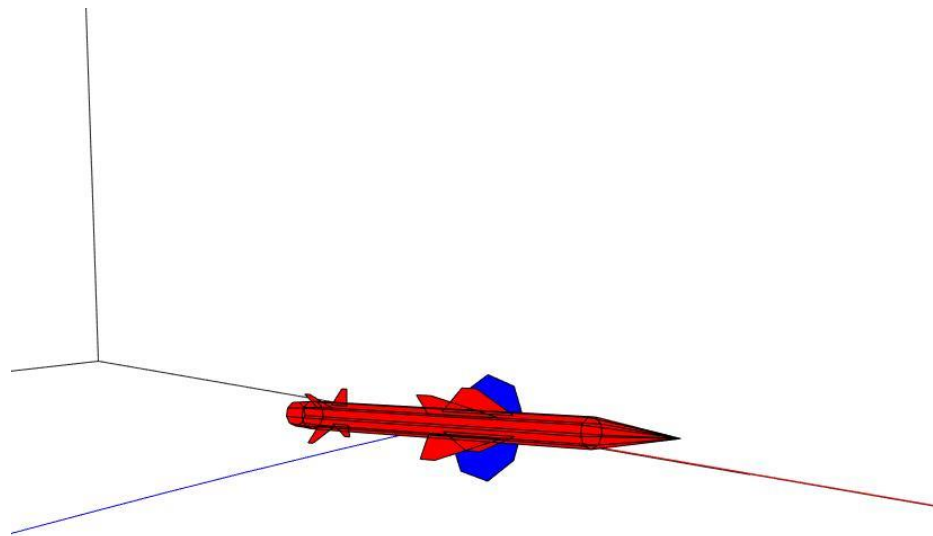


Figure 6. 45: Missile Target Interception Animation.

Fig 6.46 depicts demanded acceleration generated by proportional navigation with a seeker, alongside the measured acceleration from the missile dynamics for Case 3.

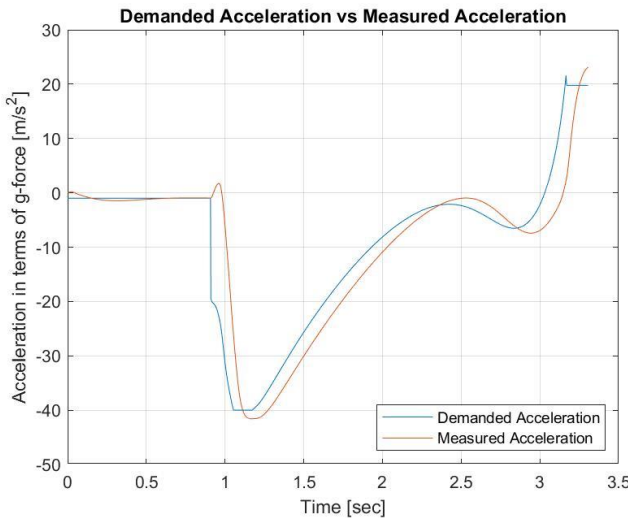


Figure 6. 46: Demanded vs Measured Acceleration.

Fig 6.47 represents missile's and target's followed trajectory until interception using proportional navigation with a seeker for Case 3.

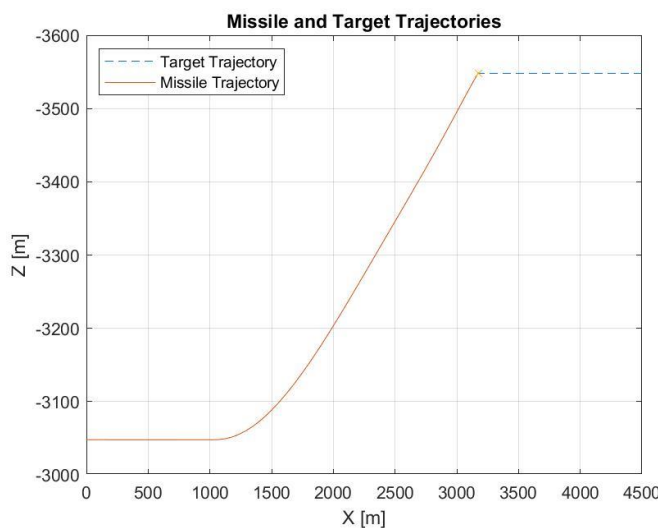


Figure 6. 47: Missile Target Trajectory.

6.3.2 Proportional Navigation

Graphical results of the proportional navigation for case three is demonstrated in this section.

Figure 6.48 illustrates the missile-target interception instant using the simple proportional navigation algorithm for Case 3.

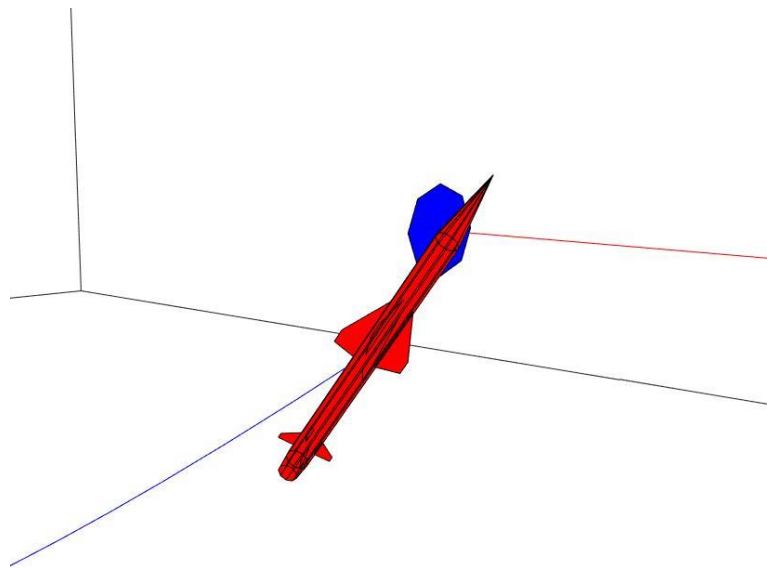


Figure 6. 48: Missile Target Interception Animation.

Fig 6.49 depicts demanded acceleration generated by proportional navigation, alongside the measured acceleration from the missile dynamics for Case 3.

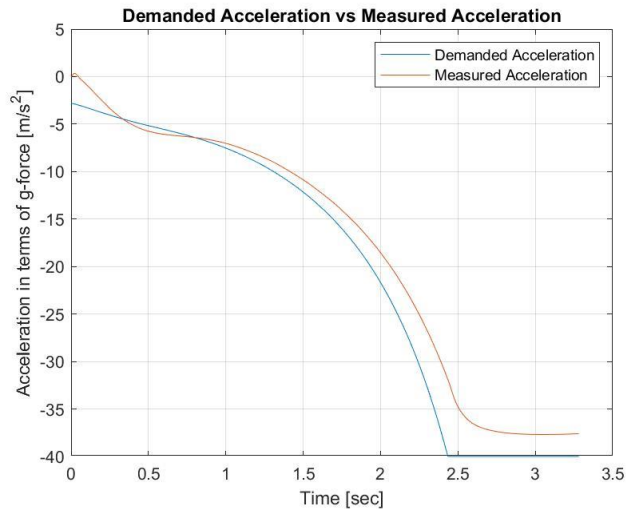


Figure 6. 49: Demanded vs Measured Acceleration.

Fig 6.50 represents missile's and target's followed trajectory until interception using proportional navigation for Case 3.

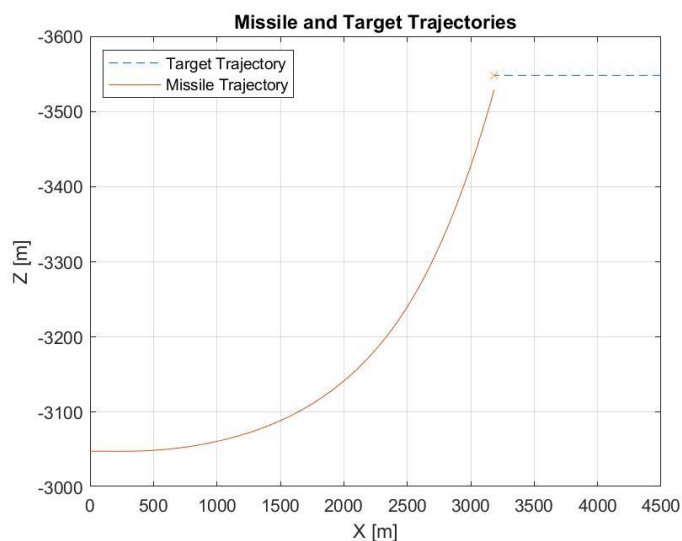


Figure 6. 50: Missile Target Trajectory.

6.3.3 Proportional Navigation with ZEM

Graphical results of the proportional navigation with zero effort miss (ZEM) for case three is demonstrated in this section.

Figure 6.51 illustrates the missile-target interception instant using the simple proportional navigation with ZEM algorithm for Case 3.

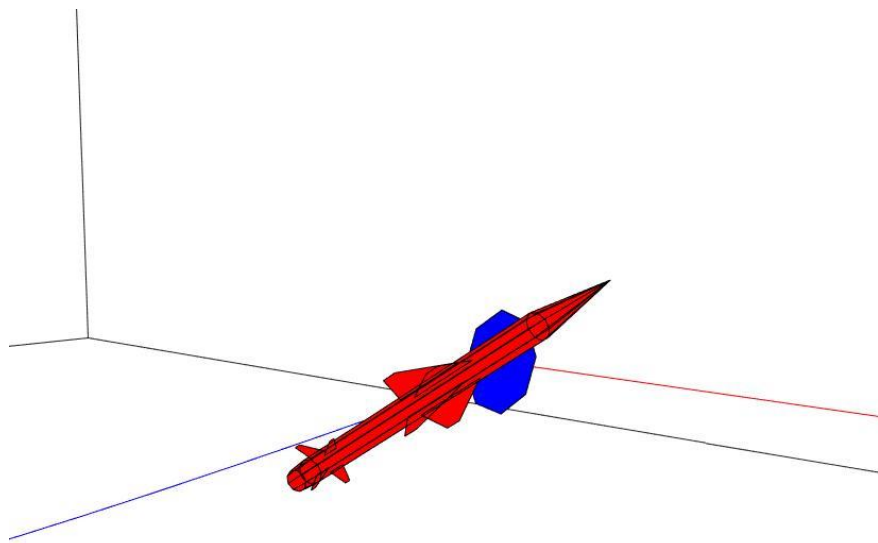


Figure 6. 51: Missile Target Interception Animation.

Fig 6.52 depicts demanded acceleration generated by proportional navigation with ZEM, alongside the measured acceleration from the missile dynamics for Case 3.

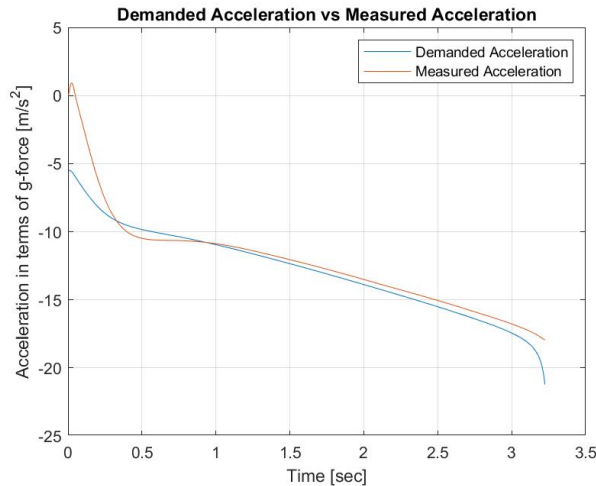


Figure 6. 52: Demanded vs Measured Acceleration.

Fig 6.53 represents missile's and target's followed trajectory until interception using proportional navigation with ZEM for Case 3.

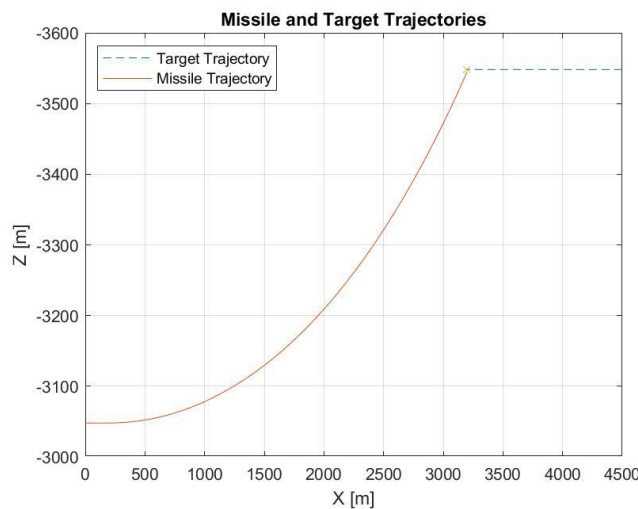


Figure 6. 53: Missile Target Trajectory.

6.4 Case 4

This case is exactly the same as the first and third cases, with the only difference being the speed of the target. However, in this case, the speed of the target is taken as very high to push the limits of the GNC algorithms. The initial separation of target and missile are same. The table below represents the initial conditions and the target's speed. In this section, three graphs, which are demanded vs measured acceleration, missile target trajectory, and fin deflection, are presented.

Table 6. 4: Numerical parameters for case five.

Parameters	Numerical Values
V_T	800 m/s
X_{sep}	4500 m
Z_{sep}	-500 m

6.4.1 Proportional Navigation + Seeker

Graphical results of the proportional navigation with a seeker for case four is represented in this section .

Fig 6.54 depicts demanded acceleration generated by proportional navigation with a seeker, alongside the measured acceleration from the missile dynamics for Case 4.

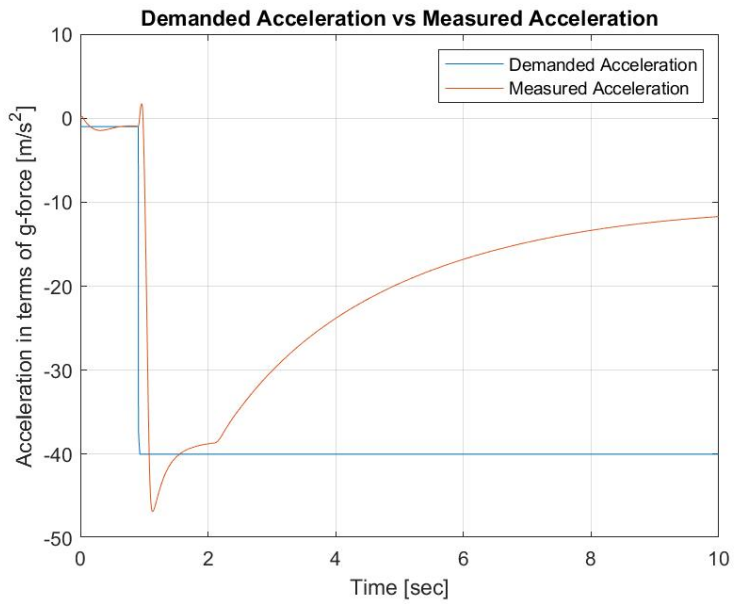


Figure 6.54: Demanded vs Measured Acceleration.

Fig 6.55 represents missile's and target's followed trajectory using proportional navigation with a seeker for miss case (4).

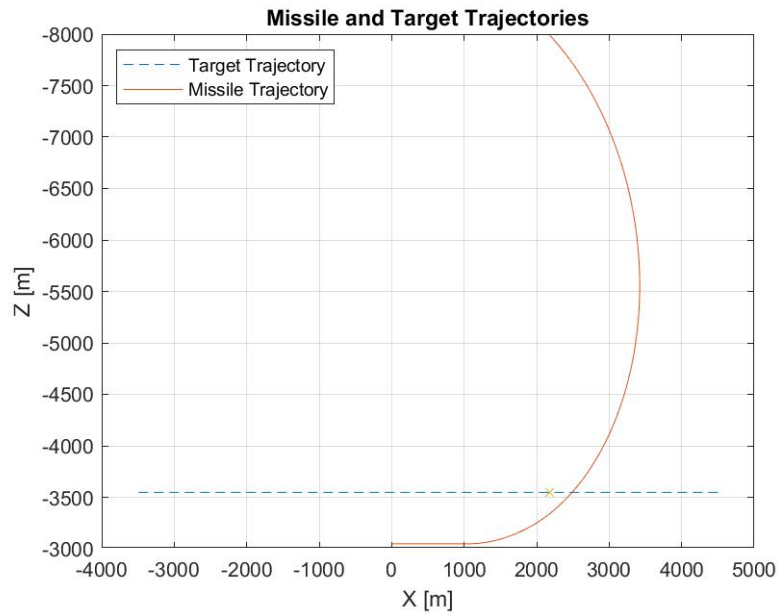


Figure 6.55: Missile Target Trajectory.

Fig 6.56 presets the change of fin deflection(δ_e) of the missile utilizing proportional navigation with a seeker for miss case (4).

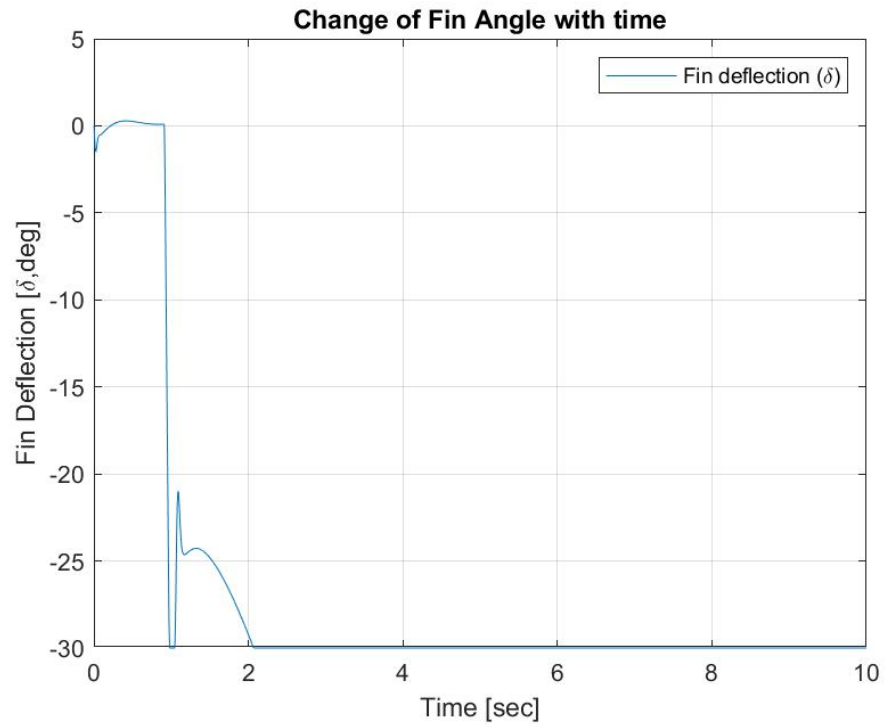


Figure 6. 56: Change of Fin Deflection.

6.4.2 Proportional Navigation

Graphical results of the proportional navigation for case four is demonstrated in this section.

Fig 6.49 depicts demanded acceleration generated by proportional navigation, alongside the measured acceleration from the missile dynamics for Case 4.

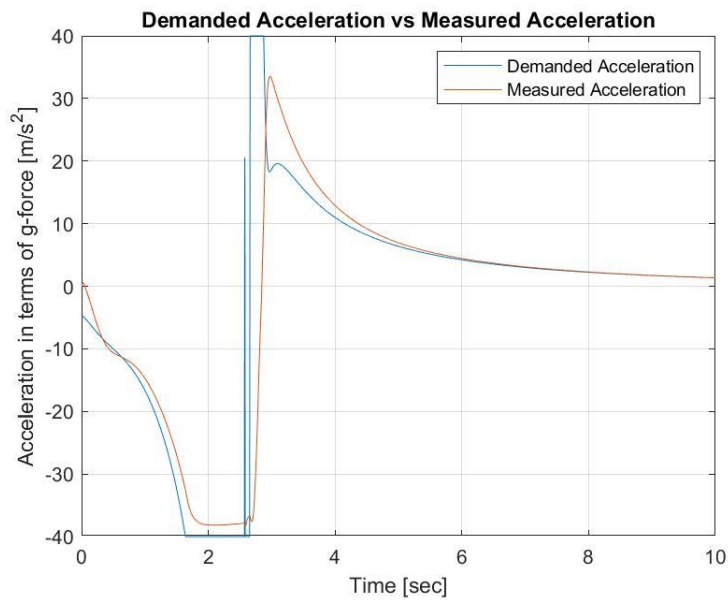


Figure 6. 57: Demanded vs Measured Acceleration.

Fig 6.58 represents missile's and target's followed trajectory using simple proportional navigation for miss case (4).

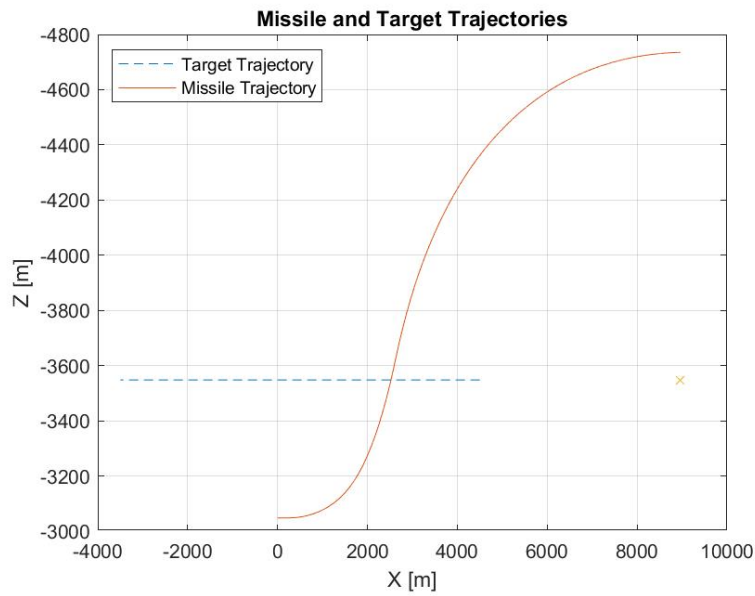


Figure 6. 58: Missile Target Trajectory.

Fig 6.59 presets the change of fin deflection(δ_e) of the missile utilizing simple proportional navigation for miss case (4).

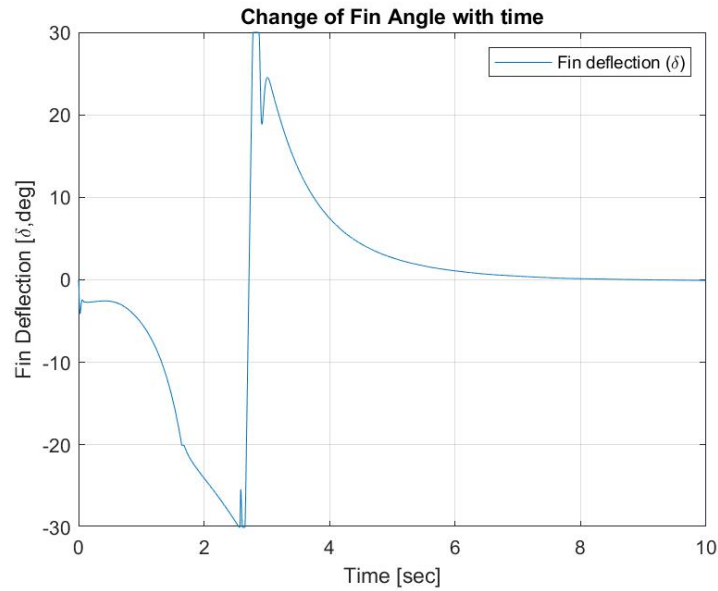


Figure 6. 59: Change of Fin Deflection.

6.4.3 Proportional Navigation with ZEM

Graphical results of the proportional navigation with zero effort miss (ZEM) for case four is demonstrated in this section.

Fig 6.60 depicts demanded acceleration generated by proportional navigation with ZEM, alongside the measured acceleration from the missile dynamics for Case 4.

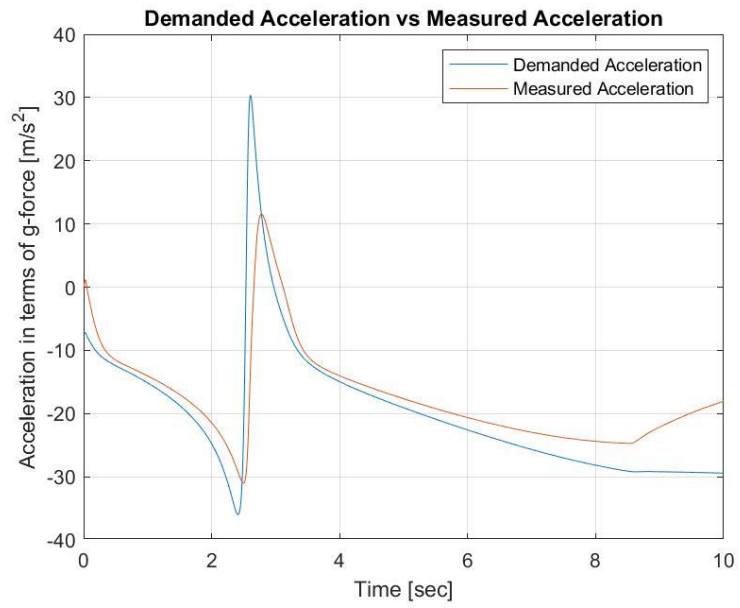


Figure 6.60: Demanded vs Measured Acceleration.

Fig 6.61 represents missile's and target's followed trajectory using proportional navigation with ZEM for miss case (4).

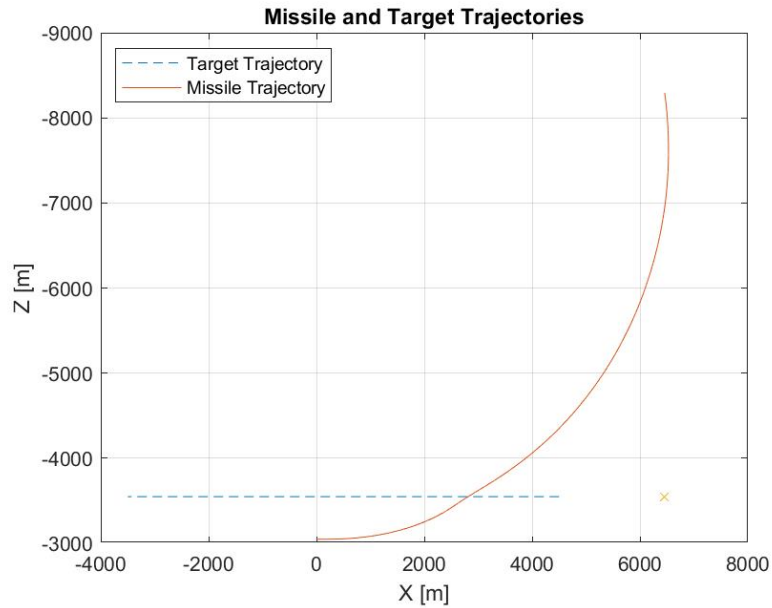


Figure 6.61: Missile Target Trajectory.

Fig 6.62 presets the change of fin deflection(δ_e) of the missile utilizing proportional navigation with ZEM for miss case (4).

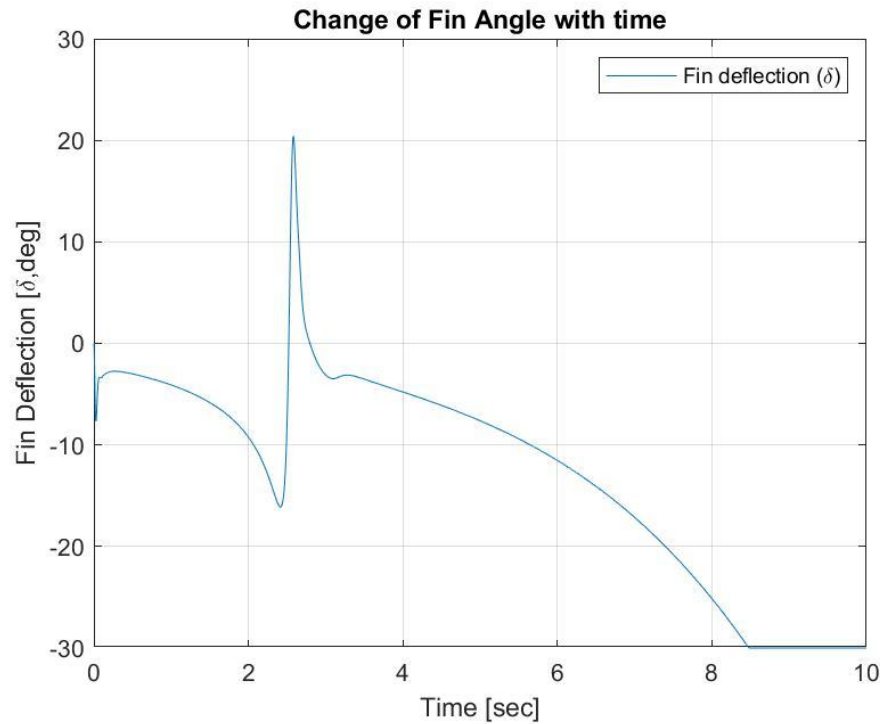


Figure 6. 62: Change of Fin Deflection.

In this case (4), with these initial position conditions, the speed of the target is too fast for the Guidance Navigation and Control (GNC) algorithms in order to create the correct command in the shortest time to make the missile and target interception happen, in other words, missile misses the target in this condition as seen from the missile target trajectory graphs. As a result, this shows that this used missile, like all missiles, has some limits. To find these limits, multiple different case studies have been done, and the limits of the missile have been found, which will be shown in the next part.

6.5 Limitations

A comprehensive analysis was conducted to estimate the limitations of the missile under various initial conditions, which are the positions and speed of the target. Numerous cases were simulated to assess the maximum speed at which the target could fly at the given separations while ensuring interception. With the data collected from the simulations, two tables and their graphs are created. These graphs represent the velocity of the target that could go up as maximum in the y-axis for the specific relative distance in the x-axis and they are shown down below.

Table 6. 5: Case analysis for z-separation target velocity.

Case	$x_{separation}(m)$	$z_{separation}(m)$	$V_{tgt}(m/s)$
1	4500	500	800
2	4500	750	550
3	4500	1000	425
4	4500	1500	250

Table 6. 6: Case analysis for x-separation target velocity.

Case	$x_{separation}(m)$	$z_{separation}(m)$	$V_{tgt}(m/s)$
1	2500	500	0
2	3000	500	200
3	4000	500	500
4	4500	500	800

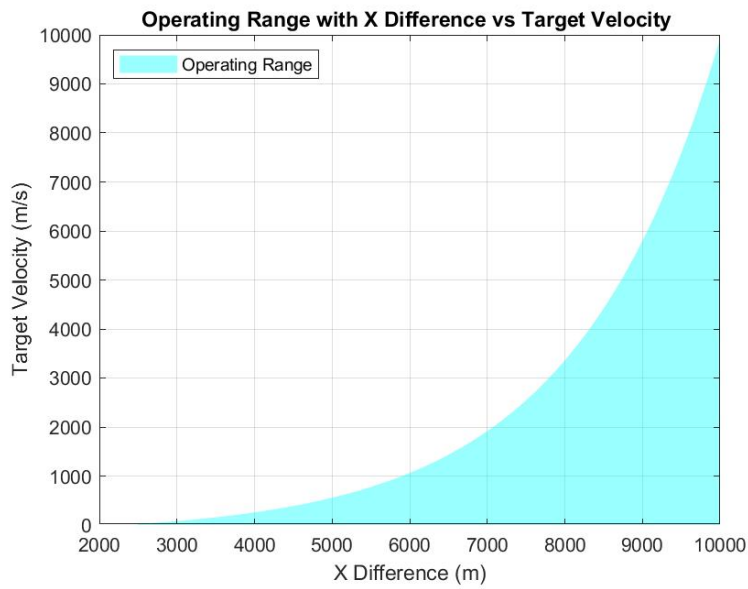


Figure 6. 63: Limitation of the missile according to the target velocity and x-direction relative separation.

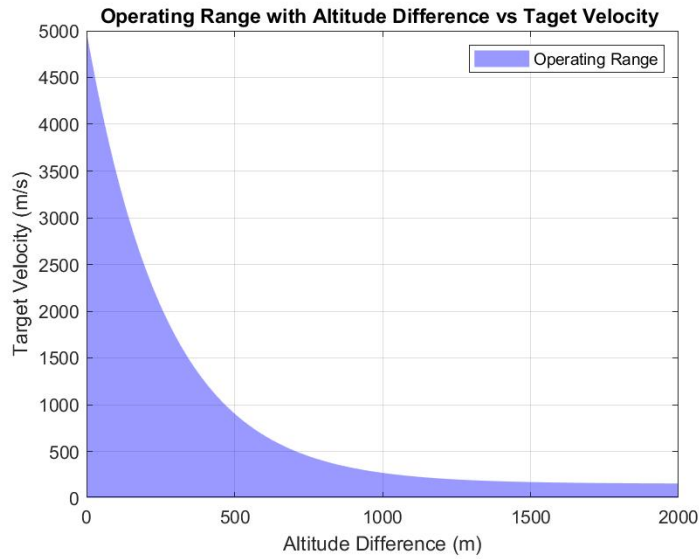


Figure 6. 64: Limitation of the missile according to the target velocity and z-direction relative separation

CHAPTER 7

DISCUSSION

In this part of the thesis, the discussion and comparison of the Guidance Navigation and Control (GNC) algorithms are done using case analysis. This case analysis can show which GNC algorithm is the best of all. In order to determine the best algorithm, some detailed comparisons need to be conducted. However, at first simulation validation needs to be done.

Validation of simulations is one of the crucial things that needs to be done to prove the computational model represents the real world systems. It helps to confirm that the simulations results are reliable and can be used to make informed decisions. In order to validate the correctness of done simulations two references, which were used in primarily in the dynamical modelling and simulating part, can be considered. In those journals similar mathematical and dynamical modelling with different controller algorithms is used and results are presented. By comparing the open loop response acceleration to a pulse function the validation can be done. In the first reference journal, state-dependent riccati equation method is used, while in the second one a gain scheduled controller is used and in this thesis simulation a PID controller with pitch rate feedback is used as mentioned previously.

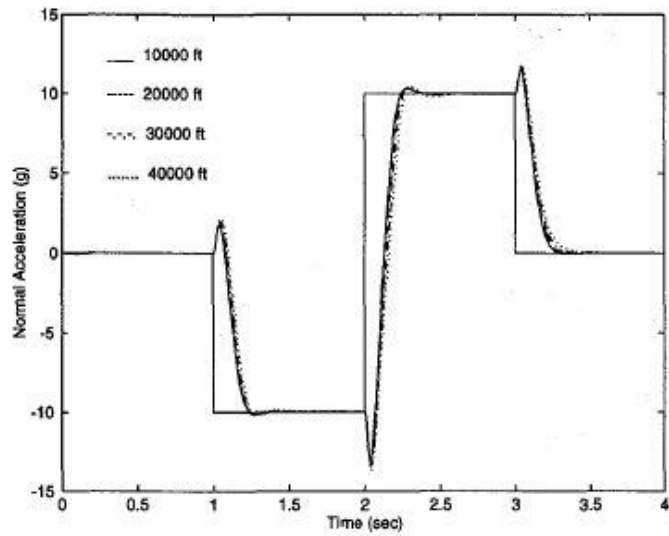


Figure 7. 1: Acceleration response to a pulse function. [15]

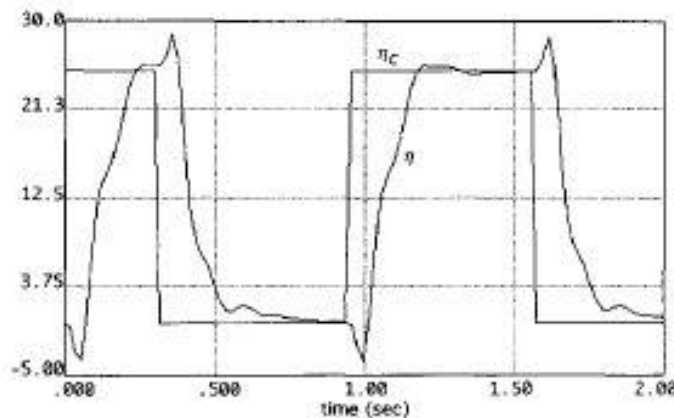


Figure 7. 2: Acceleration response to a pulse function.[11]

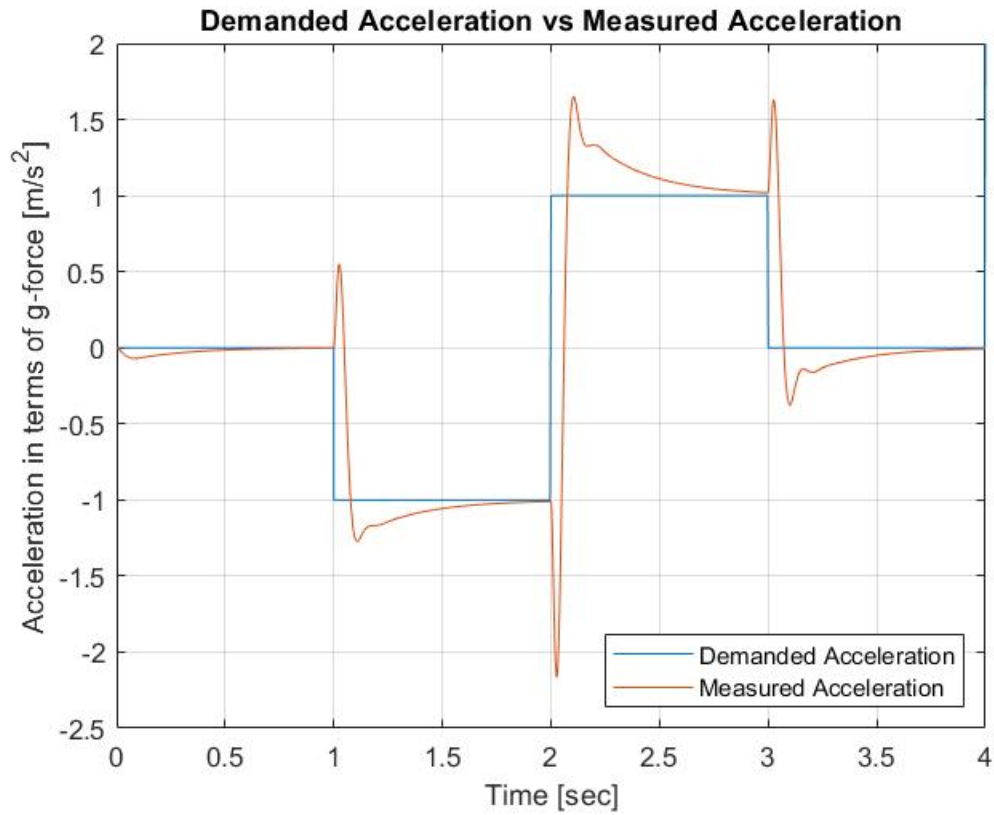


Figure 7. 3: Acceleration response to a pulse function.

By comparing these three figures (Fig 7.1, 2 and 3), it is seen that even though the controller algorithms are different , each of them has similar behaviour and trend for the pulse function in the open loop simulations. The consistency across all three figures, including simulation used in this thesis, demonstrates that the model accurately reflects the real-world system under study. This alignment with established research provides strong evidence that simulations are valid and reliable, confirming their suitability for further analysis and application in this context.

After validation of the simulation, the comparison of the GNC algorithms can be done by comparing one of the most crucial parameters is the comparison between the

demanded and measured acceleration since it creates the input command and affects all the other parameters, such as angle of attack (α), fin deflection (δ_e), missile target trajectory, Mach number (M), and hitting angle. For a better comparison, case one is chosen, and the comparisons are carried out on this case. Comparing the figures 6.3, 6.10 and 6.17, it is seen that the proportion navigational with a seeker does not provide any commands until the seeker finds the target, which roughly takes one second. After the seeker finds the target, navigational guidance provides a sharp command at first, then shows a downward trend. On the other hand, the proportional navigation and proportional navigation with ZEM show a gradually increasing trend and proportional navigation reaches the maximum allowable acceleration. Overall, all the GNC algorithms create their own commands in order to give the proper fin deflection to the missile to make the interception happen, but with different acceleration commands.

The other crucial parameter is the fin deflection (δ_e), since it is the only input command for the missile, which affects the whole system and directs the missile towards the target. For comparison the fin deflections for the first case from all the algorithms figures 6.7, 6.14, and 6.21 are evaluated. Similar to the acceleration response, proportional navigation with a seeker provides a sharp first fin deflection and then gradually decreases by slowly adjusting itself. Secondly, the proportional navigation (PN) algorithm creates a fin command that continuously increases and reaching to almost -25° deflection at the end. Finally, proportional navigation with ZEM has a similar behaviour to the simple PN algorithm, with the only difference having a sharp increase at the end.

Another parameter is the angle of attack (α), since it shows the whole behaviour of the missile pitching and the hitting angle et the end. Analysing figures 6.6, 6.13, and

6.20, it is seen that, angle of attack (α) increases very sharply at the beginning then slowly decreases and has the same mirror trend with the acceleration command for proportional navigation with the seeker. On the contrary, simple proportional navigation and proportional algorithm with ZEM have similar trends with each other and mirror trends with their acceleration commands.

Additionally, the end values of the angle of attack represent the missile's hitting angle to the target. From the figures 6.2, 6.9 and 6.16, it is perceived that the missile with a proportional navigation algorithm with seeker hits the target from almost opposite sides, while a simple proportional algorithm hits the target from the underside. Lastly, a proportional algorithm with ZEM hits the target diagonally. These hitting angles are important because if the target is small, the target may be missed depending on this angle.

The target missile trajectory is another important graph that shows how the Guidance Navigation and Control (GNC) algorithms work. Evaluating figures 6.4, 6.11, and 6.18, it is observed that each algorithm has a different trajectory. Proportional navigation with seeker has a constant ascent through the flight, while classical proportional and proportional navigation with ZEM navigations have parabolic ascent curves with a steeper curve for classical PN and a smoother curve for PN with ZEM.

Overall, it can be said that all the guidance navigation and control (GNC) algorithms are working and creating successful commands for the missile dynamics for the proper trajectory to follow in order to have an interception with the missile. However, they are creating different acceleration commands which effect all the other parameters of the algorithms. The crucial component is the acceleration; when the accelerations are

investigated, it is seen that the proportional navigation algorithm with seeker creates a sudden big magnitude acceleration command at first, then has a decline acceleration throughout the flight. On the other hand, the other two algorithms have a constantly increasing acceleration. These acceleration trends are seen in all the other performance parameters as well. When all the cases and previously explained figures are investigated a decision can be made to choose which one of the GNC algorithms is the most effective and robust among them. As a result, the proportional navigation with a seeker is concluded as the optimal algorithm since its ability to provide the required acceleration, maintain effective fin deflection (δ_e) and angle of attack (α), achieving a precise hitting angle, and ensuring an accurate trajectory. This actually shows the importance of the seeker in the algorithm. Proportional navigation with zero effort miss (ZEM) effectively mirrors the proportional navigation with the seeker algorithm in its performance. It ensures robust trajectory and accurate hitting angle by adjusting its acceleration commands to maintain close proximity to the target even with slight derivations, thus achieving high accuracy and minimal miss distance. Lastly, classical proportional navigation effectively creates the required acceleration commands, but it reaches to the maximum allowable acceleration limit, which is a drawback for the algorithm. Although it reaches the limit, it guarantees a proper trajectory to hit the target, but the hitting angle is too steep compared to the others, which could be problematic for small targets. Additionally, not pursuing the target by turning back towards in case of a miss can be shown as another drawback for this algorithm. All these drawbacks make the simple proportional navigation the least effective and robust among them.

CHAPTER 8

CONCLUSION

In this study, a short-range supersonic air-to-air tactical missile is considered, which flies around Mach 3 and has five kilometres in the x direction and five hundred meters in the z direction separations with the target in order to design different guidance navigation and control (GNC) algorithms and validate them to find the most effective one among them. Firstly, equations of motion were developed, and then three degrees of freedom (3-DOF) assumptions were discussed and applied to the EOM. After the equation of motions, other forces, aerodynamical forces, acting on the missile were handled, and the ones acting on the missile were found out. Additionally, aerodynamical coefficients were found by using polynomial estimation and look up tables were created. All these equations and coefficients were then used to model the missile in the dynamic modelling part.

An assessment of the missile stability was done by checking the poles of the system. In order to find the poles of the system, first the linearization of the equations of motion around a trim point was done. After that, stability derivatives were found using empirical equations and state space form obtained by using a trim condition. By checking the real parts of eigenvalues, poles, of the A matrix, the stability of the missile was found. According to the poles, the system is not stable, so using a closed loop system with a PI controller with pitch rate feedback, system brought it back to a stable condition.

The primary objective, designing a guidance navigation and controller (GNC) algorithm, was performed after linearization. First, the navigational algorithm, the inertial

navigation system (INS), and then the three navigational algorithms were investigated. Lastly, the PI controller and its mathematical expression are given with both pitch rate and without pitch rate feedback.

After all the equations of motion, aerodynamical forces and moment, and three guidance navigation and control algorithms were obtained, the dynamic modelling and simulation aspect of this study was delved into. Using MATLAB Simulink, the missile's dynamic model with target model and GNC algorithms was created. By using this simulation, different case studies were carried out, and in the end, results for each case were obtained. After multiple cases with different initial conditions were simulated, missile's limitations were found and represented graphically. In light of these results, the second objective, most efficient and robust algorithm, was investigated, and a ranking was made among the algorithms. Thus, proportional navigation with a seeker is found to be the best working algorithm for this missile system, while proportional navigation with ZEM is the second and simple proportional navigation is the least efficient one.

Future research directions could explore the integration of more advanced navigation guidance algorithms, such as multi-sensor fusion for seekers and adaptive observers for state estimation, to enhance interception performance. Investigating the application of advanced control strategies like Linear Quadratic Regulator (LQR) and Model Predictive Control (MPC) could provide insights into improving control performance and stability in dynamic interception scenarios and compare the advanced algorithm results with the obtained results to visualize if the performance of the missile will increase. Furthermore, developing and validating a six-degree-of-freedom (6DOF) model would offer a more realistic representation of missile target interactions, facilitating the assessment of navigation guidance algorithms and controllers in dynamic environments.

In summary, the first objective of developing and successfully implementing guidance, navigation, and control (GNC) algorithms for a three-degree-of-freedom missile model was achieved. The secondary objective, identifying the most effective GNC algorithm through comprehensive simulations, was also accomplished.

REFERENCES

- [1] R. Yanushevsky, *Modern missile guidance*. Florida: CRC Press, 2008.
- [2] P. Zarchan, *Tactical and Strategic Missile Guidance*, 6th ed., vol. 239. Atlanta, Georgia: AIAA, 2012.
- [3] G. M. Siouris, *Missile Guidance and Control Systems*. Ohio: Springer, 2004.
- [4] C.-F. Lin, *Modern Navigation, Guidance, and Control Processing*. New Jersey: Prentice Hall, 1991.
- [5] D. Titterton, J. L. Weston, I. of Electrical Engineers, A. I. of Aeronautics, and Astronautics, *Strapdown Inertial Navigation Technology*. Institution of Engineering and Technology, 2004.
- [6] T. A. Herring, “The Global Positioning System ,” *Sci. Am.*, pp. 44–50, Feb. 1996.
- [7] H. C. Gong, “Development of terrain contour matching algorithm for the aided inertial navigation using radial basis functions,” *J.Astron. Sp. Sci.* , vol. 15, no. 1, pp. 229–234, 1998.
- [8] N. A. Shneydor, *Missile guidance and pursuit: kinematics, dynamics and control*. Elsevier, 1998.
- [9] K. J. Åström and T. Hägglund, *PID controllers - theory, design, and tuning (2nd edition)*. ISA, 1995.
- [10] B. Friedland, *Control System Design: An Introduction to State-Space Methods*. Dover Publications, 2012.
- [11] J. S. Shamma and J. R. Cloutier, “Gain-scheduled missile autopilot design using linear parameter varying transformations,” *J. Guid. Control. Dyn.*, vol. 16, no. 2, pp. 256–263, Mar. 1993, doi: 10.2514/3.20997.
- [12] M. J. Anderson B., *Optimal control: Linear quadratic methods (no p.229)*. PH, 1989.
- [13] E. F. Camacho and C. Bordons, *Model Predictive control*. London: Springer London, 2007. doi: 10.1007/978-0-85729-398-5.
- [14] R. C. Nelson, *Flight Stability and Automatic Control*. McGraw-Hill Education, 1998.
- [15] C. Mracek and J. Cloutier, “Full envelope missile longitudinal autopilot design

using the state-dependent Riccati equation method," Aug. 1997. doi: 10.2514/6.1997-3767.

- [16] S. Bennani, D. Willemsen, and C. Scherer, "Robust LPV control with bounded parameter rates," in *Guidance, Navigation, and Control Conference*, Aug. 1997, pp. 1080–1089. doi: 10.2514/6.1997-3641.
- [17] A. Elsherbiny, "A CONTROL STRATEGY FOR THE POWERED LANDING OF A REUSABLE ROCKET BOOSTER," Middle East Technical University Northern Cyprus Campus, Kalkanlı, 2024.
- [18] F. K. İpek, "DESIGN, CONTROL, AND GUIDANCE OF A TACTICAL MISSILE WITH LATERAL THRUSTERS," Middle East Technical University, 2015. Accessed: Jun. 08, 2023. [Online]. Available: <https://etd.lib.metu.edu.tr/upload/12619056/index.pdf>
- [19] B. Etkin, *Dynamics of Atmospheric Flight*. Wiley, 1972.
- [20] J. N. Nielsen, *Missile Aerodynamics*. Palo Alto, California: McGRAW-HILL BOOK COMPANY, INC., 1960.
- [21] J. D. Anderson, *Fundamentals of aerodynamics*, Sixth edit. McGraw Hill Education, 2017.
- [22] R. A. Nichols, R. T. Reichert, and W. J. Rugh, "Gain scheduling for H-infinity controllers: a flight control example," *IEEE Trans. Control Syst. Technol.*, vol. 1, no. 2, pp. 69–79, 1993, doi: 10.1109/87.238400.
- [23] J. Jim Zhu and M. C. Mickle, "Missile Autopilot Design Based on a Unified Spectral Theory for Linear Time-Varying Systems," *IFAC Proc. Vol.*, vol. 29, no. 1, pp. 7558–7563, 1996, doi: [https://doi.org/10.1016/S1474-6670\(17\)58905-3](https://doi.org/10.1016/S1474-6670(17)58905-3).
- [24] "AIM-9 Sidewinder." https://en.wikipedia.org/wiki/AIM-9_Sidewinder (accessed Aug. 22, 2024).
- [25] K. Ogata, *Modern Control Engineering*. Prentice Hall, 2010.
- [26] C. M., *Flight dynamics principles: A linear systems approach to aircraft stability and control*, 2ed ed. Elsevier, 2007.
- [27] K. J. Åström and T. Hägglund, "The future of PID control," *Control Eng. Pract.*, vol. 9, no. 11, pp. 1163–1175, Nov. 2001, doi: 10.1016/S0967-0661(01)00062-4.
- [28] K. J. Åström, T. Hägglund, C. C. Hang, and W. K. Ho, "Automatic Tuning and Adaptation for PID Controllers - A Survey," *IFAC Proc. Vol.*, vol. 25, no. 14, pp. 371–376, Jul. 1992, doi: 10.1016/S1474-6670(17)50762-4.

APPENDICES

A. Linearization

Linearization of equation of motions [10], [19], [25]:

$$\Delta \dot{u} = f_0 + \frac{\partial f}{\partial X} |_{trim} \Delta X + \frac{\partial f}{\partial w} |_{trim} \Delta w + \frac{\partial f}{\partial q} |_{trim} \Delta q + \frac{\partial f}{\partial \theta} |_{trim} \Delta \theta,$$

$$\Delta \dot{u} = \frac{\Delta X}{m} - w_0 q - g \cos \theta_0 \Delta \theta, \quad (\text{A.1})$$

$$\Delta \dot{w} = f_0 + \frac{\partial f}{\partial Z} |_{trim} \Delta Z + \frac{\partial f}{\partial u} |_{trim} \Delta u + \frac{\partial f}{\partial q} |_{trim} \Delta q + \frac{\partial f}{\partial \theta} |_{trim} \Delta \theta$$

$$\Delta \dot{w} = \frac{\Delta Z}{m} + u_0 \Delta q - g \sin \theta_0 \Delta \theta, \quad (\text{A.2})$$

$$\Delta \dot{q} = f_0 + \frac{\partial f}{\partial M} |_{trim} \Delta M \rightarrow \Delta \dot{q} = \frac{\Delta M}{I_{yy}}, \quad (\text{A.3})$$

$$\Delta \dot{\theta} = \Delta q. \quad (\text{A.4})$$

Using small angle assumption, these linearized equations are further simplified.

$$w_0 = 0 \quad (\text{A.5})$$

$$\sin(\theta_0) \approx \theta_0 \quad (\text{A.6})$$

$$\cos(\theta_0) \approx 1 \quad (\text{A.7})$$

$$u_0 = V\cos(\theta_0) \quad (\text{A.8})$$

When free stream velocity (V_∞) is acting with the same direction of the x-axis of the earth reference frame pitch angle (θ) and angle of attack (α) are same.

$$w = V\sin\alpha \rightarrow w = V\alpha \quad (\text{A.9})$$

$$\dot{w} = V\dot{\alpha} \quad (\text{A.10})$$

Using these assumptions and equations linearized equations become:

$$\Delta\dot{u} = \frac{\Delta X}{m} - g\Delta\theta, \quad (\text{A.11})$$

$$\dot{\alpha} = \frac{\Delta Z}{m} + \Delta q. \quad (\text{A.12})$$

$$\Delta\dot{q} = \frac{\Delta M}{I_{yy}}, \quad (\text{A.13})$$

$$\Delta\dot{\theta} = \Delta q. \quad (\text{A.14})$$

These aerodynamical forces are functions of u, w, q, α, θ , and δ_c , so they need to be expanded and written in terms of these variables. Additionally, in the condition of pitching missile only control variable δ_c is the elevator, so it can be represented as δ_e . As a result, these forces are expressed as [10], [19], [25]:

$$\Delta X = X_u \Delta u + X_\alpha \Delta \alpha + X_{\delta_e} \Delta \delta_e \quad (\text{A.15})$$

$$\Delta Z = \frac{Z_u}{V} \Delta u + \frac{Z_\alpha}{V} \Delta \alpha + Z_{\delta_e} \Delta \delta_e \quad (\text{A.16})$$

$$\Delta M = M_u \Delta u + M_\alpha \Delta \alpha + M_q \Delta q + M_{\delta_e} \Delta \delta_e \quad (\text{A.17})$$

By putting these equations into the previous equations ,which are eq. 3.55, 3.56, 3.57, 3.58, updated linearized version can be obtained as [19], [25] :

$$\Delta \dot{u} = \frac{1}{m} [X_u \Delta u + X_\alpha \Delta \alpha + X_{\delta_e} \Delta \delta_e] - g \Delta \theta, \quad (\text{A.18})$$

$$\Delta \dot{w} = \frac{1}{m} \left[\frac{Z_u}{V} \Delta u + \frac{Z_\alpha}{V} \Delta \alpha + Z_{\delta_e} \Delta \delta_e \right] + \Delta q, \quad (\text{A.19})$$

$$\Delta \dot{q} = \dot{q} = \frac{1}{I_{yy}} [M_u \Delta u + M_\alpha \Delta \alpha + M_q \Delta q + M_{\delta_e} \Delta \delta_e], \quad (\text{A.20})$$

$$\Delta \dot{\theta} = \Delta q. \quad (\text{A.21})$$

Equations 3.63 and 3.64 can be simplified even more, so final version of linearization becomes as [19], [25], [26]:

$$\Delta \dot{u} = \frac{X_u}{m} \Delta u + \frac{X_\alpha}{m} \Delta \alpha + \frac{X_{\delta_e}}{m} \Delta \delta_e - g \Delta \theta, \quad (\text{A.22})$$

$$\Delta \dot{w} = \frac{Z_u}{mV} \Delta u + \frac{Z_\alpha}{mV} \Delta \alpha + \frac{Z_{\delta_e}}{mV} \Delta \delta_e + \Delta q, \quad (\text{A.23})$$

$$\Delta \dot{q} = \dot{q} = \frac{M_u}{I_{yy}} \Delta u + \frac{M_\alpha}{I_{yy}} \Delta \alpha + \frac{M_q}{I_{yy}} \Delta q + \frac{M_{\delta_e}}{I_{yy}} \Delta \delta_e, \quad (\text{A.24})$$

$$\Delta \dot{\theta} = \Delta q. \quad (\text{A.25})$$

Where

$$\begin{aligned} X_u &= \frac{\partial X}{\partial u}, X_\alpha = \frac{\partial X}{\partial \alpha}, Z_u = \frac{\partial Z}{\partial u}, Z_\alpha = \frac{\partial Z}{\partial \alpha}, M_u = \frac{\partial M}{\partial u} \\ M_\alpha &= \frac{\partial M}{\partial \alpha}, M_q = \frac{\partial M}{\partial q}, X_{\delta_e} = \frac{\partial X}{\partial \delta_e}, Z_{\delta_e} = \frac{\partial Z}{\partial \delta_e}, M_{\delta_e} = \frac{\partial M}{\partial \delta_e} \end{aligned} \quad (\text{A.26})$$

B. Aerodynamical Stability Derivatives

$$\text{Angle of attack: } \alpha = \arctan(-w/u), \quad (\text{B.1})$$

$$\text{Missile velocity: } V = \sqrt{u^2 + w^2}, \quad (\text{B.2})$$

$$\text{Missile velocity in x-direction: } u = V \cos(\alpha) = V \cos(\theta), \quad (\text{B.3})$$

$$\text{Mach Number: } M = \frac{V}{a} = \frac{\sqrt{u^2 + w^2}}{a}, \quad (\text{B.4})$$

$$\text{Change in angle of attack w.r.t } u: \frac{\partial \alpha}{\partial u} = \frac{w}{w^2 + u^2} = \frac{w_0}{V_0^2}, \quad (\text{B.5})$$

$$\text{Change in Mach number w.r.t } u: \frac{\partial M}{\partial u} = \frac{u}{a \sqrt{w^2 + u^2}} = \frac{u_0}{a V_0}, \quad (\text{B.6})$$

$$\text{Change in velocity w.r.t } u: \frac{\partial V}{\partial u} = \frac{u}{V} = \cos(\theta), \quad (\text{B.7})$$

Derivation of Aerodynamical Stability Derivatives

Aerodynamical statical derivatives are calculated by using empirical methods in x, z and pitching moment directions separately as:

Aerodynamical stability derivatives for force X:

$$X = \frac{1}{2} \rho V^2 S(C_x) \quad (\text{B.8})$$

Since C_x is a constant number there is not any partial derivative term coming from aerodynamical coefficients, only velocity term is used and $X_u, X_\alpha, X_{\delta_e}$ becomes as :

$$X_u = \frac{\partial X}{\partial u} = \frac{1}{2} \rho 2 V \frac{\partial V}{\partial u} S C_x = \rho V \cos \theta S C_x = \rho V_0 \cos \theta_0 S C_{x_0} \text{ (in trim)} \quad (\text{B.9})$$

$$X_\alpha = 0, X_{\delta_e} = 0 \text{ (in trim)} \quad (\text{B.10})$$

Aerodynamical stability derivatives for force Z :

$$Z = \frac{1}{2} \rho V^2 S(C_z) \quad (\text{B.11})$$

Aerodynamical coefficient in z direction is function of angle of attack, Mach number and fin deflection , where velocity (V), angle of attack (α) and Mach number(M) are functions of velocity components in x and z directions (u, w).

$$Z_u = \frac{\partial Z}{\partial u} = \frac{1}{2} \rho V^2 S \left(\frac{\partial C_z}{\partial u} \right) + \frac{1}{2} \rho 2 V S \frac{\partial V}{\partial u} (C_z)$$

$$\text{where, } \frac{\partial C_z}{\partial u} = \frac{\partial C_z}{\partial \alpha} \cdot \frac{\partial \alpha}{\partial u} + \frac{\partial C_z}{\partial M} \cdot \frac{\partial M}{\partial u} + \frac{\partial C_z}{\partial \delta_e} \cdot \frac{\partial \delta_e}{\partial u}$$

$\frac{\partial \delta_e}{\partial u} = 0$, since there is no change in fin deflection as u changes

$$Z_u = \frac{1}{2} \rho V^2 S \left(\frac{\partial C_z}{\partial \alpha} \cdot \frac{\partial \alpha}{\partial u} + \frac{\partial C_z}{\partial M} \cdot \frac{\partial M}{\partial u} \right) + \rho V \cos \theta S (C_z)$$

Change in aerodynamical force in z-direction with respect to speed in the x-direction u is represented in trim condition as:

$$Z_u = \frac{1}{2} \rho V_0^2 S \left(\frac{\partial C_z}{\partial \alpha} \Big|_{M_0} \cdot \frac{w_0}{V_0^2} + \frac{\partial C_z}{\partial M} \Big|_{\alpha_0} \cdot \frac{u_0}{aV_0} \right) + \rho V_0 \cos \theta_0 S(C_{z_0}) \text{ (in trim)} \quad (\text{B.12})$$

$$Z_\alpha = \frac{\partial Z}{\partial \alpha} = \frac{1}{2} \rho V^2 S \left(\frac{\partial C_z}{\partial \alpha} \right)$$

Change in aerodynamical force in z-direction with respect to angle of attack α is represented in trim condition as:

$$Z_\alpha = \frac{1}{2} \rho V_0^2 S \left(\frac{\partial C_z}{\partial \alpha} \Big|_{M_0} \right) \text{ (in trim)} \quad (\text{B.13})$$

$$\begin{aligned} Z_{\delta_e} &= \frac{\partial Z}{\partial \delta_e} = \frac{1}{2} \rho V^2 S \left(\frac{\partial C_z}{\partial \delta_e} \right) \\ Z_{\delta_e} &= \frac{1}{2} \rho V^2 S C_{z_{\delta_e}} \end{aligned}$$

Change in aerodynamical force in z-direction with respect to fin deflection represented in trim condition as:

$$Z_{\delta_e} = \frac{1}{2} \rho V_0^2 S C_{z_{\delta_e}} \text{ (in trim)} \quad (\text{B.14})$$

Aerodynamical stability derivatives for pitch moment M:

$$M = \frac{1}{2} \rho V^2 S d_{ref}(C_m) \quad (\text{B.15})$$

$$M_u = \frac{\partial M}{\partial u} = \frac{1}{2} \rho V^2 S \left(\frac{\partial C_m}{\partial u} \right) + \frac{1}{2} \rho 2 V \frac{\partial V}{\partial u} S d_{ref}(C_m)$$

$$\text{where, } \frac{\partial C_m}{\partial u} = \frac{\partial C_m}{\partial \alpha} \cdot \frac{\partial \alpha}{\partial u} + \frac{\partial C_m}{\partial M} \cdot \frac{\partial M}{\partial u} + \frac{\partial C_m}{\partial \delta_e} \cdot \frac{\partial \delta_e}{\partial u} + \frac{\partial C_z}{\partial q} \cdot \frac{\partial q}{\partial u}$$

$$\frac{\partial \delta_e}{\partial u} = 0, \quad \frac{\partial q}{\partial u} = 0,$$

$$M_u = \frac{1}{2} \rho V^2 S d_{ref} \left(\frac{\partial C_m}{\partial \alpha} \cdot \frac{\partial \alpha}{\partial u} + \frac{\partial C_m}{\partial M} \cdot \frac{\partial M}{\partial u} \right) + \rho V \cos \theta S d_{ref}(C_m)$$

Change in pitch moment with respect to speed in the x-direction u represented in trim condition as:

$$M_u = \frac{1}{2} \rho V_0^2 S d_{ref} \left(\frac{\partial C_m}{\partial \alpha} \Big|_{M_0} \cdot \frac{w_0}{V_0^2} + \frac{\partial C_m}{\partial M} \Big|_{\alpha_0} \cdot \frac{u_0}{aV_0} \right) + \rho V_0 \cos \theta_0 S d_{ref}(C_{m_0}) \text{ (in trim)} \quad (\text{B.16})$$

$$M_\alpha = \frac{\partial M}{\partial \alpha} = \frac{1}{2} \rho V^2 S \left(\frac{\partial C_m}{\partial w} \right)$$

Change in pitch moment with respect to angle of attack (α) in trim condition represented as:

$$M_\alpha = \frac{1}{2} \rho V_0^2 S d_{ref} \left(\frac{\partial C_m}{\partial \alpha} \Big|_{M_0} \right) \text{ (in trim)} \quad (\text{B.17})$$

$$M_q = \frac{\partial M}{\partial q} = \frac{1}{2} \rho V^2 S d_{ref} \left(\frac{\partial C_m}{\partial q} \right)$$

Change in pitch moment with respect to pitch rate (q) in trim condition represented as:

$$M_q = \frac{1}{2} \rho V_0^2 S d_{ref} \left(C_{m_q} \right) \text{ (in trim)} \quad (\text{B.18})$$

$$M_{\delta_e} = \frac{\partial M}{\partial \delta_e} = \frac{1}{2} \rho V^2 S d_{ref} \left(\frac{\partial C_m}{\partial \delta_e} \right)$$

$$M_{\delta_e} = \frac{1}{2} \rho V^2 S d_{ref} C_{m_{\delta_e}}$$

Change in pitch moment with respect to fin deflection (δ_e) in trim condition represented as:

$$M_{\delta_e} = \frac{1}{2} \rho V_0^2 S d_{ref} C_{m_{\delta_e}} \text{ (in trim)} \quad (\text{B.19})$$

Overall, an aerodynamic stability derivatives table for trim condition has been created below to summarize all these processes.

Table B. 1: Aerodynamical Stability Derivative Equations

	X	Z	M
u	$\rho V_0 \cos \theta_0 S C_{x_0}$	$\frac{1}{2} \rho V_0^2 S \left(\frac{\partial C_z}{\partial \alpha} \Big _{M_0} \cdot \frac{w_0}{V_0^2} + \frac{\partial C_z}{\partial M} \Big _{\alpha_0} \cdot \frac{u_0}{aV_0} \right) + \rho V_0 \cos \theta_0 S (C_{z_0})$	$\frac{1}{2} \rho V_0^2 S d_{ref} \left(\frac{\partial C_m}{\partial \alpha} \Big _{M_0} \cdot \frac{w_0}{V_0^2} + \frac{\partial C_m}{\partial M} \Big _{\alpha_0} \cdot \frac{u_0}{aV_0} \right) + \rho V_0 \cos \theta_0 S d_{ref} (C_{m_0})$
α	0	$\frac{1}{2} \rho V_0^2 S \left(\frac{\partial C_z}{\partial \alpha} \Big _{M_0} \right)$	$M_\alpha = \frac{1}{2} \rho V_0^2 S d_{ref} \left(\frac{\partial C_m}{\partial \alpha} \Big _{M_0} \right)$
q	0	0	$\frac{1}{2} \rho V_0^2 S d_{ref} (C_{m_q})$
δ_e	0	$\frac{1}{2} \rho V_0^2 S C_{z_{\delta_e}}$	$\frac{1}{2} \rho V_0^2 S d_{ref} C_{m_{\delta_e}}$